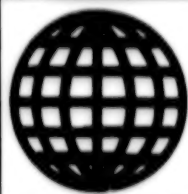


JPRS-UMS-92-002
25 FEBRUARY 1992



**FOREIGN
BROADCAST
INFORMATION
SERVICE**

JPRS Report

Science & Technology

***Central Eurasia:
Materials Science***

Science & Technology

Central Eurasia: Materials Science

JPRS-UMS-92-002

CONTENTS

25 February 1992

ANALYSIS, TESTING

Low-Carbon Raw Material—A Resource for Thermal Power Generation and Ferrous and Nonferrous Metallurgy [V.V. Mechev, V.V. Ivanov, et al.; IZVESTIYA AKADEMII NAUK SSSR: SERIYA METALLY, No 5, Sep-Oct 91]	1
The Formation of a Metallic Phase During the Reduction of Iron Oxides by Natural Gas [V.A. Maslov; IZVESTIYA AKADEMII NAUK SSSR: SERIYA METALLY, No 5, Sep-Oct 91]	1
A Study of the Reduction Dephosphorization of Manganese Melts [V.Ya. Dashevskiy, A.M. Katsnelson, et al.; IZVESTIYA AKADEMII NAUK SSSR: SERIYA METALLY, No 5, Sep-Oct 91]	1
Assessment of Information Value of Nondestructive Testing Methods Used in Shipbuilding and Flaw Detection [M.V. Rozina, L.M. Yablonik; DEFEKTOSKOPIYA, Apr 91]	2
Methods and Facilities of Composite Material Quality Control [I.G. Matiss; DEFEKTOSKOPIYA, Apr 91]	2
General and Particular Patterns of Eddy Current Testing Theory [Yu.M. Shkarlet; DEFEKTOSKOPIYA, Apr 91]	2
Analysis of Magnetic Field Restoration Method Capabilities With Respect to Magnetic Nondestructive Testing. I. [A.S. Shleyenkov, R.S. Melnik, et al.; DEFEKTOSKOPIYA, May 91]	3
Demagnetizing Factor's Effect on Harmonic Magnetization Components of Cyclically Magnetized Ferromagnetic Cores. I. Analysis [Yu.F. Ponomarev; DEFEKTOSKOPIYA, May 91]	3
Demagnetizing Factor's Effect on Harmonic Magnetization Components of Cyclically Magnetized Ferromagnetic Cores. II. Nondestructive Testing Applications [Yu.F. Ponomarev; DEFEKTOSKOPIYA, May 91]	3
Surface Examination of Condensed Systems by Photoelectron Spectroscopy Methods [V.A. Trapeznikov; DEFEKTOSKOPIYA, May 91]	4
Development of Methods and Devices of Nondestructive Testing of Welded Joints and Techniques for Assessing Their Quality Indicators [V.F. Davidenko, V.A. Troitskiy; DEFEKTOSKOPIYA, May 91]	4
Analysis of Magnetic Field Reconstruction Method Possibilities With Respect to Nondestructive Magnetic Field Testing. III [A.S. Shleyenkov, L.N. Krotov, et al.; DEFEKTOSKOPIYA, Jun 91]	4
Experimental Investigation of Ultrasound Velocity and Attenuation in Aqueous Saline Solutions [A.K. Brovitsyn, A.G. Akimov, et al.; DEFEKTOSKOPIYA, Jun 91]	4
Infrared Method of Testing Soldered Printed Circuit Board Connections [A.S. Oleynik; DEFEKTOSKOPIYA, Jun 91]	5
Method of Measuring Effective Dielectric Constant of Inhomogeneous Sheet Materials in Microwave Band [A.A. Kalachayev, I.V. Kukoiev, et al.; DEFEKTOSKOPIYA, Jun 91]	5
Measuring X-Ray Image Parameters During Radiographic Inspection of Steel by MIRA-D Pulsed X-Ray Units [Yu.V. Gromov, Yu.V. Gorbato; DEFEKTOSKOPIYA, Jun 91]	5
Radiographic Testing of Steam Turbine Weld Root in Hot State [S.V. Shablov, V.I. Kapustin, et al.; DEFEKTOSKOPIYA, Jun 91]	5
The Evolution of Thermal and Electromagnetic Perturbations in Composite Superconductors [N.A. Taylanov; METALLOFIZIKA, Aug 91]	6
Magnetic Film Metal Oxide Heterostructures on an Aluminum Surface [V.G. Shadrov, A.V. Boltushkin, et al.; METALLOFIZIKA, Aug 91]	6
Investigation of the Process of Annealing the Alloy AMg6 by Using Acoustic Emission [A.V. Kozlov, G.I. Prokopenko, et al.; METALLOFIZIKA, Aug 91]	6
Hyperfine Structure of $\text{Fe}_{85-x}\text{Co}_x\text{B}_{15}$ Amorphous Alloys After Irradiation With γ -Quanta [V.M. Shkapa, V.V. Polotnyuk, et al.; METALLOFIZIKA, Aug 91]	7
Experimental Observation of the Deviation of the Direction of an Energy Flux From a Reflecting Plane During the Anomalous Passage of X-Rays Through a Crystal [I.F. Zvorygin, L.V. Tikhonov, et al.; METALLOFIZIKA, Aug 91]	7
Diffusion of Bismuth in the High-Temperature Superconducting Ceramics $\text{YBa}_2\text{Cu}_3\text{O}_{7-\delta}$ and $[\text{Pb}_{1-x}\text{Bi}_x]_2\text{Ca}_2\text{Sr}_2\text{Cu}_3\text{O}_y$ [P.P. Gorbik, M.V. Bakuntseva, et al.; METALLOFIZIKA, Aug 91]	8

Nature of the Shape Memory Effect in Fe-Mn-Si Alloys [Ye.Z. Vintaykin, A.A. Gulyayev, et al.; METALLOFIZIKA, Aug 91]	8
The Effect of the Dispersivity of an Alloy's Phase Structure on the Depth of a Laser's Effect on the Alloy [O.M. Ivasishin, P.Ye. Markovskiy, et al.; METALLOFIZIKA, Aug 91]	9
Vacancies in AuCu-Type Ordered Alloys [A.A. Smirnov; METALLOFIZIKA, Aug 91]	9
Automated System for Monitoring, Documenting, and Analyzing Rail Quality [V. F. Tsarev, A. Ye. Koshelev, et al.; STAL No 8, 91]	9

COATINGS

An Investigation of the Heat Conduction of Gas-Thermal Ni-Cr-B-Si Coatings [V.D. Podzorov, V.S. Kharchenkov, et al.; POROSHKOVAYA METALLURGIYA, Aug 91]	10
The Structure, Composition, and Heat Stability of Nickel-Phosphorus Coatings [E.M. Lazarev, L.M. Petrov, et al.; IZVESTIYA AKADEMII NAUK SSSR: SERIYA METALLY, No 5, Sep-Oct 91]	10

COMPOSITE MATERIALS

The Effect of Adhesion-Active Substrates on the Structure Formation and Properties of Laminated Materials Consisting of the Hard Alloy KKhNF15 and Steel [V.A. Maslyuk, V.G. Kayuk, et al.; POROSHKOVAYA METALLURGIYA, Aug 91]	11
-----------------------------------------------------------------------------------------------------------------------------------------------------------------------------------------------------------------------------------	----

CORROSION

The Development and Assimilation of Different Methods of Protecting Powder Construction Materials Against Corrosion [G.I. Tarasova, V.A. Dovydenkov, et al.; POROSHKOVAYA METALLURGIYA, Aug 91]	12
The Effect of Medium Composition on the Propagation of Corrosion and Fatigue Cracks in X8CrNiTi18.10 Steel [I.M. Dmitrakh, V. Rayngard; FIZIKO-KHIMICHESKAYA MEKHANIKA MATERIALOV, Vol 27 No 2, Mar-Apr 91]	12
The Crack Resistance of AT3 Titanium Alloy Under Conditions of Hydrogen Brittleness [A.V. Malkov, V.K. Alekseyev, et al.; FIZIKO-KHIMICHESKAYA MEKHANIKA MATERIALOV, Vol 27 No 2, Mar-Apr 91]	12
Determination of Critical Brittleness Temperature During Impact Bending [V.I. Smirnov, A.Sh. Deych; FIZIKO-KHIMICHESKAYA MEKHANIKA MATERIALOV, Vol 27 No 2, Mar-Apr 91]	13
The Resistance of the Steels and Welded Joints of the Metal Structures of Hoisting Machinery to Cyclic Corrosion Cracks [V.N. Pustovoy; FIZIKO-KHIMICHESKAYA MEKHANIKA MATERIALOV, Vol 27 No 2, Mar-Apr 91]	13
Calculation and Rational Design of Structures Subjected to Corrosion Wear [I.G. Ovchinnikov, Yu.M. Pochtman; FIZIKO-KHIMICHESKAYA MEKHANIKA MATERIALOV, Vol 27 No 2, Mar-Apr 91]	14
The Effect of Ozonization and Selected Additives on the Corrosion and Electrochemical Behavior of 12Cr18Ni10Ti Steel in Sulfuric Acid [B.A. Gru, G.O. Tatarchenko, et al.; FIZIKO-KHIMICHESKAYA MEKHANIKA MATERIALOV, Vol 27 No 2, Mar-Apr 91]	14
Zr-V-Fe-Based Alloys—Effective Hydrogen Absorbers [V.A. Yartis, I.Yu. Zavaliy, et al.; FIZIKO-KHIMICHESKAYA MEKHANIKA MATERIALOV, Vol 27 No 2, Mar-Apr 91]	15
The Penetration of Hydrogen Through Nickel With Various Surface Element Profiles [V.P. Shestakov, I.L. Tazhibayeva, et al.; FIZIKO-KHIMICHESKAYA MEKHANIKA MATERIALOV, Vol 27 No 2, Mar-Apr 91]	15

FERROUS METALS

New Precision Alloys [V.V. Sosnin; STAL, Jun 91]	17
New Developments in Alloy and Alloy Steel Production [G. I. Kaplanov; PROBLEMY SPETSIALNOY ELEKTROMETALLURGII No 4, 91]	17
Heat Treatment of Low-Alloy Steels To Produce a Ferrite-Austenite-Bainite Structure [A.A. Petrunenkov; FIZIKA METALLOV I METALLOVEDENIYE, May 91]	17

The Properties of Hot-Stamped High-Chromium Stainless Steels [S.G. Napara-Volgina, L.N. Orlova; POROSHKOVAYA METALLURGIYA, Aug 91]	18
Effect of Nonferrous Metals on Quality of Tube and Pipe Steel [R.P. Bobova, V.V. Popov, et al.; STAL, Jul 91]	18
Structural Changes Occurring in Nonalloyed Steels With a Plastic Perlite Structure After Laser Heating [I.V. Lyasotskiy, D.V. Shatanskiy; FIZIKA METALLOV I METALLOVEDENIYE, May 91]	19
The Heat Embrittlement Tendency of Cr-Ni-Mo Steel With Ti and B Additives [V.M. Goritskiy, G.R. Shneyderov, et al.; METALLOVEDENIYE I TERMICHESKAYA OBRABOTKA METALLOV, May 91]	19
Optimization of Burden Composition for Making Vanadium Pig Iron [V.V. Volkov, B.M. German, et al.; STAL, Jul 91]	20
Pilot Tests of Copper Removal From Iron-Carbon Melts by Refining [V.I. Kashin, A.M. Katsnelson, et al.; STAL, Jul 91]	20
Problems of Removing Nonferrous Metal Impurities From Steel and Possible Solution Versions [V.A. Kudrin, V.K. Babich, et al.; STAL, Jul 91]	20
Copper in Steel and Copper Removal Problems [I.N. Zigalo, V.I. Baptizanskiy, et al.; STAL, Jul 91]	20
Production of 500 mm dia. Heat-Resistant Alloy Ingots by Vacuum Arc Remelting Method [M.S. Vulfovich, I.A. Tregubenko, et al.; STAL, Jul 91]	21
Efficiency of In-Line Cold-Deformed Stainless Steel Tube Production at Nikopol Yuzhnorubnyy Tube Works [O.A. Semenov, V.F. Frolov, et al.; STAL, Jul 91]	21
Iron Powder Production From Iron Ore Concentrate [P.K. Savorskiy, B.P. Khlivenko, et al.; STAL, Jul 91]	21
Stratification Kinetics and Phase Composition During the Aging of Cold-Rolled Foils Made of the Alloy Cr15 and 08Cr14Ni5Cu2Ti Steel [T.M. Makhneva, Ye.P. Yelsukov, et al.; FIZIKA METALLOV I METALLOVEDENIYE, May 91]	22

NONFERROUS METALS, ALLOYS, BRAZES, SOLDERS

The Role of Microorganisms in Molybdenum Extraction [G.M. Yashina, S.V. Nesterova; TSVETNYYE METALLY, Jul 91]	23
An Investigation of the Isothermal Upsetting of the High-Damping Alloy G55D45 [A.S. Anishchenko, A.P. Andryushchenko, et al.; TSVETNYYE METALLY, Jul 91]	23
Reducing Scaling When Copper Ingots Are Heated [T.V. Shvedchikova, I.A. Dmitriyev, et al.; TSVETNYYE METALLY, Jul 91]	24
The Dislocation Structure and Deformation Hardening of Copper-Based Solid Solutions [M.I. Tsypin, E.V. Kozlov, et al.; TSVETNYYE METALLY, Jul 91]	24
Determination of Regimens for the Induction Annealing of Brass Strips [N.M. Shirokov, V.D. Kozhin, et al.; TSVETNYYE METALLY, Jul 91]	24
Current Trends in the Development and Use of Rhenium as a Catalyst [M.A. Ryashentseva; TSVETNYYE METALLY, Jul 91]	25
Contemporary Rhenium Determination Methods [L.N. Vasilyeva, Yu.A. Karpov, et al.; TSVETNYYE METALLY, Jul 91]	25
The Use of Membrane Processes in the Technology of Rhenium Extraction [M.V. Istrashkina, Z.A. Peredereyeva, et al.; TSVETNYYE METALLY, Jul 91]	26
Extracting Rhenium While Processing Molybdenite Concentrates [V.K. Rumyantsev, S.G. Voldman, et al.; TSVETNYYE METALLY, Jul 91]	26
Boosting Rhenium Production at Nonferrous Metallurgy Enterprises [A.D. Besser, A.V. Peredereyev; TSVETNYYE METALLY, Jul 91]	27
Comprehensive Use of Slags of Ural Nickel Enterprises [A.N. Fedorenko, Yu.A. Karasev, et al.; TSVETNYYE METALLY, Jul 91]	27
Cobalt Extraction in the Smelting Shop of the Severonikel Combine [I.D. Reznik, V.M. Khudiyakov, et al.; TSVETNYYE METALLY, Jul 91]	28
Oxysulfide Formation During the Pyrometallurgical Treatment of Nickel Mattes and Converter Slags [I.D. Reznik, Ye.N. Selivanov, et al.; TSVETNYYE METALLY, Jul 91]	28
The Effect of Deformation in a Superplasticity Regimen on the Structure and Properties of Ingots of the Alloy Al-Li [V.M. Sovenko, Yu.B. Timoshenko; IZVESTIYA AKADEMII NAUK SSSR: SERIYA METALLY, No 5, Sep-Oct 91]	29
The Occurrence of Low-Energy Interfaces During the Annealing of Titanium Alloys [M.I. Mazurskiy; FIZIKA METALLOV I METALLOVEDENIYE, May 91]	29

The Effect of Directed Crystallization and Heat Treatment Conditions on Porosity in Monocrystals of Nickel Refractory Alloys [V.N. Tolorayia, A.G. Zuyev, et al.; IZVESTIYA AKADEMII NAUK SSSR: SERIYA METALLY, No 5, Sep-Oct 91]	30
Alterations in the Crystalline Structure of Martensite After Co-W and Co-Mo Alloys Have Been Doped With a Third Element [B.I. Nikolin, A.Yu. Babkevich, et al.; FIZIKA METALLOV I METALLOVEDENIYE, May 91]	30
Features of Avalanche (Explosive) Crystallization of Bi-Pb Amorphous Films [V.M. Kuzmenko, Yu.V. Navozenko; FIZIKA METALLOV I METALLOVEDENIYE, May 91]	30
Carbide Formation in a Cast Nickel Refractory Alloy [A.V. Shulga, V.V. Nikishanov, et al.; IZVESTIYA AKADEMII NAUK SSSR: SERIYA METALLY, No 5, Sep-Oct 91]	31
Spin Fluctuations in Weakly Ferromagnetic Ni-Al Alloys [Yu.V. Kudryavtsev, I.N. Mishchenko, et al.; FIZIKA METALLOV I METALLOVEDENIYE, May 91]	31

NONMETALLIC MATERIALS

Use of the Kunzler Method To Produce Wires From $\text{YBa}_2\text{Cu}_3\text{O}_{7-x}$ Superconductor Ceramics [M.I. Karpov, V.P. Korzhov, et al.; FIZIKA METALLOV I METALLOVEDENIYE, May 91]	33
Partial Displacements of Atoms in $\text{YBa}_2\text{Cu}_3\text{O}_7$ Under the Effect of High-Energy Particles [N.N. Degtyarenko, V.F. Yezesin, et al.; FIZIKA METALLOV I METALLOVEDENIYE, May 91]	33
The Heat Conduction of Turbostrate Boron Nitride [Sh.Sh. Abelskiy, A.L. Zilichikhis, et al.; POROSHKOVAYA METALLURGIYA, Aug 91]	34

PREPARATIONS

Development and Assimilation of the Production of Microcables Made of Corrosion-Resistant Steels for Computers [Kh.Yu. Latipov, B.A. Nikiforov, et al.; STAL, Jun 91]	35
Assimilating the Production of Extraprecise Pipes for the Casings of Immersion Pumps and Electric Motors [A.I. Kozlovskiy, V.Ya. Karmazin, et al.; STAL, Jun 91]	35
Development of the Pilger Method of Pipe Production [A.K. Vashchenko, A.A. Ksenz; STAL, Jun 91]	36
Trends in the Development of Cold Sheet-Rolling Shops [V.L. Mazur; STAL, Jun 91]	36
Using Low-Phosphorus Concentrates in Smelting Conversion Silicomanganese [P.Sh. Tsinadze, S.G. Grishchenko, et al.; STAL, Jun 91]	36
Selected Problems of the Status and Development of the Ferroalloy Subsector [V.A. Matviyenko; STAL, Jun 91]	37
Improvement of Steel Smelting Processes at Sector Enterprises. Western Siberian Metallurgy Combine [R.S. Ayzatulov, N.A. Fomin, et al.; STAL, Jun 91]	37
Past STAL Publications on Blast Furnace Processes Reviewed [STAL, Jun 91]	38
The Properties of Highly Disperse Tungsten Carbide Powders Produced by the Method of High-Temperature Electrochemical Synthesis [O.N. Grigoryev, Kh.B. Kushkhov, et al.; POROSHKOVAYA METALLURGIYA, Aug 91]	38
A System To Design Processes for the Hot Isostatic Compaction of Powder Materials. 2. Description of "Lower"-Level Models. A Method of Determining Rheological Coefficients. An Overall Schematic of the System's Operation [A.A. Frolov, O.B. Sadykhov, et al.; POROSHKOVAYA METALLURGIYA, Aug 91]	39
Radiation-Accelerated Sintering of Powder Materials [Yu.M. Annenkov, T.S. Frangulyan, et al.; POROSHKOVAYA METALLURGIYA, Aug 91]	39
The Effect of the Stability of the Phase Composition of Powders of Fe-Nd-B Alloys on the Structure and Hysteresis Properties of Sintered Permanent Magnets [A.A. Pavlyukov, O.S. Opanasenko, et al.; POROSHKOVAYA METALLURGIYA, Aug 91]	40
The Effect of Calcium Fluoride and Lead Content on the Structure Formation and Tribotechnical Characteristics of Copper-Based Powder Material [N.G. Baranov, V.S. Ageyeva, et al.; POROSHKOVAYA METALLURGIYA, Aug 91]	40
The Production and Properties of a Cu-Ni Powder Alloy for Thermostatic Bimetals [R.G. Samvelyan, S.G. Agbalyan, et al.; IZVESTIYA AKADEMII NAUK SSSR: SERIYA METALLY, No 5, Sep-Oct 91]	41

TREATMENTS

The Structure and Properties of Welded Joints of Different Titanium Alloys [A.A. Popov, A.G. Illarionov, et al.; <i>METALLOVEDENIYE I TERMICHESKAYA OBRABOTKA METALLOV</i> , Jul 91]	42
The Quality of Ingots Forged From Low-Alloy Steel Subjected To Pulsation Treatment During Hardening [A.N. Smirnov, Yu.B. Bychkov, et al.; <i>METALLOVEDENIYE I TERMICHESKAYA OBRABOTKA METALLOV</i> , Jul 91]	42
Quality Control of Heat Treatment of Components [V.V. Pleshakov, S.A. Alimova, et al.; <i>METALLOVEDENIYE I TERMICHESKAYA OBRABOTKA METALLOV</i> , Jul 91]	42
High-Temperature Thermoplastic Hardening of Steels St3sp and 09Mn2C [A.G. Ksenofontov, M.Yu. Sinelnikova, et al.; <i>METALLOVEDENIYE I TERMICHESKAYA OBRABOTKA METALLOV</i> , Jul 91]	43
The Effect of Hardening Regimens Entailing Electrocontact Heating on the Structure and Properties of 36NiCrTiAl Spring Alloy [G.M. Klykov, A.G. Rakhshadt, et al.; <i>METALLOVEDENIYE I TERMICHESKAYA OBRABOTKA METALLOV</i> , Jul 91]	43
The Effect of Nitrocarburization Regimens and Subsequent Oxidation on the Properties of Components [G. Wal; <i>METALLOVEDENIYE I TERMICHESKAYA OBRABOTKA METALLOV</i> , Jul 91]	44
A Study of the Kinetics of the Dissolution and Formation of Complex Carbides and Their Effect on the Martensite Transformation in Corrosion-Resistant Steels [G. Garcia, L.F. Alvarez, et al.; <i>METALLOVEDENIYE I TERMICHESKAYA OBRABOTKA METALLOV</i> , Jul 91]	44
The Dissolution of Carbides and Nitrides During the Austenitization of Steels [V.V. Popov, M.I. Goldshteyn; <i>METALLOVEDENIYE I TERMICHESKAYA OBRABOTKA METALLOV</i> , Jul 91]	45
The Reverse Martensite Transformation of Ferrite Into Austenite [Ya. Prokhazka, K.G. Maroti; <i>METALLOVEDENIYE I TERMICHESKAYA OBRABOTKA METALLOV</i> , Jul 91]	45
The Link Between Martensite and Bainite Transformation in Carbon and Alloy Steels [V.M. Schastlivtsev, D.A. Mirzayev, et al.; <i>METALLOVEDENIYE I TERMICHESKAYA OBRABOTKA METALLOV</i> , Jul 91]	45
The Effect of Pressing on the Texture of Powder Magnets Made of Barium Ferrite [A.S. Kotenev; <i>IZVESTIYA AKADEMII NAUK SSSR: SERIYA METALLY</i> , No 5, Sep-Oct 91]	46
The Mechanical Properties of the Alloy KhN35VTYu at Low Temperatures [P.F. Koshelev, P.N. Nikitin, et al.; <i>METALLOVEDENIYE I TERMICHESKAYA OBRABOTKA METALLOV</i> , May 91]	46
The Structure and Properties of Cast Bimetal Composites for Tools [V.V. Chekurov; <i>METALLOVEDENIYE I TERMICHESKAYA OBRABOTKA METALLOV</i> , May 91]	47
An Investigation of the Chemical Composition of the Surface of Specimens of High-Speed Steel With a Titanium Nitride-Based Coating After a Thermal Effect [V.D. Kalner, A.K. Verner; <i>METALLOVEDENIYE I TERMICHESKAYA OBRABOTKA METALLOV</i> , May 91]	47
The Effect of the Structure of the Hot-Rolled Band on Texture Formation in 80kp Steel [V.Ya. Goldshteyn, A.V. Seryy, et al.; <i>METALLOVEDENIYE I TERMICHESKAYA OBRABOTKA METALLOV</i> , May 91]	48
The Effect of the Duration of High-Temperature Tempering on the Elimination of Superheating Texture in Rotor Steels [I.A. Borisov; <i>METALLOVEDENIYE I TERMICHESKAYA OBRABOTKA METALLOV</i> , May 91]	48
Chemical and Heat Treatment of 5CrNiMo Die Steel [N.Ya. Kudryavtseva, Yu.N. Gromov, et al.; <i>METALLOVEDENIYE I TERMICHESKAYA OBRABOTKA METALLOV</i> , May 91]	49
Carburization of Molybdenum- and Titanium-Containing Heat-Resistant Steels [Ye.L. Gyulikhandanov, A.D. Khaydorov; <i>METALLOVEDENIYE I TERMICHESKAYA OBRABOTKA METALLOV</i> , May 91]	49
Resource-Saving Technologies for Nitriding Steel in a Closed Space [Ya.D. Kogan, Yu.A. Konovalov; <i>METALLOVEDENIYE I TERMICHESKAYA OBRABOTKA METALLOV</i> , May 91]	49

Blast-Furnace Smelting With Injection of Hot Reducing Gases [A. P. Pukhov, G. M. Stepin, et al.; <i>STAL</i> No 8, 91]	50
---------------------------------------------------------------------------------------------------------------------------	----

WELDING, BRAZING, SOLDERING

The Resistance of Type 14CrNi3MoCuN Steel to Delayed Fracture During Double-Arc Welding [G.V. Burskiy, D.P. Novikova, et al.; <i>AVTOMATICHESKAYA SVARKA</i> , Aug 91]	51
The Structural Transformations and Properties of Metal in the Heat-Affected Zone of Welded Joints of the Steel 10CrNiCu [P. Seyffarth, H.G. Gross, et al.; <i>AVTOMATICHESKAYA SVARKA</i> , Aug 91]	51
The Effect of Preliminary Heating and Local High-Temperature Tempering on the Fracture Toughness of Welded Joints of 09Mn2C Steel [V.S. Girenko, M.D. Rabkina, et al.; <i>AVTOMATICHESKAYA SVARKA</i> , Aug 91]	52
The Effect of Carbide-Forming Elements on the Properties of Welds of Martensite Steels Containing 12% Chromium [V.Ye. Lazkov, V.G. Kovalchuk, et al.; <i>AVTOMATICHESKAYA SVARKA</i> , Aug 91]	52
The Effect of Design Parameters on Durability During the Thermal Cycling Life of Soldered Joints of Electronic Components Mounted on a Printed Circuit Board Surface [V.I. Makhnenko, N.I. Pivtorak, et al.; <i>AVTOMATICHESKAYA SVARKA</i> , Aug 91]	53
Preprocessing Welding Current and Voltage Signals for Input Into a Computer [G.A. Butakov, V.V. Dolinenko, et al.; <i>AVTOMATICHESKAYA SVARKA</i> , Aug 91]	53
Magnetic Phenomena Occurring When ONi9 Steel Is Welded and Ways of Eliminating Their Effect on the Quality of Welded Joints [K.A. Yushchenko, V.A. Pestov, et al.; <i>AVTOMATICHESKAYA SVARKA</i> , Aug 91]	54
Heating Devices in Units To Weld Dielectrics in an Electric Field [N.N. Khomenko, O.A. Moseyev, et al.; <i>AVTOMATICHESKAYA SVARKA</i> , Aug 91]	54
Radiative Heat Transfer Coefficient Measurement in Heating Parameter Analysis of Infrared Radiation-Welded Polymer Tube Surfaces [V.V. Koshelev, V.V. Chigarev; <i>SVAROCHNOYE PROIZVODSTVO</i> , No 6(680), Jun 91]	54
Welding Electrodes for Low-Alloy Heat-Treated Steel Operating at Subzero Temperatures [Yu.M. Nyagay, O.S. Kakovkin, et al.; <i>SVAROCHNOYE PROIZVODSTVO</i> , No 6(680), Jun 91]	55
Formation Features and Properties of N-2.5 Zirconium Alloy Joints With PT-3V Titanium Alloy During "Sharp Face" Projection Welding [A.A. Chularis, M.M. Mikhaylova, et al.; <i>SVAROCHNOYE PROIZVODSTVO</i> , No 6(680), Jun 91]	55
Welding Characteristics of Porous Wire Mesh Materials [A.F. Tretyakov; <i>SVAROCHNOYE PROIZVODSTVO</i> , No 6(680), Jun 91]	55
Characteristics of Light-Beam Welding of Copper Hookup Wires [M.I. Oparin, V.S. Mamayev, et al.; <i>SVAROCHNOYE PROIZVODSTVO</i> , No 6(680), Jun 91]	56
Connection of High-T _c Superconductors With Normal Conductors [S.K. Sliozberg, A.I. Tokarev, et al.; <i>SVAROCHNOYE PROIZVODSTVO</i> , No 6(680), Jun 91]	56

EXTRACTIVE METALLURGY, MINING

Effect of Cryogenic Treatment on Wear Resistance of Diamond Drill Bits [V.I. Vlasyuk; <i>RAZVEDKA I OKHRANA NEDR</i> , May 91]	57
Type Test Outcome of Drill Bits Reinforced With Metallized Diamond [N.I. Kornilov, A.I. Osetskiy, et al.; <i>RAZVEDKA I OKHRANA NEDR</i> , May 91]	57
'Garmonika-411' Laser Microscope in Engineering Mineralogy [L.B. Meysner, Ye.Yu. Yefimkina, et al.; <i>RAZVEDKA I OKHRANA NEDR</i> , May 91]	57
Coal Sampling by Petrographic Parameters of Unified Classification [A.S. Artser, I.V. Yerevin; <i>RAZVEDKA I OKHRANA NEDR</i> , May 91]	57
Geological-Economic Assessment of Eastern Donbass Coal Deposits [V.K. Kabalov, G.I. Starokozheva, et al.; <i>RAZVEDKA I OKHRANA NEDR</i> , May 91]	58

Low-Carbon Raw Material—A Resource for Thermal Power Generation and Ferrous and Nonferrous Metallurgy

927D0050C Moscow IZVESTIYA AKADEMII NAUK
SSSR: SERIYA METALLY in Russian No 5,
Sep-Oct 91 (manuscript received 18 Apr 90) pp 38-41

[Article by V.V. Mechev, V.V. Ivanov, V.N. Demikhov,
A.B. Yermakov, and A.L. Kovalenko, Moscow]

UDC 662.61+662.65:669.2/8

[Abstract] The increasing demands for thermal power have made it necessary to find new raw materials for use in thermal power generation. One possible solution to the problem is to burn the low-grade coals and oil shales that are located near industrial centers throughout the country. The burning of such materials, which are plagued with a very high ash content, poses a number of problems, however. Estimates from the losses resulting from processing fuels with an elevated ash content at thermal electric power plants range from 10 to 12 rubles per ton of fuel equivalent. One way of reducing these losses that appears promising is to burn low-grade carbon-containing materials in special devices to burn fuel while in a melt. The main product resulting from such devices is a silicate slag that may be used to produce a slag portland cement or binder as well as to produce concrete fillers. The mineral portion of the low-carbon material may, moreover, contain iron along with various nonferrous and rare metals (including germanium, gallium, uranium, molybdenum, gold, silver, zinc, and lead). These may be recovered by combining a metallurgical unit in loop with a power-generating boiler. Systems of this type were used successfully at the Ryazan Pilot Metallurgy Plant of the Gintsvetmet Institute in 1987-1989. Low-grade Donetsk coal that could not normally be burned at electric power plants in the Ukraine without intensifying the jet with natural gas or mazout was burned in the new special devices to burn fuel in a melt without any complications. The new furnace differs from conventional furnaces in several ways: A combined method is used to provide the blast, the capacity of the port section is greatly reduced, and the shaft is lengthened. Its tuyere section is closer in design to fuming furnaces. The blast is delivered directly to the melt, which makes it possible to leave a greater portion of the sulfur in the bottom calm portion of the vat and to constantly maintain a reducing atmosphere in the top bubbled layer. Elemental sulfur is assimilated by the melt and not released into gases. All of these factors, coupled with the intensive mixing of the silicate melt, give the new furnace a high burning and gasification efficiency. The heat of the off gases may be processed into thermal or electric power; the silicate slag may be used in the construction industry; and the matte, dusts, and alloy produced during the burning process may serve as raw materials for use in ferrous and nonferrous metallurgy. Figure 1; references 10 (Russian).

The Formation of a Metallic Phase During the Reduction of Iron Oxides by Natural Gas

927D0050A Moscow IZVESTIYA AKADEMII NAUK
SSSR: SERIYA METALLY in Russian No 5,
Sep-Oct 91 (manuscript received 11 May 90) pp 12-17

[Article by V.A. Maslov, Mariupol]

UDC 669.094.1/2.004.67.001.5

[Abstract] The author of the study reported herein analyzed the laws governing the formation of a metal phase during the reduction of iron oxides by natural gas. The said reaction is studied as a representative topochemical reaction. The focus of the study is those kinetic laws that are observed to occur at low degrees of transformation (not exceeding 10 to 30%), and the examination is based on a model of the independent growth of nuclei, which is to say, a model in which the overlapping of nuclei in the growth process in the initial stage may be ignored. Specifically, the author has studied the kinetics of the metallization of mill scale by natural gas in the temperature interval from 870 to 970°C. Specimens of finished and rough mill scale of low-carbon steel were used as the study material. Municipal natural gas (at a flow rate of 0.5 to 1.5 l/min) that had been scrubbed to remove the CO₂, CO, H₂S, O₂, and H₂O was used as the reducing agent. It contained the following (%): CH₄, 92.8-93.5; C₂H₆, 3.8-3.2; and N₂, 3.1. The mill scale specimens weighed 6 g. Temperature was found to have a very significant effect on the speed of the metallization process. At 870°C metallization took 50 minutes; at 970°C it only required 18.5 minutes. The results were examined in two coordinate systems: ϕ/τ -W and ϕ/τ^3 -W/ τ^3 . In the first of the two coordinate systems, the dependences were linear, thus confirming that the law governing the formation of metal phase nucleation centers is a power law. As the temperature changes, the parameters of the power law remain unchanged. When the experiment results are plotted in the second coordinate system, however, the dependences are not linear, thus indicating that the formation of metal phase nuclei does not occur in accordance with an exponential dependence. This finding was taken as an indication that the law governing nucleation center formation during the metallization process is a power law. After analyzing the experimental data obtained, the author determined that the growth of a new phase in the beginning of the metallization process may be described by a Roginskiy-Schultz equation. The calculated value of the apparent activation energy (219 kJ/mol) was taken as an indication that in its initial stages, the metallization process is limited by crystalline-chemical transformations. Figures 2; references 10 (Russian).

A Study of the Reduction Dephosphorization of Manganese Melts

927D0050B Moscow IZVESTIYA AKADEMII NAUK
SSSR: SERIYA METALLY in Russian No 5,
Sep-Oct 91 (manuscript received 30 Aug 90) pp 22-26

[Article by V.Ya. Dashevskiy, A.M. Katsnelson, D.L. Maslov, A.D. Chizhikov, and V.I. Kashin, Moscow]

UDC 669.743.2

[Abstract] One possible method of the reduction refining of manganese ferro alloys to remove phosphorus and sulfur is to process the said alloys with calcium and calcium carbide. In previous communications, the authors have reported the results of their research on the systems Mn-P and Mn-S. In a continuation of this line of research herein, they have performed a thermodynamic analysis of the reaction of calcium and calcium carbide with phosphorus and sulfur dissolved in manganese-based melts. They have demonstrated that processing the manganese-based melts with calcium and calcium carbide results in comparatively low concentrations of phosphorus and very low concentrations of sulfur in the final metal. They focused their experiments on the simultaneous dephosphorization and desulfurization of the said melts by the two forms of calcium. In the case of calcium, the degree of dephosphorization was found to depend on the starting content of phosphorus: Dephosphorization reached 35% when the starting phosphorus content was between 0.35 and 0.40%, and the degree of desulfurization was between 60 and 80%. In the case of calcium carbide, the degree of dephosphorization was found to depend on the doping technique used and reached 65%. The degree of desulfurization ranged from 90 to 95%. Dissolution of carbon in the metal occurred during the calcium carbide processing. For this reason, the authors concluded that the use of calcium carbide to remove phosphorus and sulfur from manganese alloys is feasible in the case of both low- and medium-carbon melts. Overall, the results of the experiments performed were in rather good agreement with thermodynamic analysis data. Figures 3, tables 3; references 12: 10 Russian, 2 Western.

Assessment of Information Value of Nondestructive Testing Methods Used in Shipbuilding and Flaw Detection

927D0043C Sverdlovsk DEFEKTOSKOPIYA in Russian No 4, Apr 91 pp 87-94

[Article by M.V. Rozina, L.M. Yablonik, Prometey, Leningrad]

UDC 620.179

[Abstract] The use of probabilistic reliability or efficiency indicators for comparing and optimizing nondestructive testing systems in order to make a decision on whether to accept or reject an item, particularly in shipbuilding, is addressed and the need to develop an approach to estimate the information value of various nondestructive testing system is recognized. It is suggested that Shannon's entropy estimate of information quantity used in measurement methods be used to calculate the information content value of flaw detection in shipbuilding. In contrast to the probabilistic estimates of reliability, the information content value estimate makes it possible to characterize the nondestructive testing system's ability to detect flaws reliably while at the same time conveying the information about their

parameters, primarily the size, type, and orientation. Engineering methods of information content value analysis are developed for different types of nondestructive testing. The method of ultrasonic testing of the anticorrosion hard-facing is used to illustrate the evaluation of measurement information. It is shown that the information value estimate of nondestructive testing systems is especially efficient for items where more than two alternative decisions may be made on the basis of the nondestructive testing results. References 11: 10 Russian, 1 Western.

Methods and Facilities of Composite Material Quality Control

927D0043B Sverdlovsk DEFEKTOSKOPIYA in Russian No 4, Apr 91 pp 77-87

[Article by I.G. Matiss, Polymer Mechanics Institute at the Latvian Academy of Sciences]

UDC 620.179

[Abstract] The need to improve the physical and mechanical properties of composites (KM) with help of new reinforcing and binding materials, improving the reinforcement configuration, forming hybrid structures, etc., necessitated by the expanding applications of composites is identified and it is shown that such improvement may be attained only if new methods and facilities of quality control and load-carrying capacity diagnostics of structures and products from composites are developed. The findings of applied research carried out at the Polymer Mechanics Institute at the Latvian Academy of Sciences in this field are summarized and examples of new instrument for monitoring the ultrasonic (u.z.), thermal, electric, and mechanical characteristics of composites are described. Studies aimed at developing the methods and facilities of acoustic and dielectric spectrometry are described. The studies are carried out in two stages: examining the effect of various composite manufacturing conditions and structural parameters on the load-carrying capacity (i.e., ascertaining the so-called relevant factors) by phenomenologically statistical methods and then developing the methods and devices of nondestructive testing for the relevant factors thus established. The need to use real-time computer routines for this purpose is identified. Figures 11; tables 2; references 12: 10 Russian, 2 Western.

General and Particular Patterns of Eddy Current Testing Theory

927D0043A Sverdlovsk DEFEKTOSKOPIYA in Russian No 4, Apr 91 pp 71-76

[Article by Yu.M. Shkarlet, Moscow]

UDC 620.179.14

[Abstract] Efforts of leading experts in Germany, the United States, and the USSR in the field of electromagnetic methods and devices of nondestructive testing, primarily in addressing the issue of the interaction of eddy current transducers (VTP) with various test objects

(OK) are outlined and it is noted that since most of these efforts are not coordinated, there is no satisfactory unity of the physical patterns, generalized parameters, or sound techniques for extending the findings to non-standard problems. Consequently, ways are outlined for developing a theory of nondestructive eddy current testing from a unified position. To this end, a general concept of representing the system of eddy current pickups and test object by a system of magnetically coupled coils is considered and a unified system of physically sound generalized parameters is proposed; the study is limited to nonferromagnetic materials. The solenoid coil and inside coil methods of eddy current testing of tubes as well as other examples are considered. The study is dedicated to Academician M.N. Mikheyev. The author is soliciting offers of cooperation. Figures 9.

Analysis of Magnetic Field Restoration Method Capabilities With Respect to Magnetic Nondestructive Testing. I.

927D0044A Sverdlovsk DEFEKTOSKOPIYA in Russian No 5, May 91 pp 33-38

[Article by A.S. Shleyenkov, R.S. Melnik, L.N. Krotov, V.Ye. Shcherbinin, Institute of Physics of Metals at the Urals Department of the USSR Academy of Sciences and Perm Polytechnic Institute]

UDC 620.179.14

[Abstract] The shortcomings of computer-aided tomography in the field of X-ray and ultrasonic (u.z.) nondestructive testing (NK) for discontinuities are addressed and the need for developing and analyzing the method of magnetic field reconstruction is identified. The task of reconstruction is a classical incorrect problem since the scalar potential of the magnetostatic field of the defect in the air is a harmonic function. In order to estimate how well a truncated series of harmonic polynomials represents the field potential and make recommendations for placing the specific magnetic pickups, one has to consider certain problems of magnetic field reconstruction from sources whose functional relationships are already known. Since the scalar potential of the flaw's static magnetic field in the air depends on its configuration and dimensions, it would be possible to identify telltale signs by reconstructing the field in a certain area and then determine the configuration and size. The authors are grateful to A.B. Zolotovitskiy for discussing the effort, giving valuable advice, and helping to improve it. References 21: 20 Russian, 1 Western.

Demagnetizing Factor's Effect on Harmonic Magnetization Components of Cyclically Magnetized Ferromagnetic Cores. I. Analysis

927D0044D Sverdlovsk DEFEKTOSKOPIYA in Russian No 5, May 91 pp 61-69

[Article by Yu.F. Ponomorev, Institute of Physics of Metals at the Urals Department of the USSR Academy of Sciences]

UDC 620.179.14

[Abstract] The effect of the magnetizing factor on the type of valuated static magnetic hysteresis loops of rod-type cores is examined on the basis of a function describing the magnetization reversal curve of the substance while the static magnetization reversal curve of the core is plotted allowing for the demagnetizing field from induced fictitious magnetic charges on the core surface. An analysis shows that as the demagnetizing factor rises from 0 to 1, core magnetization reversal curves approach the simplest piecewise-linear anhytetic approximation regardless of the material's magnetic hysteresis type. The amplitudes and phases of the first, third, and fifth harmonics of the secondary electromotive force (eds) are calculated under the effect of a sinusoidal magnetic field on the core. For the material under study, the number of independent variables for the harmonic components of the secondary emf is three and for rod-like cores it rises to four. Figures 5; references 13.

Demagnetizing Factor's Effect on Harmonic Magnetization Components of Cyclically Magnetized Ferromagnetic Cores. II. Nondestructive Testing Applications

927D0044E Sverdlovsk DEFEKTOSKOPIYA in Russian No 5, May 91 pp 70-79

[Article by Yu.F. Ponomorev, Institute of Physics of Metals at the Urals Department of the USSR Academy of Sciences]

UDC 620.179.14

[Abstract] Magnetic methods of nondestructive testing are classified briefly into three categories: deterministic, formally correlational, and combined methods; on this basis, the procedure for assessing the capabilities of nondestructive testing of products with a high demagnetizing factor by the method of higher harmonics is formulated. To this end, a simplified mathematical model of the magnetization reversal curve is used; despite the fact that it imposes constraints on the validity of the results important for practical applications, it obviously increases the deterministic element of the higher harmonic method. Quality control of rolling-contact bearings' ball and roller hardening is used to illustrate the procedure. A method of determining the optimal alternating magnetic field amplitude is described. It is shown that the nondestructive testing method's capabilities are limited primarily not by the dependence of the magnetic parameters on the hardening temperature but by the dependence of the non-dimensional parameter on the hardening temperature; moreover, given a zero demagnetizing factor, testing of products from steel ShKh15SG by the higher harmonic method is equivalent to the magnetic susceptibility method. Figures 3, tables 3, references 7.

Surface Examination of Condensed Systems by Photoelectron Spectroscopy Methods*927D0044C Sverdlovsk DEFEKTOSKOPIYA in Russian No 5, May 91 pp 54-60*

[Article by V.A. Trapeznikov, Engineering Physics Institute at the Urals Department of the USSR Academy of Sciences]

UDC 535.215+543.422

[Abstract] Siegbahn's contribution to the development of the electron spectroscopy method and the work of his colleagues in the USSR, particularly in the Urals, in this field are recognized; the role played by M.N. Mikheyev in developing the first domestic X-ray magnetic spectrometers is mentioned. The advantages of the electron spectroscopy methods in investigating the surface of solids in the crystal and amorphous state and liquid melts with the help of special instruments, e.g., magnetic electron spectrometers, over other methods are discussed and the possibility of examining and testing rapidly passing processes on the surface of various materials by the method of pulsed electron spectroscopy is considered. It is shown that the sensitivity of the pulsed electron spectroscopy method is higher by 3-4 orders of magnitude than that of conventional methods and magnetic electron spectrometers with a large electron orbit radius (up to 100 cm) have a higher resolution, making it possible to shorten the spectrum measurement time considerably. Combined with the use of multianode microchannel plates, the method makes it possible to expand the range of traditional surface examinations within the milli- and microsecond time span and opens up new opportunities for studies in kindred fields, e.g., in nuclear physics for estimating the lower bound of electron neutrino mass on the basis of tritium β -decay. Figures 2; references 24: 23 Russian; 1 Western.

Development of Methods and Devices of Nondestructive Testing of Welded Joints and Techniques for Assessing Their Quality Indicators*927D0044B Sverdlovsk DEFEKTOSKOPIYA in Russian No 5, May 91 pp 47-54*

[Article by V.F. Davidenko, V.A. Troitskiy, Electric Welding Institute imeni Ye.O. Paton, Kiev]

UDC 620.170.16

[Abstract] Nondestructive testing management practices abroad whereby a specialized firm provides the service upon request is evaluated and it is shown that this method may be implemented in the USSR. The conditions for setting up specialized nondestructive testing (NK) enterprises are outlined and the experience accumulated in the field of nondestructive testing at the Electric Welding Institute (IES) imeni Ye.O. Paton, primarily in the area of acoustic inspection methods and techniques for estimating the qualitative characteristics, which is applicable under the conditions of new economic relations among the producers and consumers is summarized. In particular, the possibilities of sonic

testing and insonifying of welded joints in order to obtain data on the coordinates of the points on the surface of the flaw are investigated and methods of processing these data for plotting an ultrasonic (u.z.) image of the defects are suggested. Procedures are developed for estimating the errors and confidence of the ultrasonic nondestructive tests results. In addition to sonic testing using the acoustic air jet method (PSA), radiographic testing and X-ray TV inspection (RTK) methods are considered.

Analysis of Magnetic Field Reconstruction Method Possibilities With Respect to Nondestructive Magnetic Field Testing. III*927D0045A Sverdlovsk DEFEKTOSKOPIYA in Russian No 6, Jun 91 pp 34-42*

[Article by A.S. Shleyenkov, L.N. Krotov, R.S. Melnik, V.Ye. Shcherbinin, Institute of Physics of Metals at the Urals Department of the USSR Academy of Sciences and Perm Polytechnic Institute]

UDC 620.179.14

[Abstract] Continuing the studies described in the previous issue, the potential of the dipole magnetic field and leakage field over a discontinuity flaw on the ferromagnetic material's surface is represented as a series of harmonic polynomials. It is shown that there is no need to increase the number of sensors and that four pickups are sufficient for reconstructing the field in a certain region. Thus, the magnetostatic field components of a flaw with a random configuration can be reconstructed as a section of a harmonic polynomial series whose coefficients can be found most efficiently with the help of the fast Fourier transforms on the basis of known field components. The use of the magnetic field reconstruction method in nondestructive testing makes it possible to significantly increase the information content value of magnetic measurements with the optimum transducer positioning and obtain new indirect symptoms conveying information about the parameters of the magnetic disturbance source. Figures 8; tables 4; references 5.

Experimental Investigation of Ultrasound Velocity and Attenuation in Aqueous Saline Solutions*927D0045F Sverdlovsk DEFEKTOSKOPIYA in Russian No 6, Jun 91 pp 90-92*

[Article by A.K. Brovtsyn, A.G. Akimov, M.S. Gadzhiev, Obninsk Nuclear Power Institute]

UDC 620.179.16

[Abstract] The dependence of ultrasound attenuation on the concentration of salts in aqueous solutions at various temperatures and the dependence of ultrasound velocity on the salt concentration in aqueous solutions are plotted and the design of the special unit for investigating these characteristics is presented. In addition, the solubility of K_2CO_3 , K_2CrO_4 , Na_2CO_3 , $NaCl$, and $CaCl_2$ at 20°C and the molecular mass of these salts are

measured. An analysis demonstrates that the dependence of the ultrasound velocity and attenuation in medium-concentration solutions (i.e., up to 7%) is virtually linear while at concentrations above 7%, the dependence of the ultrasound velocity and attenuation is nonlinear. The ultrasound velocity is measured by an UD2-12 nondestructive flaw detector with a 1-2% accuracy while attenuation is measured by PEP P11-2.5-K-20-002 pickups at a 2.5 Mhz frequency with a ± 0.1 dB accuracy. Figures 3; tables 1; references 2.

Infrared Method of Testing Soldered Printed Circuit Board Connections

927D0045E Sverdlovsk DEFEKTOSKOPIYA in Russian No 6, Jun 91 pp 73-78

[Article by A.S. Oleynik]

UDC 620.179.13

[Abstract] The reliability and quality of soldered printed circuit board connections are largely determined by the soldering process level and testing reliability while the soldered connection quality assessment objectivity calls for using nondestructive testing methods; consequently, the relationship of the soldering process conditions and the level of infrared irradiation of these soldered connections with the help of an infrared radiometry microscope is investigated in order to develop a nondestructive testing procedure. A method of measuring infrared radiation from the thermal field of soldered connections is described and infrared profiles of soldered connections made with various departures from standard process conditions are plotted and analyzed. It is shown that infrared profile variations are uniquely related to soldered connection defects. The infrared nondestructive testing method makes it possible to increase the soldered connection reliability on printed circuit boards. In addition, the testing method may be used for testing planar electronic circuits and chips since their infrared profile is a function of the electric and thermal coupling of the circuit elements. Figures 4; tables 1; references 3: 2 Russian, 1 Western.

Method of Measuring Effective Dielectric Constant of Inhomogeneous Sheet Materials in Microwave Band

927D0045D Sverdlovsk DEFEKTOSKOPIYA in Russian No 6, Jun 91 pp 64-69

[Article by A.A. Kalachayev, I.V. Kukolev, S.M. Matytsin, K.N. Rozanov, A.K. Sarychev, High Temperature Institute at the USSR Academy of Sciences]

UDC 621.317

[Abstract] Interest in examining effective electrophysical properties of materials containing spatial irregularities whose dimensions are commensurate with the radiation wavelength, e.g., composite materials (KM) with conducting inclusions, is due primarily to the manifestations of unusual electrophysical properties, particularly an unusual behavior of the dielectric constant. A method of

measuring effective values of the complex dielectric constant of sheet materials whose spatial irregularities are comparable in size to the wavelength in the microwave band (SVCh), including composites, is proposed. In so doing, the issue of the correctness of describing the properties of composites with such inhomogeneities is not discussed. The method is based on measuring the magnitude of electromagnetic wave reflectance R from the sample and the planar metallic screen placed behind it as a function of the distance d between them and finding the complex dielectric constant from the measured $R(d)$ dependence by nonlinear programming methods. When using panoramic voltage standing wave ratio (KSVN) meters, the measurement error does not exceed 10%. The method's applicability range is estimated as 0.5-4. The experimental values are found to be consistent with the results obtained from existing theoretical models. Figures 1; references 9.

Measuring X-Ray Image Parameters During Radiographic Inspection of Steel by MIRA-2D Pulsed X-Ray Units

927D0045C Sverdlovsk DEFEKTOSKOPIYA in Russian No 6, Jun 91 pp 56-63

[Article by Yu.V. Gromov, Yu.V. Gorbatov, Montazhspeystroy All Union Scientific Research Institute]

UDC 620.179.15

[Abstract] The use of MIRA-2D portable X-ray units which generate radiation pulses with a 10^{-8} s duration and a 12-15 Hz repetition frequency for nondestructive testing (NK) of various types of steelwork during erection and the difficulty of selecting the best radiographic conditions for obtaining a good image on film are discussed. The main pulse parameters are the most important factors affecting the tested entity's X-ray image quality while the contrast of the direct shadow image determining the detectability of flaws and the radiation dose in the film plane depend primarily on the damping factor and cumulative radiation factors. The damping factors of broad and narrow pulsed beams from the MIRA-2D unit in steel parts up to 20 mm thick are measured experimentally; the results make it possible to determine the X-ray image parameters for radiographic inspection of welded joints as well as calculate the exposures of various types of film. It is shown that the use of high gamma films increases the radiation image contrast and facilitates the detection of small flaws. Figures 3; tables 2; references 9: 8 Russian, 1 Western.

Radiographic Testing of Steam Turbine Weld Root in Hot State

927D0045B Sverdlovsk DEFEKTOSKOPIYA in Russian No 6, Jun 91 pp 50-56

[Article by S.V. Shablov, V.I. Kapustin, V.B. Nazaruk, Scientific Production Association of the Central Scientific Research Institute of Machine-Building Technology]

UDC 620.179.15

[Abstract] The importance of testing the root of the steam turbine rotor weld produced by argon-arc welding in a protective gas medium while it is hot and is accessible for removing defects is emphasized. Radiographic testing (RK) must therefore be performed in a hot state (GS), so the testing procedure is characterized by the simultaneous effect of ionizing radiation and high temperature on the radiographic film; consequently, an attempt is made to develop a radiographic method of testing the steam turbine rotor weld root in the hot state. To this end, the following parameters are investigated: the testing technique, the focal distance, the size of the radioactive nuclide's active part, the type of the radio-nuclide source, and radiographic film's sensitometric characteristics. The characteristics of the radiation image development with subsequent enhancement of the optical image density by using the silver dispersion method are examined. The results indicate that it is expedient to use radionuclide sources with a 3.0x3.0 mm active part and that the testing procedure must be shortened to 18-30 min to minimize the film exposure by amplifying the optical image. This ensures that the film retains its sensitometric and physical and mechanical properties in the hot state. The use of the procedure makes it possible to detect weld flaws of 0.5 mm in size. Figures 5; references 4.

The Evolution of Thermal and Electromagnetic Perturbations in Composite Superconductors

927D00221 Kiev *METALLOFIZIKA in Russian* Vol 13 No 8, Aug 91 (manuscript received 8 Apr 91) pp 109-111

[Article by N.A. Taylanov, Dzhizak affiliate, Tashkent Polytechnic Institute]

UDC 537.312.8

[Abstract] The author of the study reported herein examined the evolution of thermal and electromagnetic disturbances in the critical state of composite superconductors of the second type. Specifically, he examined a superconducting cylindrical specimen with the radius R located in an external magnetic field of $H = (0, 0, H_z)$ increasing at a constant rate of $\delta H/dH = \text{const}$. In this particular formulation of the problem, the most "dangerous" perturbation from the standpoint of the stability of the critical state is that of unidimensional perturbations of T and E that are dependent on the radial portion of the cylindrical coordinate system. After solving a series of equations the author concludes that value of the critical field (H_c) amounts to 10^4 Oe and the maximum radius of the cylinder (R_m) is 10^{-2} cm. References 2 (Russian).

Magnetic Film Metal Oxide Heterostructures on an Aluminum Surface

927D0022H Kiev *METALLOFIZIKA in Russian* Vol 13 No 8, Aug 91 (manuscript received 1 Apr 91) pp 105-109

[Article by V.G. Shadrov, A.V. Boltushkin, A.V. Semeshko, R.I. Tagirov, and V.P. Korolev, Solid-State Physics and Semiconductors Institute, BSSR Academy of Sciences, Minsk]

UDC 620.197:669.71

[Abstract] The authors of the study reported herein examined film metal oxide heterostructures produced by electrochemical deposition of metals of the Fe group into the pores of an anodic oxide film formed on the surface of AD-1 aluminum by anodizing in a sulfuric acid electrolyte. They also studied the effect of isothermal annealing on the properties of the said heterostructures. The thickness of the anodic oxide film was varied between 5 and 20 μm by varying the anodizing time between 10 and 40 minutes. The electrochemical deposition of the metals was implemented by using a current of variable polarity (50 Hz) and a terminal voltage of 14 to 17 V. The metals were precipitated from electrolytes based on sulfates of the respective metals at 18 to 23°C. The amount of metal deposited into the pores of the anodic oxide films was determined by the photocolormetric method. The films' structure was studied by using a DRON-2 x-ray diffractometer and Jeol-100 CX scanning microscope, and their magnetic characteristics were studied by using a vibration magnetometer in fields up to 1,200 kA/m. The annealing was performed at temperatures up to 270°C in a vacuum of 10^{-5} mm Hg. The studies performed indicated that the content of metals deposited in the pores of the anodic oxide films depends on the film thickness, the nature of the metal, and the deposition conditions and ranges from 0.03 to 0.14 mg/cm². When all other deposition conditions are kept equal, the content of metal in the pores increases in the order Ni, Co, Fe. The content of Al and O in the test films amounted to 30 and 60 atomic percent respectively (i.e., the Al and O atoms were in a 1:2 ratio). The diameter of the acicular metal particles deposited in the pores was found to be between 15 and 30 nm. It was discovered that the diameter of the metal particles could be controlled by changing the pore diameter. This could be done either by varying the anodizing conditions or else by using different chemical methods of treating the already-formed anodic oxide films. The studies performed demonstrated that the coercive force of coatings as measured along the normal is determined by the diameter of the pores and is virtually independent of the cell diameter. The coercive force of the coatings was also found to depend on the angle of remagnetization of the films. The changes discovered to occur in the films' magnetic characteristics during annealing were attributed to the perfection of the crystalline structure of the acicular particles and to an increase in their effective magnetic separation due to (1) bonding of the excess oxygen in the oxide film primarily along the cell boundaries and (2) the formation of fine-crystal regions of $\gamma\text{-Al}_2\text{O}_3$ and a redistribution of the anions in the amorphous matrix of the anodic oxide. Figures 2, table 1; references 11: 3 Russian, 8 Western.

Investigation of the Process of Annealing the Alloy AMg6 by Using Acoustic Emission

927D0022G Kiev *METALLOFIZIKA in Russian* Vol 13 No 8, Aug 91 (manuscript received 28 Mar 91) pp 101-104

[Article by A.V. Kozlov, G.I. Prokopenko, V.A. Glyva, and G.I. Kuzmich, Metal Physics Institute, UkSSR Academy of Sciences, Kiev]

UDC 669.715:539.374

[Abstract] The acoustic emission of a preliminarily deformed and then annealed specimen of the alloy AMg6 is nonmonotonically dependent on the duration of the annealing. A great number of works have investigated the processes occurring in metals and alloys during heating after preliminary plastic deformation. In a continuation of this line of research, the authors of the study reported herein examined the effect that short-term and protracted annealing of deformed AMg6 aluminum alloy has on the parameters of the said alloy's acoustic emission during subsequent stretching of the specimens. Plane specimens of AMg6 with working section dimensions of $30 \times 3 \times 2$ mm were annealed at 623 K for 2 hours. Immediately thereafter, the specimens were subjected to tension tests on an IMASH 20-78 testing machine. As the specimens were stretched by 4% at a rate of $1.5 \times 10^{-3} \text{ s}^{-1}$, the activities and amplitudes of the acoustic emission signals radiated by the test specimens were recorded along with the total number of pulses during the deformation period. Wideband sensors providing a sensitivity on the level of $15 \mu\text{V}$ were used. After 4% stretching the specimens were again annealed at 623 K for various periods ranging from 2 minutes to 2 hours. The different batches of specimens were again stretched, and their acoustic emission parameters were again recorded. Electron microscopy studies (using a Tesla BS-540 electron microscope) were then performed on the specimens. The specimens' acoustic emission was found to initially increase as the holding time was increased. This was linked to a reduction in the density of the linear and point defects and to the resultant increase in the free run of the dislocations and in the rate at which the moving dislocations were generated. A process of coagulation of the particles of the β -phase Al_3Mg_2 was also found to occur as the holding time was increased. The electron microscopy studies revealed that the large particles of the second phase (diameter, $\geq 1 \mu\text{m}$) underwent a significant increase in size as the annealing time was increased. The small particles ($d < 0.3 \mu\text{m}$) remained virtually unchanged, although they did serve as barriers to the moving dislocations. The simultaneous occurrence of these two processes during heating was found to result in a nonmonotonic dependence of the acoustic emission parameters on the holding time of preliminarily deformed specimens. Initially, the defects formed during the course of the preliminary deformation underwent an intensive redistribution and decrease in density. Then, as the annealing time increased, consolidation of the particles of the second phase appeared to be the decisive mechanism of the occurrence of emission. The occurrence of this stage was accompanied by a reduction in the specific area of those boundaries that were impermeable to the dislocations. Figures 2; references 7: 5 Russian, 2 Western.

Hyperfine Structure of $\text{Fe}_{85-x}\text{Co}_x\text{B}_{15}$ Amorphous Alloys After Irradiation With γ -Quanta

927D0022F Kiev METALLOFIZIKA in Russian Vol '3 No 8, Aug 91 (manuscript received 3 Dec 90; after revision 26 Jun 91) pp 75-80

[Article by V.M. Shkapa, V.V. Polotnyuk, A.M. Shalayev, and S.P. Likhtorovich, Metal Physics Institute,

UkSSR Academy of Sciences, Kiev, and G. Vlasak, Physics Institute, Electrophysics Research Center, Slovak Academy of Sciences, Bratislava]

UDC 539.213:620.18

[Abstract] The authors of the study reported herein used the methods of γ -resonance spectroscopy and electron-positron annihilation to examine $\text{Fe}_{85-x}\text{Co}_x\text{B}_{15}$ ($x = 12, 15, 17, 21$, and 25) amorphous alloys in their initial state and after irradiation with γ -quanta. The said metal alloys were produced by the method of hardening a plane stream in the form of a strip 10 mm wide and about 25 μm thick. The test specimens were subjected to γ -irradiation with an energy of 1.2 MeV in a dose of $2.5 \times 10^5 \text{ K/kg}$ and at a temperature not exceeding 60°C . All measurements were taken at a temperature of 20°C . Mossbauer spectra of the specimens were taken on a YaGRS-4M unit with a Cr^{57}Co source. The studies performed provided a basis for concluding that the amorphous alloys studied likely contain regions with a qualitatively different local atomic structure, each reacting differently to γ -irradiation. Specifically, the study alloys likely contain regions that are relatively well ordered and regions saturated with free space, i.e., regions that are relatively disordered. Figures 3; references 14: 6 Russian, 8 Western.

Experimental Observation of the Deviation of the Direction of an Energy Flux From a Reflecting Plane During the Anomalous Passage of X-Rays Through a Crystal

927D0022E Kiev METALLOFIZIKA in Russian Vol 13 No 8, Aug 91 (manuscript received 23 Apr 91) pp 71-75

[Article by I.F. Zvorygin, L.V. Tikhonov, G.V. Kharova, Metal Physics Institute, UkSSR Academy of Sciences, Kiev]

UDC 548.732:539.2

[Abstract] The authors of the study reported herein conducted a series of experiments examining the deviation of an energy flux in a crystal from the reflecting plane in the case of the anomalous passage of x-rays through the crystal. A perfect germanium monocrystal containing single growth dislocations intersecting a plane-parallel plane from one of its surfaces to the other was used as the study object. To exclude the effect of all factors other than diffraction, the researchers decided to use different orders of reflection by one and the same crystallographic plane of the type (110). A two-crystal scheme was used to exclude the effect of multiwave diffraction. In this article the authors present topograms of the dislocation images obtained at the reflexes 022 and 044 along with an example of graphic determination of the deviation of an energy flux from a reflecting plane by the characteristic meridian method. The experiments performed indicated that for a germanium crystal approximately 0.5 mm thick, the energy flux deviation from the reflecting plane due to Laue diffraction geometry amounts to approximately 2° for a reflection of 220. For a reflection of 440 it is approximately 15° . The first

result (2°) was found to conform to the result obtained by theoretical calculation; the second result (15°) was somewhat higher than the calculated value. This discrepancy was attributed to the fact that the actual center of the image was determined during the experiments whereas in the computations it was calculated for the average and the energy flux was maximal. The fan width of the energy fluxes was found to conform to data obtained by computer simulation. The study results are deemed important for application in precision x-ray topography and for use in obtaining a deeper understanding of the dynamic scattering of radiation by real crystals. Figures 2, table 1; references 5 (Russian).

Diffusion of Bismuth in the High-Temperature Superconducting Ceramics $\text{YBa}_2\text{Cu}_3\text{O}_{7-x}$ and $[\text{Pb}_x\text{Bi}_{1-x}]_2\text{Ca}_2\text{Sr}_2\text{Cu}_3\text{O}_y$

927D0022D Kiev METALLOFIZIKA in Russian Vol 13 No 8, Aug 91 (manuscript received 3 Jun 91) pp 62-66

[Article by P.P. Gorbik, M.V. Bakuntseva, and G.M. Shalyapina, Surface Chemistry Institute, UkSSR Academy of Sciences, Kiev]

UDC 537.312.539

[Abstract] The authors of the study reported herein used the radioactive indicator method to study the diffusion of bismuth in the high-temperature superconducting ceramics [HTSC] $\text{YBa}_2\text{Cu}_3\text{O}_{7-x}$ and $[\text{Pb}_x\text{Bi}_{1-x}]_2\text{Ca}_2\text{Sr}_2\text{Cu}_3\text{O}_y$ in the temperature interval from 200 to 500°C. The study $\text{YBa}_2\text{Cu}_3\text{O}_{7-x}$ was produced from ultrapure Y_2O_3 , BaCO_3 , and CuO powders in a 1-2-3 composition. The powder charge was ground and mixed in a ball mill and then subjected to annealing for 30 hours at 850°C in an oxygen current. After annealing, the powder was pressed into tables 10 mm in diameter and 1-2 mm thick under a pressure of 30 kbar. It was then sintered in an oxygen atmosphere at 950°C for 10 hours. The specimens were cooled at a rate of about 200°C/h to 400°C, held at that temperature for 3 hours, and then cooled to room temperature at a rate of about 50°C/h. The study $[\text{Pb}_x\text{Bi}_{1-x}]_2\text{Ca}_2\text{Sr}_2\text{Cu}_3\text{O}_y$ was produced from ultrapure PbO , Bi_2O_3 , CaCO_3 , SrCO_3 , and CuO powders. The powders were mixed and homogenized, and the resultant charge was heat-treated at 800°C for 16 hours and then pressed into cylindrical blanks. The blanks were subjected to solid-phase synthesis at 854°C in an air atmosphere. The synthesis temperature was regulated with a precision of $\pm 0.1^\circ\text{C}$ continuously for 324 hours. The study HTSC were subjected to x-ray phase analysis [RFA], x-ray spectral microanalysis, and phase contrast studies. RFA of the $\text{YBa}_2\text{Cu}_3\text{O}_{7-x}$ revealed it to be a single-phase system with an orthorhombic structure. It was found to have a granular structure with a mean crystallite size of 5 to 20 μm . Chemical analysis confirmed that the grains conformed to a 1-2-3 phase, and no significant deviations in chemical composition were detected at the intergrain boundaries. The $[\text{Pb}_x\text{Bi}_{1-x}]_2\text{Ca}_2\text{Sr}_2\text{Cu}_3\text{O}_y$ was found to be a single-phase system, with the phase 2223 constituting at least 95% of its volume. ^{207}Bi -tagged nitric acid was used

for the radioactive indicator analysis of both ceramics. The analysis indicated that the surface mechanism of diffusion is dominant in both ceramics. After plotting the temperature dependences of the diffusion coefficient of bismuth in each of two study HTSC (which each possess different physicochemical properties from the other), the authors concluded that the diffusion parameters D_0 and E_a (activation energy) are only weakly dependent on the type of HTSC. This led them to conclude that there must be some factor determining the nature of bismuth diffusion in the two ceramics and leveling out of the differences between the two ceramics. They hypothesized that this factor may be the polycrystalline structure of the two materials. As confirmation of this hypothesis they cited their observation that the temperature dependences of the diffusion coefficient are linked to the migration of bismuth along the intergrain boundaries and surface of the pores of the two study HTSC. Figure 1; references 17: 13 Russian, 4 Western.

Nature of the Shape Memory Effect in Fe-Mn-Si Alloys

927D0022C Kiev METALLOFIZIKA in Russian Vol 13 No 8, Aug 91 (manuscript received 19 Feb 91; after revision 21 Jun 91) pp 43-51

[Article by Ye.Z. Vintaykin, A.A. Gulyayev, A.B. Oralbayev, N.A. Polyakova, and Ye.L. Svistunova, Central Scientific Research Institute of Ferrous Metallurgy]

UDC 669.15.112.227.34

[Abstract] The authors of the study reported herein examined the nature of the shape memory effect in Fe-Mn-Si alloys. Specifically, they studied two series of Fe-Mn-Si alloys. In the first series, the Mn content was varied from 26 to 36% (by mass), and in the second series, the Si content was varied from 0 to 6.5%. The alloys were produced in an open induction furnace, subjected to coking at 1,100°C in blank and bar form, and rolled into sheets at the same temperature. The study specimens were hardened from 1,000°C in water and then subjected to mechanical tests on an Instron-type machine. They were then subjected to x-ray structural studies on a DRON-3 using FeK_α radiation and to dilatometry studies and two structural studies on a Neofot-2 light microscope and BS-540 electron microscope. The studies performed established that the shape memory effect observed in the study specimens is caused by several factors. Included among these are blocking of the $\gamma \rightarrow \alpha$ (and $\epsilon \rightarrow \alpha$) transformations, the strength of the austenite, the magnitude of the packing defect energy, the bulk effect of the reversible γ - ϵ transformations, the temperature of the initial Martensite transformation, and the Neel point. The maximum degrees of shape restoration and shape restoration stress characterizing thermomechanical return during the occurrence of the shape memory effect were observed to occur at an Mn content of about 30% and an Si content of about 5.5%. Figures 6, tables 2; references 9: 1 Russian, 8 Western.

The Effect of the Dispersivity of an Alloy's Phase Structure on the Depth of a Laser's Effect on the Alloy

927D0022B Kiev *METALLOFIZIKA in Russian* Vol 13 No 8, Aug 91 (manuscript received 25 Jan 91) pp 34-42

[Article by O.M. Ivasishin, P.Ye. Markovskiy, A.F. Zhuravlev, and I.I. Obozhin, Metal Physics Institute, UkSSR Academy of Sciences, Kiev]

UDC 539.385

[Abstract] The authors of the study reported herein examined the effect that the dispersivity of the initial structure of the two-phase titanium alloys VT6 and VT23 have on the depth to which the alloys are affected by the action of a laser operating in a pulsed mode. Commercial-grade VT6 and VT23 alloys were subjected to preliminary heat treatment to produce different sizes of β -grains and intragrain α -phases of different geometries and sizes. The single-phase α -alloy VT1-0 in a broad range of grain sizes was also studied for the sake of comparison. The test and control specimens were subjected to pulsed laser radiation from a Kvant-18m laser with an energy density of $W = 5$ and 7 J/mm^2 . To keep the scattering of the light energy to a minimum the specimens were treated with M40 abrasive paper and subsequently coated with a 5% solution of picric acid. The depth of the fused layer on each specimen was determined by using end sections and the metallographic method. As a result of the studies performed, the authors were able to establish that the thickness of the fused zone is a nonmonotonic function of the size of the crystals of the starting α -phase. They hypothesized that this dependence is the result of intensification of the chemical inhomogeneity of the high-temperature β -phase formed during polymorphous transformation under conditions of laser heating as the α -crystals become coarser. They proceeded to propose a model for use in calculating the possible contribution of the following thermophysical parameters to the change in depth of fusion as a function of the dispersivity of the starting structure: reflection factor, melting temperature, heat conduction, latent heat of polymorphous transformation, and melting. Figures 5, tables 2; references 12: 10 Russian, 2 Western.

Vacancies in AuCu-Type Ordered Alloys

927D0022A Kiev *METALLOFIZIKA in Russian* Vol 13 No 8, Aug 91 (manuscript received 12 Nov 90) pp 22-26

[Article by A.A. Smirnov, Metal Physics Institute, UkSSR Academy of Sciences, Kiev]

UDC 539.21:536.42

[Abstract] The author develops a theory of ordered alloys of the AuCu type containing sublattice vacancies of the first and second types of node. He derives equilibrium equations for the distribution of the concentrations c_1

and c_2 of these vacancies and the long-range order parameter. He also derives the temperature dependence of the quantities c_1 and c_2 at rather low temperatures corresponding to the absence of residual vacancies (i.e., those vacancies remaining at absolute zero). At low temperatures the distribution of vacancies throughout the sublattices may be very uneven and may have a layered appearance. In other words, they may appear as parallel atomic planes containing alternately large and small concentrations. Figures 2; references 9: 8 Russian, 1 Western.

Automated System for Monitoring, Documenting, and Analyzing Rail Quality

927D0019A Moscow *STAL in Russian* No 8, 91 pp 49-52

[Abstract of article by V. F. Tsarev, A. Ye. Koshelev, G. Ya. Anisimov, V. K. Butorin, and Ye. A. Shchelokov, Kuznets Metallurgical Combine and the Novokuznets branch of the Promavtomatika State Institute of Design Engineering]

UDC 621.771.26:658.012.011.56

[Abstract] An automated system for monitoring, documenting, and analyzing rail quality has been developed. The new system is organized along the lines of the old "manually" administered system, but it automates and centralizes all functions related to rail quality-control data processing and utilization. The system, which operates in MS-DOS with SUBD RBASE 2.1, is made up of a network of five PC/XT and PC/AT computerized user-friendly workstations connected to a central computer. The system tracks rails through all stages of the quality control process 24 hours a day. Quality-control information from the reports filled out by the quality-control inspectors is entered into the data base at least four to five times per shift by a data entry operator working at one of the workstations. The other four workstations are utilized by the inventory/invoicing department, shipping, the quality-control inspector, and the senior quality-control inspector. Users can retrieve information at specified intervals or upon request. The system is equipped with a magnetic tape back-up and a code system to prevent unauthorized access. The new system has increased data-processing efficiency 10- to 12-fold, reduced data entry errors, increased the productivity of quality-control personnel by reducing the volume of calculations they have to perform, and provided for real-time process analysis and control. It is planned to expand the scope of the system to include functions such as keeping track of customer orders and processing information related to mechanical testing, chemical analysis, and the certification of various products. Eventually, the rail mill computer system will be incorporated into a plant-wide computer network. Figures 1, tables 1; references 4: Russian.

An Investigation of the Heat Conduction of Gas-Thermal Ni-Cr-B-Si Coatings

927D0029C Kiev POROSHKOVAYA

METALLURGIYA in Russian No 8, Aug 91

(manuscript received 16 Aug 89) pp 22-23

[Article by V.D. Podzorov, V.S. Kharchenkov, and A.I. Kadin, Bryansk Process Equipment Plant]

UDC 621.793.7

[Abstract] The authors of this concise report used the method of regular heat conditions (as published elsewhere) to determine the effective coefficient of heat conduction of a PG-SR4 Ni-Cr-B-Si plasma coating on a type 40 steel substrate in the temperature range from 290 to 1,278 K. In essence, the said method involved determining the coefficient of the coating's heat conduction through the cooling rate of the system coating-substrate. This cooling rate (m) was determined based on experimentally obtained data regarding the change in temperature. They then proceeded to calculate the thermal resistance of the coating by using a formula provided. The results, which are presented in table form, were used in the mathematical design (by the grid method) of regimens for heat-treating Ni-Cr-B-Si coatings in liquid coolants. The discrepancy between the calculated data and that obtained by experimentation amounted to less than 9%. Table 1; references 4 (Russian).

The Structure, Composition, and Heat Stability of Nickel-Phosphorus Coatings

927D0050G Moscow IZVESTIYA AKADEMII NAUK

SSSR: SERIYA METALLY in Russian No 5,

Sep-Oct 91 (manuscript received 16 Aug 90) pp 128-132

[Article by E.M. Lazarev, L.M. Petrov, S.Ya. Betsofen, N.A. Korotkov, and A.A. Morozov, Moscow]

UDC 621.762

[Abstract] The authors of the study reported herein examined the structure, composition, and heat stability of amorphous electrolytic coatings consisting of Ni and 15% (mass) P. The methods of x-ray crystallographic analysis, electronographic phase analysis, and electron and optical microscopy were used to structure specimen Ni-P coatings that had been chemically deposited onto carefully degreased sheets of 30CrMnCN steel in a solution of NiSO_4 , NaHPO_3 , and CH_3COONa at a pH of 4.5 to 5.5. Specimen coatings ranging in thickness from 10 to 60 μm were heated in air to a temperature between 300 and 450°C. The starting Ni-P layers were dense, had good adhesion, and were found to be x-ray amorphous. The diffractograms of the heated specimens displayed only the characteristic amorphous halos of an Ni-P phase and the reflexes from crystalline copper of the interlayering. A thin surface layer of each coating, amounting to <1,000 angstroms in thickness, was found (according to electronographic data) to have the crystalline structure of an Ni_3P phase. The studies performed revealed a relatively uniform distribution of phosphorus (22.45 and 22.36% (atomic)) that was somewhat in excess of the eutectic (Ni + Ni_3P) concentration. Heating the specimens (to 450°C, for example) was found to result a very nonuniform phosphorus distribution (23.20 and 28.42% (atomic)). The latter value even exceeded the lower concentration corresponding to the phosphide Ni_3P_2 with a hexagonal lattice. On a structural plane, heating was found to cause a significant change in the pattern observed: The halo on the diffractogram became flatter, and the individual reflexes became sharper. Heating to 400°C resulted in the appearance of very weak reflexes from Ni_3P_2 . Upon heating to 450°C, the said reflexes became more numerous and began to differ distinctly from one another. These structural changes were also reflected in changes in the microhardness of the test specimens following heating. After heating to 400 and 450°C, the test specimens developed a microhardness of 1,000-1,200 and 1,300-1,600, respectively. Crystallization in the form of finely dispersed segregations of Ni_3P_2 at the sites of the catalytic centers resulted in a three- to fourfold increase in the coatings' microhardness. Figures 3, table 1; references 9: 8 Russian, 1 Western.

The Effect of Adhesion-Active Substrates on the Structure Formation and Properties of Laminated Materials Consisting of the Hard Alloy KKhNF15 and Steel

927D0029F Kiev POROSHKOVAYA
METALLURGIYA in Russian No 8, Aug 91
(manuscript received 14 Sep 89) pp 35-41

[Article by V.A. Maslyuk, V.G. Kayuk, and V.P. Smirnov, Materials Science Problems Institute, Ukraine Academy of Sciences]

UDC 621.762:669.018.45:661.65:669.26:620.178

[Abstract] The authors of the study reported herein examined the effect of adhesion-active substrates on the structure formation, physicomechanical properties, and high-temperature oxidation of type KKhNF15 hard alloy-steel laminated materials. The materials were manufactured in accordance with a method described elsewhere. Powders of iron, nickel, type MNMTs 20-20 Melchior, and type BrAZhMTs 10-3-1.5 bronze were used as adhesion-active substrates. The substrate thickness was varied within the range from 50 to 70 μm . The microstructure and distribution of elements in the zone where the chromium carbide material made contact with the steel were studied by the methods of scanning electron microscopy and x-ray spectroscopic microanalysis. Using substrates of nickel and iron powders did not change the phase composition of the hard alloy and increased the strength of adhesion to the steel by a factor of 3 to 4. In the laminated material with an MNMTs-20

substrate, the adhesion interaction of the hard alloy with the Melchior and steel was found to result from a slight redistribution of the nickel and an increase in its concentration at the boundary of the KKhNF15 alloy and steel, with the iron of the steel base dissolving in the Melchior substrate in small amounts. Structure formation in the system KKhNF15-bronze-steel was found to be accompanied by (1) a slight dissolution of the bronze's components in the binder of the hard alloy and (2) dissolution of the iron from the steel base in the bronze substrate. An investigation of the crack resistance of the study system revealed that the ductility of all of the study materials increases as the depth of the indenter's penetration increases. This was attributed to the fact that ductile fracture begins to predominate over brittle fracture. The most crack-resistant material proved to be the alloy KKhN25, which contained the greatest amount of metal binder. Chromium carbide had the lowest crack resistance. The tests conducted established that the compression strength of the study laminated materials is at least on a par with that of the alloy TN20; from a wear resistance standpoint the study material actually surpasses TN20. The corrosion resistance of the study laminated materials in a 3% solution of NaCl and a 10% solution of HCl was found to be better than that of the alloy VK6 by a factor of 27. Layers of the alloy KKhNF15 with nickel, iron, and copper alloys began to oxidize at temperatures above 1,100°C. The presence of Al, Cu, Fe, and Ni in a layer of the chromium carbide alloy was found to increase its oxidation resistance. Figures 4, tables 2; references 10: 9 Russian, 1 Western.

The Development and Assimilation of Different Methods of Protecting Powder Construction Materials Against Corrosion

927D0029J Kiev *POROSHKOVAYA METALLURGIYA* in Russian No 8, Aug 91 (manuscript received 28 Jun 89) pp 84-88

[Article by G.I. Tarasova, V.A. Dovydenkov, and L.V. Kuzhleva, Yoshkar-Ola]

UDC 621.762.864:620.193

[Abstract] The authors of this article have summarized their experience gained in more than 15 years of working to develop and assimilate methods of protecting powder construction materials against corrosion under industrial conditions. A variety of corrosion protection methods are recommended, including hermetic sealing (vacuum impregnation) of inner pores by using various sealants and then applying protective coatings, vapor oxidation, vapor-oil oxidation, treatment of powder parts with corrosion inhibitors, and oil impregnation. PK-80 impregnation compound and GFZh 136-41 water repellent (a 10 to 15% solution in perchloro- and trichloroethylene and other solvents) are highly recommended for use in protecting powder products. Although highly effective in many application areas, GFZh 136-41 does have the problem of dissolving in alkaline electrolytes. PK-80 is therefore deemed preferable and said to result in a cost savings of about 40,000 rubles per ton of product (as opposed to 2,000 rubles per ton of product in the case of GFZh 136-41). The type and thickness of the coating applied has also been demonstrated to be a key factor in its effectiveness as a corrosion inhibitor. Specific recommendations are therefore given for selecting coatings for articles that have been impregnated with either PK-80 or GFZh 136-41. The need to protect powder products against corrosion between the various operations entailed in their manufacture as well as when they are transported and stored is emphasized. It is recommended that copper-based powder products not be stored for more than 10 days without anticorrosion protection and that unprotected iron-based products not be stored for more than 7 days. Low- and medium-volatility corrosion inhibitors such as types NDA, VNKh, IFKhAN, and VNKh-L-49 or mixtures thereof are recommended for use in preserving products that are between manufacturing operations or else in transit or storage. The simplest and most effective method of preservation is said to be packing in inhibitor-treated paper with an additional barrier layer of polyethylene film. This practice is said to result in a cost savings of 250,000 rubles per kilogram of product. An added benefit of the practice is that there is no need for depreservation because it occurs spontaneously when the preserved product makes contacts with the air. Figures 2; references 10 (Russian).

The Effect of Medium Composition on the Propagation of Corrosion and Fatigue Cracks in X8CrNiTi18.10 Steel

927D0047B Kiev *FIZIKO-KHIMICHESKAYA MEKHANIKA MATERIALOV* in Russian Vol 27 No 2, Mar-Apr 91 (manuscript received 17 Jun 90) pp 19-23

[Article by I.M. Dmitrakh and V. Rayngard, Physics and Mechanics Institute imeni G.V. Karpenko, Ukraine Academy of Sciences, Lvov, and Central Solid-State Physics and Materials Science Institute, Dresden, Germany]

UDC 620.191.33:620.194.8

[Abstract] The authors examined the effect that the chemical composition of the medium surrounding X8CrNiTi18.10 steel has on the growth of corrosion and fatigue cracks in the steel. They calculated the dependences of the growth of these cracks on the stress intensity coefficient (ΔK) values obtained during tests of the steel in an active medium (distilled water with an NaOH additive and a pH up to 8) containing different concentrations of NaCl and CuCl₂. They then proceeded to analyze these data in conjunction with electrochemical measurements of the pH of the medium and the electrode potential of the metal near the apex of each developing crack and data on the fracture surface obtained by electron microscopy and mass spectrometry. Their analysis demonstrated that additions of CuCl₂ in the stage of the propagation of a primary corrosion-fatigue crack have a positive effect: They intensify the process of the formation of microcracks and thus reduce the concentration of stresses at the primary crack's apex. Additives of NaCl, on the other hand, stimulate local corrosion and the release of hydrogen, which in turn results in an increase in the crack's growth rate. Figures 5; references 9: 8 Russian, 1 Western.

The Crack Resistance of AT3 Titanium Alloy Under Conditions of Hydrogen Brittleness

927D0047E Kiev *FIZIKO-KHIMICHESKAYA MEKHANIKA MATERIALOV* in Russian Vol 27 No 2, Mar-Apr 91 (manuscript received 5 Dec 89) pp 36-38

[Article by A.V. Malkov, V.K. Alekseyev, and M.G. Mishanova, Moscow Aviation Technology Institute imeni K.E. Tsiolkovskiy]

UDC 669.017:539.56:669.788

[Abstract] The authors of the study reported herein examined the crack resistance of the titanium alloy AT3 under conditions of hydrogen brittleness. Specimens of AT3 were subjected to standard mechanical tests, fracture toughness tests, fatigue crack resistance, cyclic elongation tests, and x-ray and electron microscope microstructural analysis. The microstructure of sheets of AT3 subjected to vacuum annealing at 800°C for 2 hours was virtually the same as that of sheets of the alloy in its

shipment state. As the concentration of hydrogen in the alloy was increased to 0.01% (by mass), an increase in the dark gray regions of its structure was observed. When a 0.05% (by mass) hydrogen concentration was reached, a new black phase appeared in the form of broken plates and "worms." The x-ray and electron microscope studies performed revealed that the following changes occur as the hydrogen content of AT3 increases: 1) the amount of β -phase increases (this is especially true in regions with a clearly pronounced mechanical texture); 2) the size of the β -phase particles increases, and their morphology changes; and 3) at hydrogen concentrations from 0.015 to 0.02% (by mass), it is possible to detect a γ -phase (titanium hydride). Hydrogen was only found to increase the strength characteristics of AT3 when added in small concentrations (0.01 to 0.02% by mass). Large amounts of a hydride phase (a hydrogen content of more than 0.02% by mass) were accompanied by a decrease in both strength and plastic characteristics. Microphotography data indicated that the nature of the fracture of AT3 is very much dependent on hydrogen content. The micro-mechanism of its fracture begins to change when a hydrogen concentration of 0.02% (by mass) is reached. This change involves the appearance of a finely pitted relief of plain facets with elements of a stream-like pattern. Both the static and cyclic fracture toughness of AT3 sheets were also found to decrease as hydrogen content is increased. The authors concluded that these negative effects of the hydrogen saturation of AT3 must be taken into account when designing equipment in which AT3 is to be used and when estimating its life. Figures 2; references 7 (Russian).

Determination of Critical Brittleness Temperature During Impact Bending

927D0047G Kiev FIZIKO-KHIMICHESKAYA
MEKHANIKA MATERIALOV in Russian Vol 27 No 2,
Mar-Apr 91 (manuscript received 24 Apr 90) pp 70-74

[Article by V.I. Smirnov and A.Sh. Deych, Prometey
TsNIIKM, Leningrad]

UDC 669.14.018:620.17

[Abstract] In a continuation of research devoted to improving methods of determining critical brittleness temperatures during impact bending, the authors of the study reported herein examined the distinctive features of estimating the critical brittleness temperature for high-strength steels based on the conventional methods and the correlation of critical brittleness temperature during impact bending to critical brittleness temperature (T_{k2}) as determined during fracture toughness tests of large-sized specimens. The studies were performed on 15Cr2MoVN hull plates and the metal of their welds (10CrMoVTi wire and An-42 flux). Specimens with a V-shaped notch were tested on an MK-30 impact testing machine equipped with a system to record loading oscillograms. The tests performed demonstrated that in the case of high-strength steels, the point of the reverse

bend of the temperature dependence of fracture onset (which is used as a basis for determining critical brittleness temperature) is not always clearly expressed or else does not always correspond to the temperature of the onset of crack propagation. The authors hypothesize that this uncertainty in selecting a criterion for determining critical brittleness temperature based on fracture onset is eliminated if it is found as the point of intersection of the lower envelope of the experimental values of the total fracture and the upper envelope of the values of KCV_{onset} . The authors proceed to verify experimentally that the critical brittleness temperature determined in this manner correlates with the critical temperature of the transition from brittle to quasi-brittle fracture during crack resistance tests. In view of their findings, the authors recommend their proposed criterion for use in determining critical brittleness temperatures during impact tests on high-strength Cr-Ni-Mo-V steels. Figures 3, table 1; references 14 (Russian).

The Resistance of the Steels and Welded Joints of the Metal Structures of Hoisting Machinery to Cyclic Corrosion Cracks

927D0047H Kiev FIZIKO-KHIMICHESKAYA
MEKHANIKA MATERIALOV in Russian Vol 27 No 2,
Mar-Apr 91 (manuscript received 10 May 90)
pp 110-116

[Article by V.N. Pustovoy, Odessa Naval Engineering
Institute]

UDC 539.43:620.194

[Abstract] The authors of the study reported herein examined the effect of operating media on the resistance of the steels and welded joints of the metal structures of rotary gantry and ship hoisting machinery to the formation of cyclic corrosion cracks. The studies were conducted on specimens of 10KhSND and St-38-b2 steel and welded joints thereof. Beam-shaped specimens (10 x 30 x 200 mm) of the base metal, the metal of the weld, and the fusion zone were tested. Sprayed sea water from the Odessa area was used to simulate sea mist. The specimens (thickness, 10 mm) were loaded by cantilever bending at a frequency of 2 Hz and with asymmetry coefficients of $R = -1, 0$, and 0.7 . The kinetic fatigue fracture diagram plotted for each of the specimens was used to characterize its resistance to the formation of cyclic corrosion cracks. Tests were conducted to assess the crack resistance of the base metal and the metal of the weld as well as the role of process breaks, elevated temperatures, and hydrogen saturation in crack resistance. Studies conducted at $R = 0.7$ did not reveal any fundamental differences in the crack resistance of the two metals studied. The kinetic diagrams of their fatigue fracture in air were virtually identical. When specimens of the two base metals were exposed to the corrosive medium simulating sea mist, however, both the shapes of their kinetic diagrams and the kinetics of their fatigue crack growth changed significantly. This change was

especially apparent in the low- and medium-amplitude regions of the stress intensity coefficient. Compared with the base metal, the metal of the welded joints studied had a higher near-threshold cyclic crack resistance in air. These differences were especially apparent in the case of the St-38-b2 steel. The presence of sea mist generally delayed fatigue crack growth in the welded joints. The only exception to this rule occurred in the case of the metal of the weld in the case of St-38-b2 steel. Holding the specimens under a load simulating the normal breaks occurring during the operation of rotary gantry cranes did not appear to have a negative effect on the cyclic corrosion crack resistance of the test specimens. Elevated temperatures (i.e., temperatures up to 40°C, thus simulating operation of the study equipment under the conditions of a tropical climate) appeared to delay the effect of the corrosive medium and increase corrosion fatigue thresholds markedly. Ammonium sulfate-saturated sea mist was not found to have a negative effect on cyclic crack resistance. Instead, in the near-threshold load range, a corrosive medium simulating sea mist was found to have a positive effect on crack resistance. This effect became more significant with cathode polarization. Figures 9; references 8: 7 Russian, 1 Western.

Calculation and Rational Design of Structures Subjected to Corrosion Wear

927D0047A Kiev FIZIKO-KHIMICHESKAYA MEKHANIKA MATERIALOV in Russian Vol 27 No 2, Mar-Apr 91 (manuscript received 13 Aug 89) pp 7-19

[Article by I.G. Ovchinnikov and Yu.M. Pochtman, Dnepropetrovsk State University and Saratov Polytechnic Institute]

UDC 539.4

[Abstract] During their life, many elements of engineering structures are not only subjected to the adverse effects of loads and temperatures but are also subjected to the damaging effects of various corrosive media. It is often the case that the factors of load, temperature, and corrosive medium act jointly in the most unfavorable combinations. Failure to taken these factors into account, both individually and in combination with one another, when designing structures can lead to emergency failures of the said structures and to enormous economic loss. A great deal of research has been and continues to be done on the models and methods for optimal design of structures that will be expected to endure the effects of corrosive media. This body of research has evolved into a rapidly developing science at the crossroads of solid-state mechanics and continuum mechanics and has attracted the attention of specialists from various countries throughout the world. One approach that has been taken to modeling deformable bodies with consideration for the physicochemical effects accompanying corrosion processes on their surface and in their bulk is that of using the principles of

nonequilibrium thermodynamics and continuum mechanics. The concepts of entropy and the deformations of bodies in the presence of chemical transformations are used with this approach. Corrosion wear may also be taken into account by using a model of induced laminar inhomogeneity. Various models of fracture, including static, protracted static, low-cycle, and fatigue fracture, have been used to estimate the durability of structures subjected to corrosive media. The process of the long-term fracture of structures has been described by using the principles of continual theories of damage accumulation. Numerous publications have examined the problem of calculating thin-walled structures with consideration for corrosion wear. M.S. Kornishin and V.G. Karpunin have been particularly important in developing this aspect of the problem. Specifically, both have given consideration to the difference in corrosion rates for the outer and inner surfaces of plates and shells. Such works are based on a deterministic approach to designing structures subjected to corrosion wear. In view of the random nature of the corrosion process, however, others have taken a probability-and-statistics approach to forecasting the corrosion behavior of structures. A model of the corrosion process in the form of a nonlinear differential equation has been proposed. Equations for structural elements with different cross sections in uni- and biaxial stressed states have also been developed. The problem of optimal design of structural elements subject to mechanical and chemical failure has also received a great deal of attention in recent years. In most of these works, the mathematical models of the respective optimization problems have been formulated in terms of mathematical programming (nonlinear, dynamic, etc.) problems and have then been solved by using analytical methods. The multicriterial approach to the optimal design of structures expected to undergo corrosive wear is a particularly promising area of study. References 123 (Russian).

The Effect of Ozonization and Selected Additives on the Corrosion and Electrochemical Behavior of 12Cr18Ni10Ti Steel in Sulfuric Acid

927D0047C Kiev FIZIKO-KHIMICHESKAYA MEKHANIKA MATERIALOV in Russian Vol 27 No 2, Mar-Apr 91 (manuscript received 7 Mar 90) pp 23-26

[Article by B.A. Gru, G.O. Tatarchenko, N.F. Tyupalo, and V.S. Kuzub, GosNII metanolproyekt, Severodonetsk, Lugansk Oblast]

UDC 620.193.41:669.15

[Abstract] The authors of the study reported herein examined the effect of benzimidazole and manganese sulfate additives on the course of the polarization curves of 12Cr18Ni10Ti austenite steel in aerated and ozonized 20% H₂SO₄. The experiments were performed in a three-electrode glass cell. A P-5848 potentiostat (potential-scanning speed, 1.44 V/h) was used along with a

silver chloride standard electrode. Before the polarization curves were read, the working electrode was cathodically activated at a current density of 0.1 A/m^2 for 3 minutes. The solutions were ozonized by using a laboratory ozonizer to pass an ozone-and-air mixture through the cell's working space at a rate of 10 l/h. Four maxima in the vicinity of the anode currents were noted in the potentiodynamic polarization curves of 12Cr18Ni10Ti steel in a sulfuric acid solution (the background solution). They occurred at -0.35, 0, 0.6, and 0.85 V. Benzimidazole added in amounts of 1 and 5% reduced the current density in that leg of the curve corresponding to the beginning of the steel's passivation. The corrosion potential in unstirred aerated background solutions remained virtually unchanged when benzimidazole was added. A partial smoothing of the maxima was observed when a 20% sulfuric acid solution was used. This smoothing was attributed to neutralization of the sulfuric acid by the benzimidazole. In stirred H_2CO_4 + benzimidazole solutions the corrosion potential was shifted in a positive direction by 50-100 V. In the background solution, the 12Cr18Ni10Ti steel corroded at a rate of 2.2 to 5.6 $\text{g}/(\text{m}^2 \times \text{h})$; in a solution containing 1% benzimidazole, corrosion occurred at a rate of 2.15 to 2.6 $\text{g}/(\text{m}^2 \times \text{h})$, and in a solution containing 5% benzimidazole, corrosion occurred at a rate of 0.8 to 1.0 $\text{g}/(\text{m}^2 \times \text{h})$. The reproducibility of the test results was significantly dependent on the surface state of the steel and on the method used to activate it. Intensity of stirring was found to accelerate the depolarization process. When manganese sulfate was added to the system sulfuric acid-benzimidazole, the critical current densities at potentials of -0.15, 0.6, and 0.9 V decreased. The system H_2SO_4 -benzimidazole- MnSO_4 - O_3 was found to be characterized by lengthy intervals of cathode currents in the region of anode potentials from 0.8 to 1.0 V. Repassivation of the metal was found to begin at 1.05 V. When the solution was first saturated with ozone for 10 to 15 minutes, the active region on the polarization curve was insignificant at a potential of 0.9 V with the width of the region of stable passivation amounting to about 0.2 V and with a rapid increase in polarization current density following shortly thereafter. Overall, however, the curves coincided with one another, which confirmed the hypothesis of the quick reaction of ozone with benzimidazole and manganese sulfate. Ozone was thus found to be a depolarizer of the anode process. Changing the ozone concentration had a marked effect on the course of the polarization curves. Figure 1, table 1; references 8 (Russian).

Zr-V-Fe-Based Alloys—Effective Hydrogen Absorbers

927D0047D Kiev FIZIKO-KHIMICHESKAYA MEKHANIKA MATERIALOV in Russian Vol 27 No 2, Mar-Apr 91 (manuscript received 19 Mar 90) pp 26-36

[Article by V.A. Yartis, I.Yu. Zavalii, M.V. Lototskiy, I.I. Bulik, P.B. Novosad, and Yu.F. Shmalko, Physics

and Mechanics Institute imeni G.V. Karpenka, Ukraine Academy of Sciences, Lvov]

UDC 546.3-19'11

[Abstract] The authors of the study reported herein examined the phase equilibria and hydrogen-sorption characteristics of alloys of the system Zr-V-Fe. Specifically, they studied the affect of doping such alloys with scandium, lanthanum, and aluminum oxide. The studies performed established that the dynamics of hydrogen absorption are improved when a $\text{Zr}_3\text{V}_3\text{O}$ phase is present in the alloy and that doping with lanthanum or scandium increases the hydrogen capacity of alloys of the system Zr-V-Fe. The thermal decomposition of hydrogen-charged alloys of the said system was also studied. The studies demonstrated that using Zr-V-Fe-based alloys as the main element of metal hydride systems to provide ion sources in accelerators is one way of solving the problem of simultaneously accomplishing all of functions that such systems are expected to perform (from storing, purifying, and flooding hydrogen in to pumping it out) and simultaneously increasing the gas economy of ion sources. Figures 11, tables 3; references 22: 12 Russian, 10 Western.

The Penetration of Hydrogen Through Nickel With Various Surface Element Profiles

927D0047F Kiev FIZIKO-KHIMICHESKAYA MEKHANIKA MATERIALOV in Russian Vol 27 No 2, Mar-Apr 91 (manuscript received 3 Oct 89) pp 43-47

[Article by V.P. Shestakov, I.L. Tazhibayeva, O.G. Romanenko, L.A. Zolotova, and I.N. Bekman, Kazakhstan State University imeni S.M. Kirov, Alma-Ata]

UDC 669.788+539.2

[Abstract] The authors of the study reported herein examined the effect that the element profile of a nickel membrane's surface had on the kinetics of the penetration of hydrogen through the said membrane. To conduct their study, the authors combined hydrogen permeability method with Auger electron spectroscopy. The qualitative and quantitative makeup of the surface of each specimen was determined, as was the degree of the effect that each individual type of dopant had on the hydrogen-nickel reaction. Hydrogen permeability was studied on specimens 2.0 and 0.8 mm thick and 18 mm in diameter with specified element profiles. The hydrogen permeability experiments were performed in the temperature interval from 933 to 473 K and at hydrogen input pressures of 10^3 to 10 Pa while the change in surface composition was monitored simultaneously by Auger electron spectroscopy. The membranes were attached to the diffusion cell by welding in an argon atmosphere. The specimens were heated with an outside heater with an error of $\pm 0.5^\circ$. The establishment of a steady hydrogen flow was plotted as a function of temperature and element profile (Ni, S, and C versus Ni and

S). Only in individual cases did the kinetic dependences turn out to be straight lines. At high temperatures the curves were S-shaped. The anomalies were found to depend on temperature and hydrogen input pressure. In all cases, the anomalies in the shape of the kinetic curves of hydrogen permeability either decreased or disappeared completely as the input pressure increased. Studies of the stationary hydrogen permeability of nickel membranes revealed that when the membranes were 2 mm thick, the method used to prepare the surface had virtually no effect on the type of temperature dependence of the stationary flow or on its absolute value. The temperature dependence of the permeability constant was subject to Arrhenius' law throughout the entire temperature range studied. Investigations of the hydrogen permeability of a nickel membrane 0.8 mm thick revealed that the absolute value of the stationary hydrogen flow and type of temperature dependence are determined by the surface's purity. The effective permeability constants of specimens with an initial surface element profile of 84% Ni and 16% S and of specimens with an initial surface element profile of 19% Ni, 10% S, and 71% C were determined. The temperature dependence of the flow of hydrogen through the Ni-S-C membrane contained an anomaly in the temperature range from 643 to 933 K. Auger electron analysis confirmed that the penetration process is limited by hydrogen diffusion through the graphite film at low temperatures and through the sulfided nickel at high temperatures. The Auger electron spectroscopy studies performed confirmed that significant changes in the surface's element profile occur within this temperature interval. Consequently, the authors were able to demonstrate that the concentrations of adsorption and catalytically active centers depend on temperature whereas the

effective rate constants of the surface reactions depend on temperature and time. Because permeability is limited by the totality of processes occurring on the nickel surface, the flow of hydrogen through the membrane decreases. Anomalies found in the curves for temperatures above 873 K were also shown to be closely linked to initial surface element profile. At temperatures below 673 K in the case of a nickel specimen with an initial surface element profile of 19% nickel, 10% sulfur, and 71% carbon and a final surface element profile of 100% carbon, the dependence $s(T)$ turned out to be practically exponential. The adsorption activation energy amounted to 16.6 kJ/mol, and the pre-exponential factor amounted to $s_0 = 1.4 \times 10^{-6}$. These low values do not fall in the range of hydrogen adsorption values predicted by the transition state theory. The authors hypothesized that what happens most is that, in the case of a graphite film, the adsorption of hydrogen occurs on a small number of active centers. These centers may be individual nickel atoms on the graphite film. The subsequent increase in temperature is accompanied by an increase in the effective adhesion coefficient due to dissolution of the graphite film. Calculations enabled the authors to establish that on a nickel specimen with an initial surface composition of 84% Ni and 16% S, the adsorption activation energy equals 6.6 kJ/mol with $s_0 = 4.2 \times 10^{-7}$ when $T < 623$ K versus 22.4 kJ/mol with $s_0 = 6.5 \times 10^{-5}$ at $T > 823$ K. By combining the methods of hydrogen permeability and Auger electron spectroscopy, the authors were thus able to establish the reason for the anomalous deviations of the effective permeability and diffusion constants from a linear Arrhenius dependence and to determine the parameters of the penetration of hydrogen through a material with a specified initial surface element composition. Figures 4; references 3: 1 Russian, 2 Western.

New Precision Alloys

927D00201 Moscow STAL in Russian No 6, Jun 91
pp 76-78

[Article by V.V. Sosnin, Central Scientific Research
Institute of Ferrous Metallurgy]

UDC 669.018.5+669.018.47

[Abstract] Alloys possessing a set of physical or physico-mechanical properties resulting from some precise chemical composition, controlled impurity content, or the creation of a specified structural state are classified as precision alloys. The USSR metallurgy industry produces more than 200 types of precision alloys in the form of forgings, bars, wires, strips, thin-walled tubes, precision profiles, very thin strips, and composites. In recent years, the Precision Alloys Institute of the Central Scientific Research Institute of Ferrous Metallurgy has directed its efforts toward improving the quality of series-produced alloys and creating alloys with a qualitatively new level of properties or with a new combination of physicochemical properties. In the area of magnetically soft alloys, they have developed a process for commercial production of 27NKh in the form of fine-grained (grain diameter, $\approx 50 \mu\text{m}$) forgings 60 to 120 mm in diameter and up to 1,500 mm in length for contactless magnetic screw gears for ultraprecise machine tools. This metal has a saturation induction of 1.75 and 2.05 teslas in magnetic fields with respective intensities of 2,500 and 15,000 A/m. In the area of amorphous magnetically soft alloys, they have created the alloys 84KKhSR, 84KSR, and 86 KGSR and have developed processes for producing them in amorphous strips in three thicknesses (μm): 20-30, 25-32, and 35. The precision manganese-aluminum alloy 71GYu is produced in the form of small permanent magnets with a high coercive force, high mechanical strength, high corrosion resistance, good machinability, and highly stable magnetic characteristics at temperatures ranging from -60 to +60°C. A process has also been developed to produce the alloy 42NKhYu in 0.3-mm-thick strips for use as anode leads. Other new precision alloys produced by the institute include the nonmagnetic corrosion-resistant spring alloy 18KhNAGS, which is produced in the form of a cold-rolled strip 0.025 to 0.25 mm thick and high-cold hardened wire 0.1 to 1.2 mm in diameter. The corrosion-resistant nonmagnetic alloy 40KKhNi10MTYu is a precision alloy that was developed for medical purposes and may be implanted in the human body. It is produced in the form of a bar 12 to 25 mm in diameter and wire 0.070 to 3 mm in diameter and strips of different thickness. Its breaking resistance in softened and hardened states ranges from 860 to 1,200 and 1,750 to 2,150 N/mm², respectively, and its relative elongation in the two aforesaid states ranges from 40 to 65 and 2.0 to 5.3%, respectively. All of the aforementioned new precision alloys have performance characteristics competitive with their best foreign rivals, as well as high technical and economic indicators. Figure 1, table 1; references.

New Developments in Alloy and Alloy Steel Production

927D0017A Kiev PROBLEMY SPETSIALNOY
ELEKTROMETALLURGII in Russian No 4, 91
pp 81-84

[Abstract of article by G. I. Kaplanov]

[Abstract] The author reviews recent advances made in alloy and alloy steel production by the Ukrainian Institute of Specialty Steels in conjunction with a number of major domestic iron and steelmaking concerns. These developments include: corrosion-resistant and high-manganese steelmaking processes that combine decarbonization, direct alloying, and carbothermic reduction, thereby producing cleaner steels and conserving alloying elements; ladle-treatment of steels with specially made furnace slags used together with solid slag-forming materials to produce cleaner steels; the first domestically manufactured ladle furnace, which produces extremely clean steels with optimal alloy element content; use of recycled dust and slime from electric furnace gas scrubbing in briquet form for direct alloying utilizing the carbothermic process; a process that yields larger bearing steel ingots that have plastically deformable non-metallic inclusions and that can be rolled with high reduction drafts; a process for making low-fluoride fluxes that improve the quality of electrosag steel and help reduce electricity consumption and pollution; vacuum-arc remelting of bimetallic ingots for tubular products; plasma-spray resurfacing of worn machinery components with heat-resistant alloys; homogenizing heating of ingots and continuously cast billets that greatly reduces alloy element and impurity segregation, structural and carbide inhomogeneity, and primary carbide size; continuous production of tubular stock and products from continuously cast billets; and numerous other improvements throughout the entire range of alloy steelmaking and forming technologies. A number of the new processes and process modifications cited, such as the hot extrusion of large capsules containing high-speed steel powder, products rolled and forged from alloy steels with special deformation patterns and plastic flow lines, and artificial and natural composites made from high-alloy steels and alloys, were said to have no foreign counterparts.

Heat Treatment of Low-Alloy Steels To Produce a Ferrite-Austenite-Bainite Structure

927D0042 Sverdlovsk FIZIKA METALLOV I
METALLOVEDENIYE in Russian No 5, May 91
(manuscript received 30 May 90; after revision
7 Sep 90) pp 93-98

[Article by A.A. Petrunenkov, Quality Steels Institute
and Central Scientific Research Institute of Ferrous
Metallurgy imeni I.P. Pardin]

UDC 669.15'74'782-194:539.4.015

[Abstract] The authors of the study reported herein examined the possibility of producing high-strength low-alloy thin steel sheets with improved plasticity (thanks to the transformation-induced heating [trip] effect). In the first stage of the studies the researchers compared the properties of steels with varying amounts of C, Si, Mn, Cu, Ni, Cr, S, P, Al, and N. They decided upon a steel containing 0.37% (by weight) C, 1.35% Si, and 1.35% Mn. Ingots of the said steel were cooled in sand, heated to 1,150-1,200°C, and hot-rolled to produce a band 3 mm thick. The band was etched and cold-rolled to a thickness of 1 mm. After this rolling the steel had a perlite structure. Further experiments enabled the researchers to establish that incomplete isothermal hardening from the intercritical temperature interval makes it possible to obtain a structure with 20% ferrite, 20% austenite, and 60% bainite in which the trip effect is achieved. The optimal heat treatment regimen for the said steel was determined to be as follows: heating temperature, 780°; isothermal holding temperature, 400°C; and isothermal holding time, 5 minutes. The steel produced in this manner was found to have a combination of strength (1,000 N/mm²) and plasticity (total elongation, about 35%; even elongation, about 25%) that is unique when compared with the properties of existing low-alloy sheet steels. Figures 5; references 10: 7 Russian, 3 Western.

The Properties of Hot-Stamped High-Chromium Stainless Steels

927D0029D Kiev POROSHKOVAYA
METALLURGIYA in Russian No 8, Aug 91
(manuscript received 1 Aug 89) pp 30-35

[Article by S.G. Napara-Volgina and L.N. Orlova, Materials Science Problems Institute, Ukraine Academy of Sciences]

UDC 621.762

[Abstract] The authors of the study reported herein examined the properties of Kh17, Kh18M, and Kh13-M high-chromium hot-stamped stainless steels produced by using powder alloys that were in turn produced by pulverization and diffusion saturation. The studies were performed on specimens with dimensions of 10 x 10 x 55 mm that were manufactured by compacting porous blanks and then stamping them at temperatures between 800 and 1,200°C coupled with heating in different media. Preliminary studies showed that depending on the temperature, duration, and medium used in the process of heating the porous blanks during the hot stamping, the content of carbon in the steels could range from 0.04 to 0.10% and the nitrogen content could range from 0.02 to 0.45%, with the latter increasing after heating in nitrogen-containing media. Depending on the exact hot stamping conditions, the structure of the steel produced could range from a purely ferrite structure with a microhardness of 1.5-1.8 GPa to a martensite structure

with a microhardness of 7.7-8.0 GPa. The mechanical and corrosion properties of the study steels after the various hot stamping regimens tested are presented in table form. Directly after hardening, the Kh13M steel had a martensite-bainite or troostite-bainite structure with a high microhardness (8 and 5.9 GPa, respectively) and high tensile strength (900 and 845 MPa). After low-temperature tempering at 300°C, its strength increased to 1,073 and 859 MPa, respectively, for the two aforesaid structures, and its plasticity increased at the same time. High-temperature tempering at 600 and 780°C, on the other hand, resulted in the formation of ferrite structures with a relatively low microhardness ranging from 2 to 2.5 GPa. The Kh18M steel manufactured under the same regimen as Kh13M underwent less pronounced changes in structure and properties. Hot-stamped Kh13M steels was found to be quite similar to 10Kh13 steel. After tempering in oil at 1,050°C, however, the Kh13M was found to be much stronger but less plastic than the 10Kh13. Figures 3, tables 2; references 11: 10 Russian, 1 Western.

Effect of Nonferrous Metals on Quality of Tube and Pipe Steel

927D0059E Moscow STAL in Russian No 7, Jul 91
pp 23-24

[Article by R.P. Bobova, V.V. Popov, G.A. Oblasov, Yu.A. Starkov, Metallurgy Institute at the Urals Department of the USSR Academy of Sciences and Seversk Tube Mill]

UDC 621.746.628

[Abstract] Efforts to find the causes of tube metal rejects prompted by a large number of smeltings (usually from the same ladle) rejected at the pipe mill due to cracks (primarily of steel D) are described. Ingots cast from the 260-ton basic open hearth furnaces using scrap were investigated. An analysis shows that the ingot quality deteriorates under the simultaneous effect of several factors: an elevated metal temperature, a nonuniform skin development along the ingot perimeter, and an elevated copper and tin content with a copper:nickel ratio of more than 1.5. Taken together, these factors determine the solidification character of cracks. Ingot flaws also form after heating in furnaces or during rolling due to the internal oxidation phenomenon whereby the grain boundaries become enriched with low-melting copper-containing phases when the nickel concentration does not compensate for copper's harmful effect. Cracking can be prevented by casting metal at the lower temperature of the melting range, ensuring a copper concentration of no more than 0.2% a Cu:Ni < 1.5 ratio, and maintaining a tin concentration of no more than 0.02%. G.N. Telezhnikova, V.N. Kudryashov, and B.P. Kuzmin helped with the analysis and research. Figures 6; references 4.

Structural Changes Occurring in Nonalloyed Steels With a Plastic Perlite Structure After Laser Heating

927D0042E Sverdlovsk FIZIKA METALLOV I
METALLOVEDENIYE in Russian No 5, May 91
(manuscript received 22 Jun 90; after revision
27 Sep 90) pp 122-129

[Article by I.V. Lyasotskiy and D.V. Shatanskiy, Metal Science and Metal Physics Institute, Central Scientific Research Institute of Ferrous Metallurgy]

UDC 669.11:620.182/.186

[Abstract] The authors of the study reported herein studied laser heating-induced structural changes in three types of nonalloyed steels containing plastic perlite as a structural component. Specifically, they performed a layer-by-layer electron microscopy analysis of the various structural changes occurring in the steels after different laser heating regimens. The experiments were performed on carbonyl iron and on types 3, 45, U10 steel in an annealed state. A continuous-wave CO₂ laser with a power-flow density ranging from 4×10^3 to 4×10^4 W/cm² and an irradiation time of 0.3 to 1.0 seconds and a Kvant pulse laser with a power-flow density of 3×10^4 W/cm² and an irradiation time of 4×10^{-3} seconds were used as radiation sources. In the case of the continuous-wave laser a heating rate ranging from 10^3 to 3×10^3 K/s was used. In the second case a heating rate of 2×10^5 K/s was used. In no case did the treatment temperature on the specimen surface exceed the melting point. A JEM-200CX scanning electron microscope was used to study the specimens' fine structure in different temperature effect zones. Two processes proved to be decisive in the alteration of the phase state of the study alloys under nonisothermal conditions. These two processes were 1) the diffusion growth of an austenite grain as a result of carbon being supplied to the α - γ phase boundary and 2) a displacement process resulting in α - γ restructuring of the lattice without any noticeable involvement of carbon. The studies performed confirmed that under conditions of accelerated heating of nonalloyed steels with a starting structure containing plastic perlite or perlite and structurally free ferrite, the process of phase recrystallization of ferrite in accordance with a displacement mechanism forestalls the process of the diffusion growth of austenite. The conditions of diffusionless α - γ restructuring of the lattice were found to be affected by the contact interaction of the two phases. Specifically, this interaction facilitated the displacement α - γ transformation. The process of the ferrite-to-austenite transition in accordance with a martensite mechanism in perlite columns was found to begin by the time a heating rate of about 10^3 K/s had been reached. When the heating rate was increased to 10^5 K/s, a displacement transformation of the structurally free ferrite into austenite occurred. As the superheating temperature continued to rise higher and higher over the equilibrium temperature of the

phase transition, the transformation became more complete and the structure acquired a more pronounced grid martensite morphology. Figures 4; references 16 (Russian).

The Heat Embrittlement Tendency of Cr-Ni-Mo Steel With Ti and B Additives

927D0026D Moscow METALLOVEDENIYE I
TERMICHESKAYA OBRABOTKA METALLOV
in Russian No 5, May 91 pp 9-11

[Article by V.M. Goritskiy, G.R. Shneyderov, and V.I. Bogdanov, TsNIIProyektstallkonstruktsiya]

UDC 620.178.2:669.26'24'28

[Abstract] The martensite Cr-Ni-Mo steel 08Cr4Ni2Mo has been shown to have a greater resistance to heat embrittlement than the steel that was previously used in RBMK-type reactors. It too is only recommended for use at temperatures not exceeding 350°C, however. In view of this fact, the authors of the study reported herein examined the effect that titanium and boron additives have on the heat embrittlement of 08Cr4Ni2Mo steel. Seven laboratory melts of 08Cr4Ni2Mo steel were used in the study in plates measuring 200 x 60 x 20 mm. The test plates were subjected to hardening at 920°C in water and tempering at 650°C for 2 hours. To determine their tendency toward heat embrittlement, the specimens were kept in a muffle furnace at 450°C for 1,000, 2,000, and 5,000 hours. Impact buckling tests were also conducted at temperatures ranging from -60 to +60°C. The tests performed revealed that adding titanium, boron, and niobium additives to 08Cr4Ni2Mo steel with 1.98 to 2.05% Ni results in only an insignificant gain in strength properties (by 20 to 70 N/mm²). For all practical purposes, these additives do not have any effect on the steel's plastic properties in a hardened-temperature state either. Adding 0.02-0.03% Ti and 0.002-0.003% B to 08Cr4Ni2Mo martensite steel did turn out to significantly reduce its tendency toward heat embrittlement. The increase in the critical embrittlement temperature of 08Cr4Ni2Mo steel with 0.009-0.020% phosphorus was found to not exceed 15°C even after it was held for 2,000 hours at 450°C. The beneficial effects (i.e., enhancement of resistance to heat embrittlement) derived from the combined addition of Ti and B were found to extend to 08Cr4Ni2Mo steel with an elevated (0.035%) phosphorus content. The increase in resistance to heat embrittlement achieved by adding titanium and boron to 08Cr4Ni2Mo steel was attributed to the fact that boron prevents segregation of phosphorus at the grain boundaries while titanium binds nitrogen and thereby increases the boron's activity. Figures 3, tables 3; references 4: 3 Russian, 1 Western.

Optimization of Burden Composition for Making Vanadium Pig Iron*927D0059A Moscow STAL in Russian No 7, Jul 91
pp 5-7*

[Article by V.V. Volkov, B.M. German, V.S. Novikov, V.V. Filippov, A.V. Chentsov, S.V. Shavrin, Urals Ferrous Metallurgy Scientific Research Institute and Metallurgy Institute at the Urals Department of the USSR Academy of Sciences]

UDC 669.16.012:669.162.292

[Abstract] The effect of burden composition on the quality of vanadium pig iron is considered on the basis of the experience accumulated at the Kachkanar Mining and Ore Dressing Works (KGOK). To this end, the quality of sinter and pellets produced by the KGOK in 1980-1997 is compared with respect to such indicators as Fe, FeO, and V content, CaO/SiO₂ basicity, the amount of 5-0 mm fines, strength according to GOST 15137-77, etc. Operating indicators of blast furnace No. 1 as a function of pellet concentration in the burden are summarized and the carbon dioxide concentration distribution in the furnace top cross section is plotted at various pellet concentrations in the burden. An analysis demonstrates that Kachkanar iron-vanadium pellets are characterized by a higher iron content, an elevated reducibility, and satisfactory initial strength compared to the sinter cake but have a lower "hot" strength and a broader temperature range of plastic viscous state and filtering. It is shown that by replacing 10% of sinter cake with pellets, it is possible to increase the furnace yield by 1.0-1.3% and decrease coke outlays by 0.8-1.0%. The optimum pellet content in the burden is 55-70% and depends on the furnace volume thus confirming the need for improving the burden production process, especially increasing the "hot" strength. V.I. Grigina, the late B.V. Ipatov, B.V. Kachula, and B.A. Marsuverskiy participated in the study. Figures 1; tables 2; references 5.

Pilot Tests of Copper Removal From Iron-Carbon Melts by Refining*927D0059B Moscow STAL in Russian No 7, Jul 91
pp 15-16*

[Article by V.I. Kashin, A.M. Katsnelson, Yu.A. Danilovich, V.P. Savanin, A.M. Bigeyev, A.I. Usharov, G.S. Uvarovskiy, L.V. Goryaynova, Metallurgy Institute imeni A.A. Baykov at the USSR Academy of Sciences, Tulachermet Scientific Production Association, Magnitogorsk Mining and Metallurgy Institute, and Khrompik Production Association]

UDC 669.187.26

[Abstract] The effect of the burden contamination with nonferrous metals (primarily copper) on the quality of steel-making process and steel itself is discussed and the results of pilot tests to check laboratory studies of the

thermodynamics and kinetics of copper removal from the high carbon melt to the slag by the sulfide method are presented. The experiments were carried out at the steel-making plant of the Tulachermet Scientific Production Association. The experiments demonstrate that data on the slag-forming mixture outlays during the copper removal from Fe-C melts with an elevated initial sulfur content are consistent with the results of lab smeltings. Tentative economic and engineering analyses demonstrate that given a sodium sulfide outlay of 10% of the metal by mass, the cost of slag-type refining amounts to 20 rubles per ton of metal; this figure may be reduced further by 35-40% by means of hydrometallurgical processing of the sulfide slag in order to recover copper and the sodium-containing component. Yu.T. Dadeshkeliani, V.I. Lysenko, A.I. Mazun, M.P. Mishin, S.Yu. Nefedov, V.T. Tereshchenko, S.P. Sustavov, and V.V. Shirokov (Tulachermet) and S.N. Ishmetyev (Magnitogorsk) participated in the study. Figures 2; tables 1; references 7.

Problems of Removing Nonferrous Metal Impurities From Steel and Possible Solution Versions*927D0059C Moscow STAL in Russian No 7, Jul 91
pp 16-17*

[Article by V.A. Kudrin, V.K. Babich, G.N. Yelanskiy, Yu.F. Vyatkon, L.G. Sukhova, Moscow Continuing Education Metallurgy Institute and USSR Metallurgy Ministry]

UDC 669.18.046.5

[Abstract] The negative effect of even trace amounts of nonferrous metal impurities on the quality of steel, especially structural is discussed and the increasingly high nonferrous metal concentration in the burden components is stressed. The problem of removing nonferrous metal impurities is addressed and several methods which should be pursued for developing the technology of nonferrous metal removal are identified: oxidation by a medium with a high oxygen potential, treatment by powder materials with evacuation, treatment by calcium-containing reagents, etc. Positive results obtained by heating in a reducing atmosphere are reported and it is shown that chemical heat treatment of high-alloy scrap in a chloride melt is promising and makes it possible to recover tin and lead and thus utilize expensive high-alloy byproducts. The need to expand scientific and research efforts aimed at examining the joint effect of impurities on the quality of steel and developing technologies for removing them from steel by refining is recognized. Figures 2.

Copper in Steel and Copper Removal Problems*927D0059D Moscow STAL in Russian No 7, Jul 91
pp 18-22*

[Article by I.N. Zigalo, V.I. Baptizanskiy, Yu.F. Vyatkin, A.G. Velichko, Ye.Kh. Shakhpazov, Yu.N. Grishchenko, Dnepropetrovsk Metallurgy Institute, USSR Metallurgy Ministry, and USSR State Committee on Science and Engineering]

UDC 669.18

[Abstract] The difficulties of removing nonferrous metal impurities with the help of "classical" methods during the smelting and ladle processing of steel made from scrap in converters and open hearth and electric furnaces are discussed and data on the copper content in various types of steel are cited. It is noted that with the exception of a few plants, the copper content in steel is constantly on the rise due to the use of ferrous metal-containing scrap. Several methods of removing copper from steel, both by carefully sorting the scrap and using innovative processes, are considered. It is shown that the sulfide refining method which makes it possible to decrease the copper content in steel by 30-35% according to foreign reports and more than 60% according to Soviet data is one of the most theoretically developed and practically tested. The electric arc processing of the steel jet may lower the copper content by 30% while steel processing by ceramic materials from spinel on the basis of alumina and zinc oxide is promising. It is noted that special attention must be focused on the environmental safety issues. Figures 5; tables 2; references 11: 7 Russian; 4 Western.

Production of 500 mm dia. Heat-Resistant Alloy Ingots by Vacuum Arc Remelting Method

927D0059F Moscow STAL in Russian No 7, Jul 91
pp 32-33

[Article by M.S. Vulfovich, I.A. Tregubenko, V.A. Kalitsev, T.V. Beda]

UDC 669.187.26

[Abstract] The increased tendency of the KhN67MVTYu and KhN65KVMYuT high-temperature alloys toward the development of point discontinuities of the segregation origin in the ingot macrostructure is identified and the possibility of remelting serviceable 500 mm dia. high-temperature alloy ingots by the method of vacuum arc remelting (VDP) made possible by the development of the plasma arc surface refining technology (PDRP) is investigated. The study demonstrates that it is possible, in principle, to produce KhN67MVTYu and KhN65KVMYuT ingots with a 500 mm diameter by the new technology which has already been commercially implemented. Production of 500 mm dia. ingots from high-temperature alloys in molds makes it possible to expand the range of standard sizes of 1,300-1,400 kg forgings; moreover, casting of 400 mm dia. electrodes makes it possible to decrease the mass of the original smelting and reduce the number of smelting from five to three. The use of this virtually waste-free technology results in metal savings of 80-100 kg/t. Tables 3; references 4.

Efficiency of In-Line Cold-Deformed Stainless Steel Tube Production at Nikopol Yuzhnotrubby Tube Works

927D0059G Moscow STAL in Russian No 7, Jul 91
pp 56-58

[Article by O.A. Semenov, V.F. Frolov, S.E. Gershgorin, Scientific Production Association of the All-Union Scientific Research Tube Institute]

UDC 621.774.35.016.3.003.1:658.527

[Abstract] The anticipated impact (including the social and economic needs of the workers) from the implementation of a continuous production line for making stainless steel tubes with a diameter of 30-8 mm, a wall thickness of 3.0-0.7 mm, and a ready tube length of up to 23 m in the TVTs-5 tube mill at the Nikopol Yuzhnotrubby Tube Works is estimated; the effort is prompted by the conclusion of a study showing that continuous production is the most efficient method of making high-quality long stainless steel tubes and by the introduction of new economic mechanisms. The advantages of in-line tube production over batch production are summarized. The dependence of the mill profitability on the tube quality classification and number of double passes in the stand per minute is established and plotted. In addition, the possibility of rolling the tubes made in the drawbench at the rolling section of the line without shutting down the KhPT40PL mill is examined. Figures 2; tables 1; references 4.

Iron Powder Production From Iron Ore Concentrate

927D0059H Moscow STAL in Russian No 7, Jul 91
pp 74-76

[Article by P.K. Savorskiy, B.P. Khlevenko, Ye.A. Krashenninnikov, I.F. Dvornichenko, V.F. Bernado, A.S. Rylkova, L.A. Sharonov, Yuzhruda GPO, Ore Directorate imeni Dzerzhinskiy, Central Scientific Research Institute of Ferrous Metallurgy, Ferrous Metal Machining Institute, and Sulinskiy Integrated Iron and Steel Works]

UDC 621.762.242:669.012.22

[Abstract] The outcome of studies aimed at producing a superconcentrate from iron ore, granulating it, and making reduced iron powder at the Sulinskiy Integrated Iron and Steel Works prompted by the rising demand for reduced iron powders characterized by a higher raw compaction strength that loose powder is presented. The superconcentrate for this purpose is produced from the regular concentrate in three stages at the pilot plant of the Ferrous Metal Machining Institute: finishing by the wet magnetic separation method, magnetic flotation dressing, and chemical desilicization. The procedures involved in all three stages are outlined and the chemical and mineral compositions of concentrates and roasted

granules are summarized. The raw compacted superconcentrate with a 6.5 g/cm^3 density reaches 54 N/mm^2 which is higher than that of PZhV2.160 powder by 2.5 times; the pilot powder's caking ability corresponds to that of the best brands. The use of the superconcentrate from ferruginous quartzites makes it possible to produce high-quality iron powder which can be used for making antifriction and structural members for crucial structures. Figures 2; tables 2; references 1.

Stratification Kinetics and Phase Composition During the Aging of Cold-Rolled Foils Made of the Alloy Cr15 and 08Cr14Ni5Cu2Ti Steel

927D0042F Sverdlovsk FIZIKA METALLOV I METALLOVEDENIYE in Russian No 5, May 91
(manuscript received 28 Feb 89; after revision 12 Oct 90) pp 130-136

[Article by T.M. Makhneva, Ye.P. Yelsukov, and Ye.V. Voronina, Physics Technical Institute, Ural Department, USSR Academy of Sciences]

UDC 669.15'26-194:669.017.167.2

[Abstract] The authors of the study reported herein examined the effect that aging temperature and holding time at $375\text{--}475^\circ\text{C}$ have on the average hyperfine magnetic field (H) in 08Cr14Ni5Cu2Ti stainless maraging steel and the binary alloy Cr15. Specimens of cold-rolled foils (thickness, $30 \mu\text{m}$) of each of the aforesaid materials

were subjected to nuclear γ -resonance spectroscopy studies on a YaGRS-4M spectrometer in a constant-acceleration mode at room temperature. A DRON-1 diffractometer was used to perform a x-ray phase analysis of the specimens at room temperature. The studies performed demonstrated that H increases as holding time during the aging process is increased. The researchers linked this increase in H with stratification processes in the Fe-Cr-Ni matrix of the α -solid solution. These rate at which these stratification processes occur in 08Cr14Ni5Cu2Ti steel is twice their rate of occurrence in the alloy Cr15. By analyzing the Mossbauer spectra recorded during the studies, the researchers were able to plot the lower portion of a C-shaped curve of the decomposition of the α -matrix of 08Cr14Ni5Cu2Ti steel. This curve revealed that at temperatures close to 475° , the decomposition occurs virtually without an incubation period and is completed within 15 to 30 minutes. At the temperatures used in the practice of hardening heat treatment (425 to 450°C), the formation of chromium-enriched zones begins after 10 to 15 minutes. At $375\text{--}400^\circ\text{C}$ the incubation period is rather lengthy, requiring up to 3 hours. The C-shaped curve plotted based on the study data is in line with previously published discussions of the kinetics of the formation of chromium-enriched zones. The stratification process described for 08Cr14Ni5Cu2Ti is analogous to that occurring in Cr15, with the latter reaching a maximum at 475°C . The chromium stratification process observed in both test materials occurred simultaneously with the decomposition of residual austenite. Figures 6, table 1; references 17: 11 Russian, 6 Western.

The Role of Microorganisms in Molybdenum Extraction

927D0031M Moscow TSVETNYYE METALLY
in Russian No 7, Jul 91 pp 64-67

[Article by G.M. Yashina and S.V. Nesterova, Unpromed [not further identified]]

UDC 622.346.2

[Abstract] Several published reports have discussed the fact that the bacterium *Th. ferrooxidans* accelerates the oxidation of molybdenum. Thermophilic bacteria have been shown to be promising for use in leaching out molybdenum. In view of these reports, the authors of the study reported herein examined the effect of different microorganisms on processes of the dissolution of sulfide and sulfide-oxidized molybdenum-containing materials. For their studies, they used six molybdenum-containing specimens: three ore specimens (one sulfide-oxidized specimen and two sulfide), two specimens of molybdenum flotation tailings, and one specimen of molybdenum concentrate. The molybdenum in each of the aforesaid specimens was leached out in agitation and percolation regimens in solutions containing additives of different microorganisms, including *Th. ferrooxidans*, *Candida lipolytica*, and a culture of the fungus *Mucor*. The experiments conducted proved that it is, in principle, possible to use various heterotrophic microorganisms to leach molybdenum from ores, flotation tailings, and concentrates. The studies also established that the process of using iron- and sulfur-oxidizing bacteria to extract molybdenum is a protracted process requiring months. When *Th. ferrooxidans* was used to leach molybdenum from molybdenum-containing tailings, for example, only 50-53 mg/l (i.e., 2 to 4% of the starting amount of molybdenum present) was leached out of a test solution after 140 days. Tests comparing the effectiveness of *Th. ferrooxidans* and the yeast *Candida lipolytica* demonstrated that the concentration of molybdenum in the productive solution was increased when *Candida lipolytica* was used as opposed to *Th. ferrooxidans* but that the solution contained less molybdenum. This finding led the authors to hypothesize that *Candida lipolytica* is more selective with respect to molybdenum as compared with bacteria of the type *Th. ferrooxidans*. An agitation regimen was also used to leach the molybdenum from a molybdenum concentrate in the presence of sulfur-oxidizing bacteria. After 14 days the content of sulfur in the solid phase amounted to 6.7%, which was 1.6% lower than in the starting specimen before the leaching, whereas the concentration of molybdenum in the productive solution amounted to 1.0 mg/l. Figures 5, tables 2; references 7 (Russian).

An Investigation of the Isothermal Upsetting of the High-Damping Alloy G55D45

927D0031L Moscow TSVETNYYE METALLY
in Russian No 7, Jul 91 pp 58-60

[Article by A.S. Anishchenko, A.P. Andryushchenko, A.B. Dobychin, and D.I. Chasnikov, MF TsNIIKM Prometey [not further identified]]

UDC 669.74'35.746:539.52

[Abstract] Besides possessing a high vibration-damping capability, the manganese alloy G55D45 (Avrora) has a low plasticity during plastic metal working by conventional high-speed methods and is prone to very quick hardening (which limits its use in a deformed state). In view of these facts, the authors of the study reported herein examined the possibility of isothermal shaping of G55D45 at reduced deformation speeds. Their primary objective in so doing was to develop an alternative plastic metal working process that would reduce the energy and force parameters and increase the plastic properties of the alloy as it is deformed. The G55D45 alloy was smelted in an open induction furnace into ingots measuring 50 x 100 x 240 mm excluding the sinkhead. The ingots were heated to 850°C and rolled into blanks 25 mm thick in eight passes with a total reduction of 50%. A portion of each heated (to 850°C) blank was quenched in water. Specimens with a diameter of 20 mm by 30 mm and with a roughness of 20 were cut from the hot-deformed and quenched blanks. Experiments investigating free upsetting under isothermal conditions were conducted on a 1231U-10 testing machine equipped with an electric furnace, three chromel-alumel thermocouples connected to a KSP-3 potentiometer, strain gauges measuring up to 10 and 100 kN each, and a reverser made of the refractory nickel alloys EI 698VD and EI 868VD. The specimens were placed in the reverser, which in turn was placed in an electric furnace. They were heated for 4 to 8 hours to the required temperatures, upset, cooled in the furnace to 150-200°C over the course of 3 to 7 hours, and then removed from the furnace. The upsetting was performed at deformation rates of 0.02, 0.2, and 2.0 mm/min. Three specimens were tested in each upsetting regimen. Tests conducted at 800-850°C demonstrated that the upsetting pressure, both in the case of hot-rolled and rolled-and-quenched specimens, does not depend on the degree of deformation δ throughout the entire deformation rate range. For hot-rolled specimens, moreover, p does not depend on δ even in the case of upsetting at rates (v) of 0.02 and 0.2 mm and temperatures of 670 and 750°C. Instead, the ultimate deformation in the specified cases is determined solely by the technical data of the reverser, and the upset specimens are characterized by an absence of a network of cracks. Rather, they may be described as disks whose side surface is slightly barrel shaped. At a deformation rate of 2.0 mm and a temperature of 670 or 750°C the upsetting pressure of both types of specimens reaches a maximum at $\delta = 0.03$ to 0.08 and then diminishes monotonically as δ increases. In the quenched specimens, a decrease in p as δ increases is observed when $T = 670^\circ$ and $v = 0.02$ and 0.2 mm/min as well as at $T = 750$ and $v = 0.2$ mm/min. In all of the experiments performed, plastic deformation of the specimens begins after some specified "threshold" upsetting pressure value is reached (between 1 to 16 MPa in the case of high temperatures and low deformation rates and between 160 and 240 MPa at lower temperatures and increased deformation rates). After analyzing the results

of their experiments, the researchers concluded that they could not unequivocally determine the effect of superplasticity in the alloy G55D45 and that further research would be required for this. Figures 2; references 3 (Russian).

Reducing Scaling When Copper Ingots Are Heated

927D0031K Moscow TSVETNYYE METALLY
in Russian No 7, Jul 91 pp 56-58

[Article by T.V. Shvedchikova, I.A. Dmitriyev, B.Ye. Khaykin, and L.M. Zheleznyak, Ural Polytechnic Institute imeni S.M. Kirov]

UDC 621.771.016

[Abstract] Before copper ingots can be rolled they must be heated to 850-900°C. It is estimated that during the course of this heating, 4 to 7 kg of every ton of copper rolled is lost to scaling. One way of reducing these losses of copper is to reduce the oxidation of copper ingots during the heating process. The research that has been conducted has demonstrated that one of the most effective ways of accomplishing this is to apply a protective glass coating that has been doped with polyvalent metal oxides to the copper. Coatings made of sodium borate glass with small amounts of molybdenum and tungsten oxides added are particularly effective in this respect. The advantage of such composites is that they are inexpensive, simple, and reliable to use. This article reports the results of tests of the effectiveness of three such sodium borate glass coating compounds that have been developed to protect copper ingots while they are heated. The new coatings contained varying percentages of the following: H_3BO_3 , $Na_2B_4O_7 \times 10H_2O$, WO_3 , MoO_3 , and H_2O . Comparisons of the scaling losses incurred by untreated copper ingots and by copper ingots coated with the three new coatings demonstrated that the new coatings afford a number of benefits. Specifically, they reduce losses of metal to scaling by 54%, they cut etching time in half, they have a good wettability, and they provide good coating continuity thanks to the fact that their thermal coefficients of linear expansion are in good agreement with those of copper. Figure 1, tables 3; references 5 (Russian).

The Dislocation Structure and Deformation Hardening of Copper-Based Solid Solutions

927D0031J Moscow TSVETNYYE METALLY
in Russian No 7, Jul 91 pp 54-56

[Article by M.I. Tsylin, E.V. Kozlov, G.A. Kulikova, M.L. Matyusheva, and L.G. Danshina, Giprotsmo [not further identified]]

UDC 669.35:620.1

[Abstract] The authors of the study reported herein examined the different stages of plastic deformation and evolution of the fine structure of face-centered crystals of copper-based solid solutions. Alloys of the systems Cu-Ga (containing Ga in amounts of 1, 3, 6, 10, and 16%,

respectively) and Cu-Ge (containing Ge in amounts of 0.08, 0.4, 5, and 8%, respectively) were studied. So that the grains obtained would be of identical size (about 40 μm), the deformed Cu-Ga and Cu-Ge alloys were annealed at 600-700°C. Round specimens with a working section measuring 6 x 30 mm were subjected to tension tests at temperatures of 77 to 1,000 K and a rate of 5 mm/min on an NIKIMP-1253-U-2-2 tension testing machine. Specimens of the test alloys were also subjected to deformation and rupture tests. The deformation hardening laws discovered were found to depend on the type of dislocation structure. The second stage of the plastic deformation of alloys with a cellular structure was found to be characterizable as follows: short duration, high value of the hardening coefficient, and moderation of the hardening coefficient as the temperature was increased. The second stage of the plastic deformation of alloys with a cellular-reticular structure was found to be characterized by a lower hardening coefficient. The diminution of this coefficient as the stress decreased was more moderate than in the case of alloys with a cellular structure, and the second stage lasted longer in the case of the cellular-reticular alloys. The second stage in the case of alloys in which multilayered and multidimensional packing defects formed was markedly longer than in the case of either of the two aforesaid types of alloys, and the hardening coefficient tended to assume a constant value as the content of alloy-forming element was increased at all temperatures. Previous research called attention to the fact that the transition from stage to stage of plastic deformation was associated with a change in dislocation structure. The present study, on the other hand, demonstrated that the characteristics of the second stage (duration, temperature dependence, etc.) affect the type of substructure formed and that this in turn is a function of energy packing defects and the magnitude of the contribution of solid-solution hardening. Figures 4; references 10 (Russian).

Determination of Regimens for the Induction Annealing of Brass Strips

927D0031I Moscow TSVETNYYE METALLY
in Russian No 7, Jul 91 pp 51-52

[Article by N.M. Shirokov, V.D. Kozhin, L.Yu. Luzhina, A.A. Filippov, M.Z. Pevzner, and S.G. Khayutin, Kirov plant OOTsM [not further identified] and Giprotsmo [not further identified]]

UDC 669.6:621.78

[Abstract] The authors of the study reported herein worked to develop an optimal regimen for annealing strips of L68 brass that contain copper in an amount ranging from 67.5 to 68.0% and that have been manufactured by hot rolling, milling, and cold rolling in two passes as is the practice at the Kirov plant OTsM. The annealing experiments were conducted on specimen strips drawn on an INPP line (as described elsewhere) at rates of 30, 34, 38, 42, and 46 m/min. Because the existing All-Union State Standards [GOST] and Specifications [TU] regulate several mechanical properties

simultaneously, the authors examined the extent to which the drawing speeds required to achieve different properties coincide. Tests performed indicated that in the case of semirigid L63 strips, the ranges of permissible speed values are in good agreement for the parameters ultimate strength, elongation, and depth of ultimate drawing, so the induction annealing of such strips will not present any problems. For a number of type sizes of strips made from L63 brass, however, the speeds required to achieve different properties do not fully coincide with one another. For this reason, additional research is required before the practice of finishing induction annealing of strips of this type may be introduced. Figures 2, tables 2; references 3 (Russian).

Current Trends in the Development and Use of Rhenium as a Catalyst

927D0031H Moscow TSVETNYE METALLY
in Russian No 7, Jul 91 pp 49-51

[Article by M.A. Ryashentseva, Organic Chemistry Institute imeni N.D. Zelinskiy, USSR Academy of Sciences]

UDC 546.719:542.971.3

[Abstract] Rhenium and its compounds are very interesting as potential catalysts. Thanks to its high melting point and high density, rhenium satisfies one of the main requirements imposed on catalysts, i.e., that they be highly resistant to recrystallization during the catalysis process. Ammonium perrhenate and rhenium heptoxide dissolve well in water, which makes them suitable for catalyst preparation by the impregnation method. From 1935 to 1987, research on the properties of rhenium and its compounds has focused on the following: the catalytic properties of rhenium and rhenium compounds, the properties of rhenium and rhenium compounds on carriers, mixed rhenium-containing catalysts, the use of rhenium catalysts in oil refining, and the physicochemical properties of rhenium catalysts. In the past few years, attention has shifted to the physicochemical properties of bimetallic Pt-Re catalysts on carriers. The research that has been conducted indicates that rhenium-containing compounds are suitable for wide-scale use in certain inorganic reactions such as the reaction of aliphatic mono- and dicarbonic acids with ammonia in the presence of hydrogen. Unlike "standard" catalysts, rhenium oxides reduce carbonic acids into the respective alcohols, and they reduce amides of carbonic acids into amines. Rhenium sulfides surpass existing catalysts of the dehydrogenation of alcohols into aldehydes and ketones, and rhenium heptasulfide is more active than Mo and Co sulfides in the hydrogenation of styrene, cyclohexene, and maleic acid of selected organosulfur compounds and in the reduction of nitrobenzene and diphenyldisulfide. Research has also been conducted on the hydrogenation of compounds of the indolysine series in the presence of Re_2S_7 for the purpose of producing new compounds that are of interest because of their biological activity. Aluminorhenium catalysts have proved to be especially interesting in the hydrogenation of $\text{C}_{10}\text{-C}_{16}$ hydrocarbon fractions of synthetic fatty acids

into the respective alcohols and in the formation of H_2 , CO , and CO_2 . When rare earth elements are added to it, aluminorhenium catalyst surpasses the commercial copper-chromium catalyst GIPKh-105 in the hydrogenation of the butyl ether fraction of synthetic fatty acids. New applications areas for rhenium-containing catalysts include the production of synthetic fuel, ammonia synthesis, exhaust gas scrubbing, the automotive industry, and "minor" chemistry (the production of organic matter in small quantities). In the USSR, the Lennestekhim Scientific Production Association has developed domestic rhenium-containing catalysts of the KR series for reforming processes. Polymetallic catalysts are being produced in quantities of 200 to 300 tons yearly and are used in about half of all domestic reforming installations (and are thus used to process more than 20 million tons of raw material a year). References 27: 25 Russian, 2 Western.

Contemporary Rhenium Determination Methods

927D0031G Moscow TSVETNYE METALLY
in Russian No 7, Jul 91 pp 44-49

[Article by L.N. Vasilyeva, Yu.A. Karpov, O.A. Shiryayeva, State Scientific Research Institute of Nonferrous Metals and State Scientific Research and Design Institute of the Rare Metal Industry]

UDC 546.719

[Abstract] The use of rhenium in new areas of science and technology in recent years has spawned increased interest in increasing extraction of rhenium from various raw materials, expanding the range of sources from which rhenium is extracted, developing new technologies, and making rational use of rhenium. Analytic testing has received an especially large amount of attention. The leading institutes of the nonferrous metallurgy sector, the USSR Academy of Sciences, and other departments have been coordinating their work in this field for the past 3 years. The most complete examination of the status of analytic testing of rhenium-containing materials occurred at the Fifth All-Union Conference on the Chemistry, Technology, and Analytic Testing of Rhenium, which was held in 1990 at the State Institute of Nonferrous Metals. Two rhenium extraction techniques have proved to be extremely attention worthy. They are 1) using ketones to extract perrhenate ions from highly alkaline media following re-extraction by means of diluted acids and 2) precipitation of rhenium (VII) in the form of rhenium sulfate. The main drawback of the first method is that extraction of perrhenate from solutions with a high concentration of salts formed during the decomposition of specimens weighing more than 2 g is incomplete. The optimal conditions for implementing the second method have been determined as follows: solution acidity, 13 to 15% HCl; amount of copper (II), 5-6 mg/l; and amount of sodium thiosulfate, 45 to 50 ml of a 10% solution. The copper and rhenium sulfides may be precipitated from either a hydrochloric or sulfuric acid medium. Sorption methods of rhenium extraction have also received a great deal of attention, as

have three different classes of sorbents: complex-forming (chelate) sorbents containing donor nitrogen and sulfur atoms, complex-forming sorbents in the form of a styrene and vinylacetate copolymer with graft maleic acid groups, and heterochain polymer sorbents with a high mass fraction of heteroatoms without an inert organic matrix. Five rhenium determination methods have also gained a great deal of attention: atomic emission spectroscopy with induction plasma, atomic emission spectroscopy with arc spectrum excitation, neutron activation, photometry, and a kinetic method involving a tellurate ion. Atomic emission spectroscopy with induction plasma has been found to have a lower threshold of detecting rhenium compounds of 0.01 to 0.02 $\mu\text{g}/\text{cm}^3$ with a relative standard deviation of about 0.02 in the presence of base components, which translates into $n \times 10^{-5}\%$ for a solid specimen without preliminary concentration of the rhenium. This detection threshold may be improved to $n \times 10^{-6}\%$ with preliminary concentration. It offers the added advantage of not being affected by the presence of molybdenum. Atomic emission spectroscopy with arc spectrum excitation has a detection threshold of 2 to 5 $\times 10^{-5}\%$ when used with a high-resolution optical system. Photometric methods permit the determination of rhenium in flotation tailings, ores, mattes, and concentrates when it is present in amounts of 0.00002 to 0.00030%. Research performed in 1989-1990 has made it possible to use tellurate ions in a kinetic rhenium determination method. The new method permits the detection of rhenium in amounts ranging from 4×10^{-6} to $1 \times 10^{-4}\%$. Applied research to improve analytic chemistry-based rhenium determination methods is currently under way in several directions. These include improving concentration techniques, creating and using standard specimens, and using nontraditional (activation, etc.) laboratory rhenium determination methods. References 15: 14 Russian, 1 Western.

The Use of Membrane Processes in the Technology of Rhenium Extraction

927D0031F Moscow TSVETNYYE METALLY
in Russian No 7, Jul 91 pp 39-40

[Article by M.V. Istrashkina, Z.A. Peredereyeva, and A.A. Belskiy, State Scientific Research and Design Institute of the Rare Metal Industry]

UDC 669.849:661.074.7

[Abstract] Electrodialysis and membrane electrolysis processes are very promising in the field of the metallurgy of rare elements. They are promising on two counts: as ways of separating and concentrating liquid mixtures and as ways of isolating and obtaining ultra-pure substances. Electrodialysis and membrane electrolysis may, for example, be used to produce high-purity rhenium salts and rhenic acid from commercial-grade potassium perhenate and ammonium perhenate virtually without the loss of any reagents. At the present time, rhenium is extracted from sulfuric acid molybdenum-containing solutions by the conventional methods of ion exchange and extraction. The authors of the study

reported herein conducted a series of experiments to develop a new membrane electrolysis process to replace these conventional rhenium extraction techniques. The experiments were conducted in a three-chamber electrodialysis unit. The unit was made of acrylic plastic and had a membrane working surface of 0.01 m^2 . The anodes used in all the experiments were made of platinized titanium, and the cathodes were made of either stainless steel or titanium depending on the specific membrane and pH used in the given experiment. The experiments were designed to study the kinetics of the process of the electrodialysis of a model solution containing 1.5 g/dm^3 rhenium, 8.5 g/dm^3 molybdenum, and 65.0 g/dm^3 sulfate ion. MA-411L heterogeneous and MK-100 homogeneous membranes were used at current densities of 170 to 200 A/m^2 . After 1 hour of electrodialysis under the said conditions, the content of rhenium in the dialysate was reduced to 50%, after 4 hours, it reached 3 to 5% of the starting amount. The molybdenum remained primarily in the dialysate (about 80-90% of the starting amount). As the acidity of the solution was increased, the rate of migration of rhenium to the anode chamber decreased. This was attributed to the competing effect of the sulfate ion. Passage of rhenium through the membrane was higher when molybdenum was present in the sulfuric acid solution than when it was not. This was attributed to the fact that molybdenum reduces the competing effect of the sulfate ions by binding them. Separation of rhenium from molybdenum was virtually complete in the concentration range from 0.5 to 0.75 $\text{gEq}/\text{dm}^3 \text{H}_2\text{SO}_4$. Current density played a decisive role in the intensity of ion transfer during the electrodialysis process, with 200 A/m^2 being the optimal current density. Temperatures between 55 and 60°C proved to be best. Both MA-411L and MK-100 membranes yielded good results. Table 1; references 11: 10 Russian, 1 Western.

Extracting Rhenium While Processing Molybdenite Concentrates

927D0031E Moscow TSVETNYYE METALLY
in Russian No 7, Jul 91 pp 33-39

[Article by V.K. Rumyantsev, S.G. Voldman, V.V. Kulakova, All-Union Scientific Research and Design Institute of Refractory Metals and Hard Alloys]

UDC 553.462:669.849.3

[Abstract] Molybdenite concentrates are the main source of rhenium. Depending on their individual deposit of origin, molybdenite concentrates contain between 10^{-3} and $10^{-1}\%$ rhenium. The molybdenite concentrates and by-products processed in the USSR are comparatively rich in rhenium, containing from 0.2 to 0.7 kg rhenium per ton of concentrate. One of the main ways of extracting rhenium is that of using salts of quarternary ammonium bases to remove rhenium from solutions passed through wet gas and dust traps. The main drawbacks of the process of extraction from solutions are the need for preliminary neutralization of the sulfuric acid solutions, the high alkali (soda) consumption of the

process, the need to use perchloric acid and hydrogen sulfide, and the complexity of reprocessing the re-extract into ammonium perrhenate. The process of extracting rhenium from dusts is about as effective as processes of extraction from solutions. Molybdenum cinders contain up to 10% rhenium, and a sorption process developed to extract rhenium from them has made it possible to increase the effectiveness of extracting rhenium from molybdenite concentrates by 3 to 7%. Another rhenium extraction technique is that of extracting rhenium during the hydrometallurgical processing of molybdenite concentrates. Various extraction and sorption processes have been developed to accomplish this, and there is general agreement that trialkylamine [TAA] is the best extractive reagent for the process. The Moscow Institute of Steel and Alloys has developed an extraction technology for processing nitrate-sulfate mother liquors for two-stage nitric acid decomposition of molybdenite concentrates. The process includes the selective extraction of molybdenum by a 7-8% solution of di-2-ethylhexylphosphoric acid followed by extraction of rhenium from the raffinate by a 7-8% solution of TAA with a tributylphosphate additive. Continuous sorption processes for the formation of molybdenum from nitrate-sulfate pulps and mother liquors appear to be preferable to analogous extraction processes. In the past few years, the All-Union Scientific Research and Design Institute of Refractory Metals and Hard Alloys has been working to develop a new sorption process for rhenium extraction. It was introduced in 1989 and enabled the enterprise using it to meet its plan quotas for the year. The most complete extraction of rhenium is achieved by autoclave oxidation of molybdenite concentrates or their by-products in an alkaline medium. This is because nitrate-free solutions are obtained in the process. According to the most recent work published on this topic (Sobol, Gedgagov, et al. in TSVETNYE METALLY, No 3, 1991), sorption methods are the best approach to use in the comprehensive processing of alkaline molybdenite solutions with simultaneous extraction of rhenium and tungsten. Figures 2; references 39: 30 Russian, 9 Western.

Boosting Rhenium Production at Nonferrous Metallurgy Enterprises

927D0031D Moscow TSVETNYE METALLY
in Russian No 7, Jul 91 pp 32-33

[Article by A.D. Besser and A.V. Peredereyev, State Scientific Research Institute of Nonferrous Metals and USSR Ministry of Metallurgy]

UDC 669.849.003

[Abstract] The USSR has taken a number of steps to meet the ever-increasing demands for rhenium in such diverse sectors as electronics, the aerospace industry, and petrochemistry. An all-union scientific-technical conference entitled "Chemistry, Technology, and Analytical Control of Rhenium" was held in 1990. The conference was attended by scientists and specialists from 16 enterprises and 29 institutes of various sectors of the

national economy of the USSR Academy of Sciences, Kazakhstan Academy of Sciences, and various higher educational institutions. A comprehensive program to increase rhenium production was developed in 1989-1990. The program included scientific research, design, and planning projects directed toward increasing the engineering level of the rhenium production process and improving procedures for the analytical testing of rhenium. In 1989, production of ammonium perrhenate, the basis of rhenium production, increased by 6.13% over the 1988 level and was increased even more in 1990. New guidelines have also been developed to boost rhenium extraction at enterprises currently processing rhenium-containing ore. Among other things, these guidelines call for introducing low-waste copper-smelting technologies, constructing new shops to anneal molybdenum concentrates to obtain ferromolybdenum from which rhenium can eventually be extracted, and setting up procedures to extract rhenium from spent aluminum-platinum catalysts. Steps must also be taken to set prices for rhenium and rhenium-containing materials that would stimulate interest in increasing rhenium recovery and extraction efforts. Planning and material-and-technical supply organizations at the union, regional, and sector levels must provide additional assistance to enterprises involved in rhenium production.

Comprehensive Use of Slags of Ural Nickel Enterprises

927D0031C Moscow TSVETNYE METALLY
in Russian No 7, Jul 91 pp 19-21

[Article by A.N. Fedorenko, Yu.A. Karasev, Ye.R. Tokareva, A.L. Rozovskiy, A.P. Pigina, and L.I. Unguryan, State Scientific Research and Design Institute of the Nickel Industry and Uralniustromproyekt (not further identified)]

UDC 669.243

[Abstract] The authors of the study reported herein examined the possibility of reprocessing the granulated waste slags produced at Ural nickel enterprises for the purpose of extracting additional nonferrous metals by magnetic separation and then using them in the construction industry. Pilot studies were conducted on granulate waste slags from the smelting processes currently under way at three enterprises: the YuUNK, the UNK, and the RNZ [enterprises not further identified]. The said slags were determined to have a moisture content of 2.5 to 3.5% and to consist mainly of silicate glass containing oxide inclusions and metal sulfide beads ranging mainly from 2 to 20 μm in size. The slags were subjected to pulverization on two different drying-grinding mills at the Central Ore Enrichment Combine Mekhanohermet Production Association. The slags were ground to a consistency suitable for use as fine filler to replace the natural sand used in making concretes. After pulverization, the slags were subjected to magnetic separation on a PBSh-80 dry magnetic separator to extract the nickel and cobalt remaining in their magnetic fraction. The magnetic concentrate was found to consist

of silicates, an oxide phase, and two types of beads (i.e., metal sulfide and metal). The beads of the magnetic concentrate removed from the waste slags at the YuUNK, UNK, and RNZ contained 37.3, 27.3, and 16.9% Ni beads and 0.85, 1.54, and 0.64% Co, respectively. Because its dust loss (about 6%) and composition made it suitable for construction purposes, the remaining pulverized waste slag was diverted for use as a concrete filler. The magnetic concentrate was returned to the metallurgical process cycle. Provisions have recently been made to process 1.0 million tons of waste slag at the UNK annually. Technical and economic projections indicate that processing 0.95 million tons per year will require a capital investment of 12.6 years, that 4.7 years will be required to recoup this initial investment, and that the process will result in a profit of 2.6 million rubles. Plans are being made to adopt the process at the YuUNK and RNZ as well. It is projected that processing 3.5 million tons of waste slag annually at the YuUNK will require 24.7 million rubles in capital investment, require 5.6 years to recoup the initial investment, and result in a profit of 4.6 million rubles. In the case of the RNZ, the projections are that processing 0.995 million tons of waste slag per year will require an initial capital investment of 6.96 million rubles, require 5.5 years for the process to pay for itself, and will result in a profit of 1.28 million rubles. Figure 1, table 8.

Cobalt Extraction in the Smelting Shop of the Severonikel Combine

927D0031B Moscow TSVETNYE METALLY
in Russian No 7, Jul 91 pp 10-13

[Article by I.D. Reznik, V.M. Khudyakov, Ye.S. Kondyrev, M.S. Chetverkov, T.A. Kharlakova, and M.Yu. Kozlov, State Scientific Research Institute of the Nonferrous Metals, and Severonikel Combine]

UDC 669.243:669.25

[Abstract] In 1985 the practice of autogenous smelting was introduced at the Severonikel Combine. The authors of this article compared cobalt extraction operations in the combine's smelting shop in 1984 (the final year before autogenous smelting was adopted) and 1989. In 1984, 31.90% of the cobalt available for extraction was lost with slag. Difficulties in assimilating the new autogenous smelting process caused this indicator to rise to 34.38% in 1985 and to peak at 36.52 in 1986. Improvements made in the process resulted in a decline in cobalt losses with slag from that point on, culminating in a loss of 30.50% in 1989. This improvement was attributed to the fact that the extraction process was modified to include the additional operation of depleting the autogenous smelting slags in a specially equipped electric furnace. In addition, a number of process techniques were developed to reduce cobalt losses in the ore-smelting furnaces, which is where half of all losses of cobalt with slag occur. Other process indicators more difficult to compare directly because of changes in the relative percentages of different ores and mattes processed at the combine in the years between 1984 and

1989. Thanks to the fact that richer mattes were available, for example, the amount of converter slags produced was nearly cut in half. Another change that resulted in an improvement in process indicators was the fact ore from the Norilsk area began to be used almost exclusively instead of matte in the ore-depleting furnaces. Also because of these particular changes, cobalt extraction rose from 72.1% in 1984 to 81.5% in 1989, and nickel extraction rose from 94.2 to 95.4% in the same period. Studies performed in the smelting shop demonstrated that cobalt extraction could be improved even further within the framework of the extraction process and equipment currently being used. The following are among the recommendations offered to further improve cobalt extraction: keep the SiO_2 content in slags at a level of 43 to 45%, increase reducing agent consumption and increase the content of metallic iron in the mattes from 5 to 8-10%, do not use mattes containing less than 1.5% Co, switch completely to a mode of semicontinuous depletion so that the amount of cobalt in the waste slags of the ore-depleting furnaces do not exceed 0.06% in any one stage, improve the ore-reducing conditions in the electric furnaces by sealing the roofs, adopt the practice of pouring high-silica ore-heating furnace slags to stabilize the SiO_2 content in the slags, and equip furnaces with automatic sampling devices. Tables 6; references 5 (Russian).

Oxysulfide Formation During the Pyrometallurgical Treatment of Nickel Mattes and Converter Slags

927D0031 Moscow TSVETNYE METALLY
in Russian No 7, Jul 91 pp 6-10

[Article by I.D. Reznik, Ye.N. Selivanov, A.I. Okunev, E.Ya. Gurevich, T.A. Kharlakova, and Yu.A. Sasovskikh, State Scientific Research and Design Institute of the Nonferrous Metallurgy Industry and Metallurgy Institute, Ural Department, USSR Academy of Sciences]

UDC 669.243

[Abstract] Research has shown that in a number of pyrometallurgical processes, FeO-FeS oxysulfide forms as a separate layer during melting into matte and slag. The existence of three nonmixing phases (including a melt with a composition approximating FeO-FeS-CaO that is in equilibrium with the metal sulfide alloy) has been established in complex oxide-sulfide systems involving nickel matte. In view of these facts, the authors of the study reported herein examined the characteristic features of stratification in oxide-sulfide systems simulating the processes of conversion of nickel mattes with a calcium flux and the depletion of highly basic slags. The experiments were performed in a laboratory electric furnace at 1,300°C. Weighted portions of charge were placed in an open corundum crucible that was then placed into a heated furnace. After the melt had been held for 30 minutes, the crucible was removed from the furnace and cooled. The products of the melting process were isolated and analyzed. Nuclear gamma-ray resonance spectroscopy and chemical phase analysis were

used to determine the forms in which the iron existed. The conversion process was simulated by using different portions of nickel matte from ore smelting, converter matte, and iron oxide. Blast furnace slag and quartz were used as a flux. As the degree of oxidation was increased and as matte with 13.1% Ni was produced, three layers enriched with matte, slag, and oxysulfide alloy respectively were observed to form. The following regression equation was derived to express the dependence of oxysulfide yield (P) on the content of nickel in the matte and basicity of the slag ($r = 0.93$):

$$P = 1.02 + 205.2B - 153.5B^2 - 150[Ni] + 0.007[Ni^2].$$

The research conducted indicated that obtaining calcium silicate converter slag with a basicity close to 1 and without the formation of oxysulfide requires mixing the slag used in the conversion process with concentrated slag containing at least 35 to 40% Ni. On the basis of the studies conducted, the researchers concluded that within the framework of existing technologies, the possibility of intensifying the process of depleting slags by adding calcium-containing fluxes is limited by the conditions of the formation of an oxysulfide alloy. They also concluded that in view of the low desulfurization and accumulation of sulfur in oxysulfide alloy, it is possible to use oxysulfides as new forms of sulfidizers in a number metallurgical processes. Figures 2, tables 3; references 10 (Russian).

The Effect of Deformation in a Superplasticity Regimen on the Structure and Properties of Ingots of the Alloy Al-Li

927D0050F Moscow IZVESTIYA AKADEMII NAUK SSSR. SERIYA METALLY in Russian No 5, Sep-Oct 91 (manuscript received 10 Apr 90) pp 115-118

[Article by V.M. Sovenko and Yu.B. Timoshenko, Ufa]

UDC 669.715'884:539.52

[Abstract] The authors of the study reported herein examined that effect that deformation in a superplasticity mode has on the structure and properties of ingots of an Al-Li-Cu-Mg alloy containing aluminum and the following additional elements: Li, 2.18%; Cu, 1.35%; Mg, 0.93%; and Zr, 0.11%. The ingots were produced by the semicontinuous method. They were poured at a rate of 36 to 42 mm/min at a pour temperature of 700 to 720°C. To determine the effect of the thermomechanical parameters of the deformation process on the structure and properties of the alloy, specimens of the alloy were upset under isothermal conditions on a 1231U-10 universal testing machine at deformation rates ranging from 10^{-4} to 10^{-2} /s with the degrees of deformation of each specimen ranging from 20 to 80% and with the temperature ranging from 200 to 500°C. An Instron testing machine was used for the mechanical tests. The tests performed demonstrated that isothermal deformation in the temperature interval from 400 to 500°C and at the aforementioned deformation rates results in the formation of a

uniform fine-grained microstructure. After such treatment, the test specimens proved to have high mechanical properties. Specifically, specimens subjected to omnilateral isothermal forging in a superplasticity regimen in three mutually perpendicular directions at temperatures between 450 and 500°C followed by hardening at 525°C, cooling in water, and aging at 170°C for 18 hours had an ultimate strength that was 25% greater than the ultimate strength of specimens subjected to homogenizing annealing. Moreover, the test alloys subjected to the stated regimen had a relative elongation that was 136% of the latter. The specimens thus treated had a grain size of 8 to 25 μ m and were not marred by any clearly pronounced bands in their structure. Figures 3, table 1; references 3: 2 Russian, 1 Western.

The Occurrence of Low-Energy Interfaces During the Annealing of Titanium Alloys

927D0042G Sverdlovsk FIZIKA METALLOV I METALLOVEDENIYE in Russian No 5, May 91 (manuscript received 5 Apr 90; after revision 27 Oct 90) pp 142-147

[Article by M.I. Mazurskiy, Institute of the Problems of the Superplasticity of Metals, USSR Academy of Sciences]

UDC 669.295:620.186.8

[Abstract] The author of the study reported herein examined the process of the occurrence of interfaces when a titanium alloy is annealed. The alloy VT5-1, which contains 5.4% (by weight) Al and 2.3% (by weight) Sn, was studied. A blank of VT5-1 was first deformed at 800°C (the α -region) and then cut into sections. Sections were annealed at 1,000°C (the $\alpha + \beta$ region) for 2, 20, and 50 hours, after which they were quenched in water. The resultant microstructure was developed by a mixture of hydrofluoric acid, glycerin, and acetic anhydride. Analysis of the specimens revealed that in the beginning of the annealing process, simultaneous development of $\alpha \rightarrow \beta$ recrystallization results in the formation of a microstructure with predominantly equiaxed (polyhedral) phase grains. After 2, 20, and 50 hours the volume fraction of α -phase in the study specimens amounted to 39.7 \pm 1.5%, 32.0 \pm 2.0%, and 32.4 \pm 1.9%, respectively. The lack of any significant change in the volume fractions in the interval between 20 and 50 hours was taken as confirmation that phase equilibrium had taken place. After a holding time of 20 hours the maximum distribution was in the angle interval from 120 to 130°. After 50 hours this maximum was smeared. Detailed microstructural studies revealed that new β -particles having "unique" low-energy interfaces appeared within the α -grains during the course of the annealing. These new particles were observed mainly around the starting ternary joints in the form of triangles. They also developed on individual interfaces and intergrain boundaries. The nature of the test specimens' microstructure changed as annealing time was increased. Specifically, α -grains that had formerly been neighbors became separated from one another by the growing β -phase particles.

and many α -grains acquired a close-to-plastic form. This process of the formation of new particles was explained in terms of a tendency toward a decrease in the interface energy in the system due to the replacement of random high-energy interfaces by low-energy interfaces. Figures 4; references 12: 9 Russian, 3 Western.

The Effect of Directed Crystallization and Heat Treatment Conditions on Porosity in Monocrystals of Nickel Refractory Alloys

927D0050D Moscow IZVESTIYA AKADEMII NAUK SSSR: SERIYA METALLY in Russian No 5, Sep-Oct 91 (manuscript received 17 Apr 90) pp 70-76

[Article by V.N. Tolorayia, A.G. Zuyev, and I.L. Svetlov, Moscow]

UDC 669.24.245

[Abstract] The authors of the study reported herein examined the distribution of pores in a non-carbon-containing nickel alloy that is especially intended for casting monocrystals. Specifically, they examined pore distribution in the said alloy as a function of directed crystallization conditions and as a function of high-temperature homogenization. They also studied the effect that micropores have on the nature of the monocrystals' fracture during the process of protracted high-temperature tests. Monocrystals of the refractory metal alloy were produced by directed crystallization in the form of cylindrical ingots 18 mm in diameter with an orientation of (001). A portion of the specimens were studied in a poured state. The remaining specimens were studied after homogenization under a regimen entailing heating at 1,320°C for 4 hours and cooling in a vacuum at a rate of 40 to 60°C/min. The quantitative metallographic studies and protracted strength tests performed indicated that, in a poured state, the pores have the appearance of cracks along the interface of the $\gamma + \gamma'$ eutectic. After heat treatment, the pores assume a round shape, and their volume fraction increases. As the temperature gradient at the growth front increases, the volume fraction of the pores decreases. It increases as the growth rate increases. Fracture of the monocrystals during the creep process was found to begin in the neck zone on the working part of each specimen. Crack propagation in specimens with an orientation of (001) was found to occur perpendicular to the specimen's axis, and the rate of propagation was found to be anisotropic. Figures 3; references 4 (Western).

Alterations in the Crystalline Structure of Martensite After Co-W and Co-Mo Alloys Have Been Doped With a Third Element

927D0042D Sverdlovsk FIZIKA METALLOV I METALLOVEDENIYE in Russian No 5, May 91 (manuscript received 11 Sep 90) pp 99-105

[Article by B.I. Nikolin, A.Yu. Babkevich, T.V. Izdkovskaya, and S.N. Petrova, Metal Physics Institute, UkSSR Academy of Sciences]

UDC 669.255:620.186.1

[Abstract] The authors of the study reported herein performed a roentgenographic examination of the crystalline structure of martensite formed in Co-15% W-(2-3%) Fe, Co-(7-20) Mo, Co-13% Mo-2% (Fe, Mn, Ni), and Co-13% Mo-(2-3%) Si monocrystals after hardening and aging in the α - and β -phases. The major findings of the experiments performed may be summarized as follows. Long-period martensite structures representing martensite polytypes were observed to form in Co-15% W-(2-3%) Fe, Co-13% Mo-2% Fe, and Co-13% Mo-2% Ni monocrystals after hardening and aging in the β -phase at temperatures ranging from 500 to 750°C. A martensite α -phase with a 2H lattice was observed to form in Co-Mo, Co-13% Mo-(2-3%) (Fe, Ni, Si, Mn) monocrystals after aging at temperatures of 500 to 600°C. This martensite α -phase was not transformed into other densely packed martensite structures. Aging the α - and β -phases of Co-W-Fe, Co-Mo, and Co-Mo-(Fe, Ni, Si, Mn) monocrystals at temperatures from 500 to 700°C was found to result in a continuous decomposition of supersaturated solid solutions of the said monocrystals. This decomposition in turn resulted in the appearance of satellites on the specimens' roentgenograms. These findings led the researchers to hypothesize that the mechanism of the effect of dopant alloys on the formation of polytype-multilayer martensite structures in ternary cobalt alloys is more complicated than previously publications would indicate. They further hypothesized that this effect mechanism is connected with change in the electron structure of the alloys in question. Figure 1, tables 2; references 9: 6 Russian, 3 Western.

Features of Avalanche (Explosive) Crystallization of Bi-Pb Amorphous Films

927D0042I Sverdlovsk FIZIKA METALLOV I METALLOVEDENIYE in Russian No 5, May 91 (manuscript received 2 Oct 90; after revision 25 Dec 90) pp 169-174

[Article by V.M. Kuzmenko and Yu.V. Navozenko, Kharkov Physics Engineering Institute, UkSSR Academy of Sciences]

UDC (669.4'76+539.216.2):548.5

[Abstract] The authors of the study reported herein examined the effect of small concentrations of lead on the crystallization parameters of Bi-Pb amorphous films. Their primary objective in so doing was to determine the laws governing the process of nonattenuating (self-sustaining) and attenuating avalanche crystallization of amorphous bismuth films containing 0.5 to 5% (atomic) lead. Bi-Pb alloys containing 0.51, 0.95, 1.84, 2.32, 3.85, and 5.1% (atomic) lead were produced by the technique of vacuum melting in quartz crucibles at a temperature of 680 K or thereabout. Vaporization of the alloy to prepare the study films was accomplished by the resistive technique from tungsten vaporizers. The studies performed revealed that regardless of their lead concentration, Bi-Pb films underwent the transition from the

amorphous to the crystalline state in the range of temperatures from 13.5 to 14.5 K (approximately the same temperature as for pure Bi). Unlike in the avalanche crystallization process, however, the rate of bulk crystallization in the case in question ranged from 10^{-3} to 10^{-1} of the specimen's volume per minute. The resistivity ρ of all of the amorphous films studied also coincided (within the bounds of the measurement error) with the resistivity of pure amorphous Bi (i.e., $140 \pm 20 \mu\Omega\text{-cm}$). The temperatures at which Bi-Pb amorphous films undergo the transition to a state of superconductivity was found to have a tendency toward a slight increase relative to the T_c of amorphous Bi films as the Pb concentration increased. Directly after the $a \rightarrow k$ transition, however, the resistivity of Bi-Pb films becomes very different from the resistivity values for pure Bi films and proves to be clearly dependent on the concentration of Pb dopant. The increase in the heat conduction of Bi-Pb films that occurs as the amount of lead in the films is increased was found to result in an increase in the threshold thickness d^* , which was found to be in qualitative agreement with the existing theory. The authors further concluded that for one and the same Bi-Pb film composition, the fluctuating nature of the manifestation of the critical thickness d_c means that either of the opposite equalities may occur: $d^* > d_c$ and $d^* < d_c$. They further show that it is this fact that determines whether avalanche crystallization will be attenuating or not. Figure 4, table 1; references 15 (Russian).

Carbide Formation in a Cast Nickel Refractory Alloy

927D0050E Moscow IZVESTIYA AKADEMII NAUK SSSR: SERIYA METALLY in Russian No 5, Sep-Oct 91 (manuscript received 19 Apr 90) pp 108-110

[Article by A.V. Shulga, V.V. Nikishanov, M.S. Podolskiy, and L.G. Kuzmicheva, Moscow]

UDC 669.24.018-492.3

[Abstract] The authors of the study reported herein examined carbide formation in a nickel refractory alloy with the following composition: Ni + 9% Cr + 15% Co + 5% Al + 2% Ti + 2% Nb + 1% Mo + 10% W + 1% Fe. The study alloy was examined in its initial poured state as obtained by double vacuum remelting as well as after graduated heat treatment at temperatures of 1,230, 1,190, and 1,170°C and hot deformation. The distribution of carbon in the alloy was analyzed by activation autoradiography, and the nature and composition of the carbide phase were determined by x-ray spectral microanalysis and electrochemical isolation. The distribution of carbon in the peripheral portion of the ingot was found to be characterized by the formation of disperse agglomerates caused by the presence of carbide-phase particles. The distribution of "point" carbon agglomerates in the peripheral part of the ingot was virtually uniform throughout the bulk of the metal without preliminary isolation along grain boundaries. In the center part of the ingot the carbon was formed a pattern of carbide particles of a nonequilibrium carbide

eutectic in the dendrite structure of the ingot. The axes of the dendrites were characterized by a reduced carbon content. The interaxial segments, on the other hand, were rich in carbon and contained isolated carbon-phase particles. The ingot was demonstrated to contain type MeC carbide phase in the amount of approximately 0.6% with a lattice period of 0.443 nm. This carbide phase was rich in titanium, niobium, and tungsten, with the nickel in the phase amounting to about 3% (atomic) and the chromium and cobalt amounting to about 1% (atomic). After heat treatment, the distribution of carbon in the form of carbide-phase particles remained uniform in the peripheral part of the ingot, just as was the case prior to heat treatment. The particles were smaller and more disperse, however. The dendritic nonuniformity of the particles in the central part of the heat-treated ingots was preserved after heat treatment; however, the sizes of the "decarbonized" dendrite axes increased, as did the growth of the agglomerates of carbide-phase particles in the interaxial segments. This increase in the dispersivity of the carbide-phase particles in the peripheral part of the ingot was attributed to 1) their dissolution as the carbon passed into a solid solution, 2) the diffusion of the metal atoms of the carbide formers into the matrix and γ' -phase, and 3) the occurrence of carbide reactions. The heterogenization of the structure in the central part of the ingot was attributed to a process of the further decay and coagulation of carbide-phase particles in structurally defective interaxial areas. Heat treatment resulted in an increase in the niobium content in both the γ' -phase and the matrix. Titanium was also involved in the formation of the γ' -phase following heat treatment, albeit to a lesser extent. A uniform redistribution of the carbide-phase particles was also observed in the study specimens after hot deformation. Figure 1; references 6: 4 Russian, 2 Western.

Spin Fluctuations in Weakly Ferromagnetic Ni-Al Alloys

927D0042B Sverdlovsk FIZIKA METALLOV I METALLOVEDENIYE in Russian No 5, May 91 (manuscript received 5 Jun 90; after revision 11 Sep 90) pp 48-52

[Article by Yu.V. Kudryavtsev, I.N. Mishchenko, Ya. Dubovik, and Ye.A. Ganyshina, Metal Physics Institute, UkSSR Academy of Sciences, and Molecular Physics Institute, Poland Academy of Sciences, and Moscow State University imeni M.V. Lomonosov]

UDC 669.245:538.221

[Abstract] The authors of the study reported herein used the methods of magnetometry and optical and magneto-optical spectroscopy to examine the spin fluctuations occurring in Ni-Al alloys and to determine how their state changes with temperature. Alloys containing 75.2 and 77% (atomic) Ni and possessing a γ' -phase structure were used for the studies. These alloys are weak band ferromagnetics with Curie temperatures of 50 and 78 K.

respectively. The alloy bars from which the test specimens were obtained were made from nickel and aluminum with respective purities of 99.999 and 99.99% (atomic) that were fashioned into bar-shaped ingots 8 mm in diameter and 80 mm long by argon-arc melting of the charge and pouring the resultant melt into a copper chill mold. The test specimens were cut from the bar by the electrosark method, and the surface of each specimen was subjected to mechanical polishing followed by annealing in an ultrahigh vacuum at 620 K. The temperature dependences of reverse magnetic susceptibility were plotted for three different test specimens with different compositions and degrees of structural perfection. In the case of the most perfect monocrystal (i.e., an annealed $\text{Ni}_{75.2}\text{Al}_{24.8}$ monocrystal), the curve of the temperature dependence contained one sharp bend at about 530 K. The curves plotted for the temperature dependences of the other two specimens (a nonannealed $\text{Ni}_{75.2}\text{Al}_{24.8}$ monocrystal and a $\text{Ni}_{77}\text{Al}_{23}$ monocrystal) contained sharp bends at temperatures of about 480 K and 520 K and anomalies in the regions of higher

temperatures. In all three curves plotted, the temperature dependence of reverse magnetic susceptibility is subject to a Curie-Weiss law both below and above the first sharp bend. The temperature at which the sharp bend was observed is significantly higher than T_c and is close (from an order of magnitude standpoint) to the value of T_c calculated in accordance with the microscopic theory. The optical conduction spectra of $\text{Ni}_{77}\text{Al}_{23}$ at different temperatures (the spectra of $\text{Ni}_{75.2}\text{Al}_{24.8}$ were found to be virtually identical) revealed strong interband absorption bands in the infrared and ultraviolet regions of the spectrum. In the low-energy band below 360 K it was possible to observe a fine structure that did not undergo any changes when T_c was reached and surpassed. The magnitude of the Kerr equatorial effect also remained unchanged at the T_c transition. These findings were found to be easily explainable within the framework of a model in which spin fluctuations are microdomains with fluctuating directions of the magnetic moments. Figures 3, table 1; references 9: 1 Russian, 8 Western.

Use of the Kunzler Method To Produce Wires From $\text{YBa}_2\text{Cu}_3\text{O}_{7-x}$ Superconductor Ceramics

927D0042H Sverdlovsk FIZIKA METALLOV I METALLOVEDENIYE in Russian No 5, May 91 (manuscript received 28 Nov 90) pp 148-163

[Article by M.I. Karpov, V.P. Korzhov, A.A. Snegirev, B.A. Gnesin, R.K. Nikolayev, and N.S. Sidorov, Solid-State Physics Institute, USSR Academy of Sciences]

UDC 669.3868:(546.562+538.945):669.426.2

[Abstract] The authors summarize the results of research regarding the production of superconducting wire from $\text{YBa}_2\text{Cu}_3\text{O}_{7-x}$ by what has become known as the Kunzler method, i.e., by deforming oxide powder in a metal sheath. A copper rod 18 to 20 mm in diameter and about 80 mm long with a central blind cylindrical cavity 12 mm in diameter that had been prefilled with synthesized $\text{YBa}_2\text{Cu}_3\text{O}_{7-x}$ ceramic powder was used as the starting rod. Rods consisting of a Cu core with a blind hole, a niobium tube placed in the hold, and a $\text{YBa}_2\text{Cu}_3\text{O}_{7-x}$ powder filler were also used. The $\text{YBa}_2\text{Cu}_3\text{O}_{7-x}$ powder was prepared in accordance with a three-step process entailing solid-phase synthesis, hydrogen reduction, and oxidation. Powders manufactured by using conventional solid-phase synthesis at 950°C were also used. Y_2O_3 , CuO, and BaO_2 powders served as the starting reagents. The oxide powder produced had a grain size of <250 μm . Three types of wire were produced and examined: wire made of $\text{YBa}_2\text{Cu}_3\text{O}_{7-x}$ ceramic in Cu and Cu/Nb sheaths, wires with precious metal interlayerings, and wires with an aluminum diffusion interlayering. The studies performed revealed that superconductivity is not maintained at temperatures greater than 4.2 K in wires with 2-mm-diameter Cu and Cu/Nb sheaths. The degree of the effect of deformation on the parameters of the superconductivity transition in such wires was found to depend on the quality of the starting ceramic. Powders produced by the three-step process were found to undergo less degradation than did powders produced by conventional solid-phase synthesis. In those cases where superconductivity of the ceramic was maintained (for example, in Cu/Nb/ $\text{YBaCuO}/\text{BaO}_2$ wire), the superconductivity transition occurred far below 90 K with a ΔT_c reaching several tens of degrees. Subsequent heat treatment of wires of this type did not restore the high-temperature superconductivity of the ceramic core due to the intensity reaction of the ceramic with the copper or niobium sheath. The Cu/St3/Ag/ YBaCuO wire with an interlayering of silver 54 μm thick that the researchers produced in an attempt to conserve precious metals had the following superconductivity properties after heat treatment in an O_2 flow at 925°C for 2 hours: j_c (77K, 0 T) \approx 260 A/cm²; T_c = 89 K; and ΔT_c = 2.5 to 3.0 K. The wires produced with gold interlayerings were found to possess high-temperature superconductivity even after heat treatment; however, the gold layers contained a large amount of lengthwise cracks that could not be avoided even when rather thick (66 to 77 μm) layers were used. In the $\text{YBa}_2\text{Cu}_3\text{O}_{7-x}$ ceramic wires that the

researchers produced with Cu and Cu/Nb sheaths and aluminum interlayerings, the aluminum interlayers proved to protect the ceramic against reactions with the sheath even in the case of heat treatment all the way up to 950°C. In specimens of the said wires that were notched at a distance up to 10 mm from the ends, the ceramic had a superconductivity onset temperature up to 92.5 K, a T_c of about 91 K, a ΔT_c of or less than 16.5 K, and a j_c at 77 K and 0 T at currents up to about 380 A/cm². In wires with a continuous gap between 0.1 and 0.6 mm wide the ceramic had identical superconductive properties throughout the entire length of the wire. In wires where the Al interlayering was kept continuous (not notched), the researchers found that those segments of wire that had been cut farther from the end of the piece were characterized by worse superconductivity parameters than were segments cut closer to the end. Figures 8, tables 7; references 13: 1 Russian, 12 Western.

Partial Displacements of Atoms in $\text{YBa}_2\text{Cu}_3\text{O}_7$ Under the Effect of High-Energy Particles

927D0042A Sverdlovsk FIZIKA METALLOV I METALLOVEDENIYE in Russian No 5, May 91 (manuscript received 11 Jul 90) pp 39-47

[Article by N.N. Degtyarenko, V.F. Yelesin, and V.L. Melnikov, Moscow Physics Engineering Institute]

UDC (546.562+538.945):539.12.04

[Abstract] The authors of the study calculated the partial numbers of displacements (c_{di}) for various subsystems of the superconductive compound $\text{YBa}_2\text{Cu}_3\text{O}_7$ under the effect of different types (i.e., ion and neutron) of irradiation. The customary procedure for computing partial cascade functions involves tracking the paths of all of the knock-on atoms until their energy drops below T_{min} . To accelerate this procedure, the authors of the present study tracked the path of just the initial knock-on atom. On the basis of their computations, they concluded that in the presence of a cascade damage structure, the distribution of displacements between the subsystems of $\text{YBa}_2\text{Cu}_3\text{O}_7$ (and evidently that of other high-temperature superconductors as well) does not depend on the energy of the primary radiation. They also found that in the case of the high energies at which primary knock-on atoms are formed, it does not depend on the type of irradiation either. In the case of electron and proton irradiation, which create a comparatively soft initial knock-on atom spectrum, there was no leveling off at a constant c_{di} value as the energy was increased. The partial number of displacements for a subsystem of weakly bound oxygen is severalfold higher than for metallic subsystems. The stability of $\text{YBa}_2\text{Cu}_3\text{O}_7$ was found to be significantly dependent on the starting values of the superconductivity parameters of the given specimen. For specimens with a $T_{c0} > 88$ and a narrow transition, the values of $c_{di}(T_c/T_{c0} = 12)$ were found to coincide for the different types of irradiation. Those $\text{YBa}_2\text{Cu}_3\text{O}_7$ specimens that were of the highest quality

demonstrated the best radiation stability. In view of the linear nature of the dependence $T_c(\Phi)$ (Φ being the fluence of the irradiation), the authors hypothesized that the dependence T_c/T_{c0} is universal for the system $YBa_2Cu_3O_7$, regardless of the displacements just as the previously observed analogous dependence was for Nb_3Sn . Figures 7, tables 2; references 35: 12 Russian, 23 Western.

The Heat Conduction of Turbostrate Boron Nitride

927D0029H Kiev POROSHKOVAYA

METALLURGIYA in Russian No 8, Aug 91

(manuscript received 8 Sep 89) pp 75-78

[Article by Sh.Sh. Abelskiy, A.L. Zilichikhis, L.S. Parfenyeva, I.N. Kulikova, and E.A. Knyshev, Ural Forestry Engineering Institute, Physics Technology Institute, Kristall Scientific Production Association]

UDC 546.273.171:536.2.01

[Abstract] The authors of this article conducted an experimental study of the heat conduction (χ) of pressed specimens of boron nitride with different degrees of three-dimensional disorder (γ). The measurements were taken in the temperature range from 80 to 380 K at values of $\gamma = 0.298$ and $\gamma = 0.345$ respectively for the two test specimens, and the degree of three-dimensional

disordering of each was calculated according to a formula provided. The heat conduction of the specimens was measured parallel and perpendicular to the direction of the pressing. As was expected, polycrystalline specimens had a lesser heat conduction than did monocrystals regardless of temperature. Anisotropy increased as the degree of three-dimensional disorder increased. The background heat conduction was calculated under the assumption of the linear frequency dependence of the inverse relaxation time and with the Debye temperature serving as an adjustable parameter. Analysis of the calculations and experiments performed led the authors to conclude that in the case of specimen 1, the best agreement between the calculated and experimental results is obtained when the Debye temperature is approximately 500 K. The Debye temperature of monocrystalline graphitelike boron nitride in a perpendicular direction was previously found to equal 1,500 K. In the parallel direction (i.e., in the direction of the hexagonal axis C) it was about equal (410 K) to that of the ordered specimen (specimen 2). This was linked to the fact that in a disordered crystal, there are rather few interatomic bonds in the direction of the hexagonal. This in turn makes the properties of graphitelike boron nitride in this direction similar to the properties of an amorphous medium. The authors conclude that the most interesting results of their study was the discovery of (1) the strong dependence of the Debye temperature in the perpendicular direction on γ and (2) the fact that it may be determined from heat conduction experiments. Figures 2; references 8: 4 Russian, 4 Western.

Development and Assimilation of the Production of Microcables Made of Corrosion-Resistant Steels for Computers

927D0020H Moscow STAL in Russian No 6, Jun 91
pp 60-63

[Article by Kh.Yu. Latipov, B.A. Nikiforov, and B.A. Igmetov, All-Union Scientific Research Institute of Metal Products and Magnitogorsk Mining and Metallurgy Institute]

UDC 621.778.1-427.4.04

[Abstract] The intensive development of small manufacturing and control equipment (including printers, plotters, and manipulator robots) has created an annual demand for more than 700,000 meters of cables with very thin diameters (microcables). In an effort to improve the quality and reliability of microcables, the All-Union Scientific Research Institute has been working to develop and assimilate new processes to manufacture promising types of microcables. Because the USSR currently lacks equipment for twisting cables less than 1 mm in diameter from micron-size wires, the SRN 6 x 100, SRN 12 x 100, and BUN-90 rope-twisting machines had to be redesigned to twist microcables. Wire 100 μ m in diameter was used to produce 0.90-mm-diameter microcable with a 7 x 7 design, and wire 60 μ m in diameter was used for microcable with a 7 x 19 design. Modern SRN-type rope-twisting machines are capable of reaching speeds of 7,500 rpm. Such speeds resulted in frequent breaks in test microcables, however. A speed of 1,400 rpm was eventually found to be optimal for twisting microcables. Devices to perform and straighten the cables were also developed. Tests of the new process revealed that the best technique for thermomechanical stabilization of the microcable was to simultaneously stretch it (at a force of 0.30 to 0.45P) and heat it in a protective gas medium at temperatures between 400 and 650°C (with the exact force and temperature depending on the rope diameter and wire material). The VNIKP Scientific Production Association in Moscow, the Khimvolokno Scientific Production Association in Kiev, the Tashkabel Production Association in Tashkent, and the pilot plant of the All-Union Scientific Research Institute of Metal Products developed a process for applying protective polymer coatings to the microcable. After application of the coating, the cable had a diameter of 1.2 mm. Tests of the new coatings revealed that, to date, it only lasts 30 to 45% of the life of the cable itself. Strength tests of the new microcable revealed that nonlubricated cable has a 0.45 probability of operating without breaking for 20,000 cycles of bending on steel pulleys and a 0.99 probability of not breaking on polycaprolactame pulleys. According to the results of cyclic durability tests, nonlubricated microcables had a per-cycle wear intensity of 10^6 on polycaprolactame pulleys and 2×10^4 on steel pulleys. The new cable and cable-twisting process are being further modified in an effort to develop wires that will resist breaking at forces to 1,800-2,000 N/mm².

Assimilating the Production of Extraprecise Pipes for the Casings of Immersion Pumps and Electric Motors

927D0020G Moscow STAL in Russian No 6, Jun 91
pp 57-58

[Article by A.I. Kozlovskiy, V.Ya. Karmazin, O.N. Savchenko, A.M. Yepishev, and V.V. Sivak, Pipe Rolling Plant imeni K. Libknekht, Nizhnedneprovsk]

UDC 621.774.372

[Abstract] Pipes of class 3 precision (maximum deviations with respect to inner diameter, 0.07 to 0.09 mm) with inner diameters of 80 to 130 mm and up to 9 m long are used to manufacture standard electric centrifugal pumps and motors used to recover oil from nongushing wells. For a long time, the casings for these pumps and electric motors were produced by the method of turning and boring thick-walled hot-rolled pipes. This method did not result in pipes of the required precision and entailed losses of up to 40% of the starting metal to chips. For this reason, the Pipe Rolling Plant imeni K. Libknekht in Nizhnedneprovsk developed a new method of producing ultraprecise pipes for use as the casings of immersion pumps and electric motors. As blanks, the workers used hot-rolled pipes produced on a TPA 200 with a three-roller reeling mill. The blanks were then drawn in one or two passes by using hard-alloy (VK9 and VK12) arbors and draw dies. The finished pipes were then straightened at a pilot plant of the All-Union Scientific Research, Planning and Design Institute of the Pipe Industry on an 8 x 700 straightening machine with paired hyperboloid drive rollers. Special measuring instruments based on the electrocontact principle were jointly developed by the All-Union Scientific Research, Planning and Design Institute of the Pipe Industry and the special technological design office of the Potensial All-Union Scientific Production Association and were used to measure the rectilinearity of the generatrix and deviations of the inner diameter of the finished pipes. Special template-gauges 1 m long with three cylindrical dies were also developed for use in delivery inspection of the pipes. The new process was introduced at the plant. Pipes of the three initially planned type sizes, i.e., 92 x 6, 103 x 5.5 (6.5), and 114 x 7.0 mm, were produced in the amount of 2,000 tons a year with the following precision parameters: deviation with respect to inner diameter, +0.12 mm; deviation with respect to wall thickness, ± 0.4 mm; and nonrectilinearity of the generatrix of the inner surface throughout its entire length, 0.3 mm/m. Between 60 and 70% of the pipes produced annually were of acceptable quality. Deviations with respect to inner diameter were the main reason why pipes were rejected. The production process was further debugged, the precision of the pipes produced was improved, and a special section was designed to house the production process. After the process and process equipment were fine-tuned, the production volume was raised to 7,600 tons yearly. Because of the process' success, purchase of foreign pipes of the said class was curtailed. The new

ultraprecise pipes, which are on a par with their counterparts throughout the world, can now be produced at a rate of 5,000 tons per year.

Development of the Pilger Method of Pipe Production

927D0020F Moscow STAL in Russian No 6, Jun 91
pp 53-55

[Article by A.K. Vashchenko and A.A. Ksenz, Pipe Rolling Plant imeni K. Libknekht, Nizhnedneprovsk]

UDC 621.774.36.004

[Abstract] The Pipe Rolling Plant imeni K. Libknekht is one of the largest enterprises producing seamless steel pipes. The plant's first Pilger mill is used mainly in manufacturing general-purpose pipes and thick-walled pipes intended for special purposes. The plant's second Pilger mill was designed with assistance from Hungarian specialists. Its main distinction is that the sleeves used for rolling are produced in two stages: a stage entailing broaching on a horizontal hydraulic press and a stage of reeling on an elongator mill. At present, casing pipes accounted for two-thirds of the pipes produced in the shop. They now account for 90%. Because of this change, the initial configuration of the equipment used in the shop's finishing section has undergone considerable revision. At present, the main trends in the development of Pilger production at the shop are a reduction in the nonuniformity of the thicknesses of the pipes rolled and an increase in unit capacity. Theoretical and experimental studies have been conducted to find ways of adjusting the rollers in the various deformation cycles so as to reduce the problem of nonuniform pipe thicknesses as much as possible. The first stage of this process was to change the angle at which sleeves were fed into the mill for rolling. In the second stage of the improvement process, the Pilger cages will be equipped with devices for precision control of roller configuration. In the third stage of the improvement project, the rolling process will be placed under computer control. Other directions of the effort to improve Pilger mill pipe rolling at the plant include the installation of new threading machines, reeling machines, and presses; the introduction of a new method of heat-treating large tools used in the production process; and improvement of the steel smelting process used to make the metal that is used to form casing pipes on the Pilger mills. In an effort to achieve this last goal, the plant has begun work to develop a new mill to deform blanks and ingots before broaching in order to be able to correct the shapes of blanks whose shapes are not optimal for working on a Pilger mill.

Trends in the Development of Cold Sheet-Rolling Shops

927D0020E Moscow STAL in Russian No 6, Jun 91
pp 45-49

[Article by V.L. Mazur, doctor of technical sciences and professor]

UDC 621.771.23

[Abstract] In the USSR the demand for cold-rolled steel sheets is currently greater than the amount of such sheets being produced. The construction and subsequent operation of one or two high-capacity cold-rolling mills could fully meet both current and projected needs for cold-rolled steel sheets. In addition, the automotive and agricultural machine building sectors are currently in need of 1.5 million tons of hot-rolled etched tempered sheets, which are on a par with hot-rolled sheets from a technical characteristic standpoint but which are cheaper to produce. For this reason, the new cold rolling shop being constructed at the Magnitogorsk Metallurgy Combine is designed to produce about 3 million tons of cold-rolled sheets and 1 million tons of hot-rolled etched sheet steel annually. Analysis shows that no radical changes in the structure of the demand for cold-rolled sheets will occur by the year 2000, although the need for sheets up to 0.65 mm thick will increase somewhat. The demand is thus greatest for sheets of construction steel (mainly low-carbon steel) 0.35 to 3.0 mm thick. In view of these facts, the main needs may be summarized as follows: accelerated air or water-and-air methods of cooling rolls of hot-rolled bands of rolled stock; improvement of existing and discovery of new methods of removing scale from their surface; increasing the amount of available rolling equipment capable of producing high-quality rolled metal (i.e., increasing the amount of equipment capable of producing sheets with high degrees of precision from the standpoints of thickness, planarity, and surface purity of the finished sheets); use of the practice of bell furnace annealing cold-rolled sheets in a hydrogen medium; and unification of individual process operations and units into single flexible modular lines handling the etching, cold rolling, and annealing stages as well as the finishing stage. Figure 1; references 12 (Russian).

Using Low-Phosphorus Concentrates in Smelting Conversion Silicomanganese

927D0020D Moscow STAL in Russian No 6, Jun 91
pp 39-41

[Article by P.Sh. Tsinadze, S.G. Grishchenko, I.V. Liskovich, V.I. Ishutin, Yu.M. Bogutskiy, and T.V. Akhobadze, Zestafoni Ferroalloy Plant, Ukraine Scientific Research Institute of Special Steels, and USSR Ministry of Metallurgy]

UDC 669.168

[Abstract] The removal of obsolete martensite furnaces from service and the increased production of converter steels has increased the ferrous metallurgy sector's demand for low-phosphorus and refined manganese alloys. In view of this fact, the authors of the study reported herein examined the possibility of using low-phosphorus concentrates in smelting conversion silicomanganese. A comparative analysis of the chemical compositions of conversion slag and low-phosphorus

concentrates from the Ushkatynsk and Dzhezdy areas of central Kazakhstan confirmed that it is, in principle, possible to substitute the latter for slag, which is in such short supply, without significantly reorganizing the smelting process. Samples of ore concentrates from the Ushkatynsk and Dzhezdy areas were formed into briquettes that were in turn tested to determine the initial softening and final melting temperatures, their true and apparent densities, and their porosities. The possibility of obtaining conversion silicomanganese by using the test raw materials was evaluated in a laboratory ore-reducing furnace with a power of 240 kV-A, a working current of 1.8 kA, and a secondary voltage of 34.5 V. Four different versions of the reducing process were tested. The conversion silicomanganese obtained in all four versions of the process had a low phosphorus content (0.09 to 0.13%). The difference in manganese extraction from version to version was small (3 to 5%). The experiments thus confirmed the possibility of replacing conversion slags by the Kazakhstan concentrates. The new process was subjected to commercial-scale verification in the 22.5-MV-A furnaces in shop No. 4 at the Zestafoni Ferroalloy Plant. The commercial tests confirmed that using Ushkatynsk concentrates in amounts ranging from 0.13 to 0.27 tons per ton of alloy makes it possible to reduce the use of carbon ferromanganese slag by 13.2-22.4%, the amount of low-phosphorus slag by 21.5-46.4%, and the amount of imported ore by 15.4-57.7%. Figure 1, tables 3.

Selected Problems of the Status and Development of the Ferroalloy Subsector

927D0020C Moscow STAL in Russian No 6, Jun 91
pp 37-38

[Article by V.A. Matviyenko, USSR Ministry of Metallurgy]

UDC 669.168

[Abstract] The process of switching the country's industries over to a market economy have created a number of problems for the ferroalloy subsector. Ferroalloy enterprises are located in different regions of the country. Although each enterprises specializes in different types of ferroalloys, all of the enterprises have similar equipment and use similar production processes. At present most of the demand for ferroalloys is being met; however, only 80% of the demand for medium-carbon ferromanganese is being met, and only 90% of the demand for metallic manganese is being satisfied. This situation is largely due to the unstable operation of the Zestafoni Ferroalloy Plant due to interruptions in electric power supply and a lack of manganese ore of the required quality. Operation of the subsector's remaining enterprises is more stable. Between 1991 and 1995, however, all of the subsector's enterprises must face and solve a number common problems: develop a process of palletizing chromite raw material in view of the shortage of lump chromium ore; redesign existing shops in order to

improve the output of high-carbon ferrochrome and refine it to the necessary fractions; and switch over to a no-waste technology of producing chromium- and manganese-based alloys with complete processing of the slag, complete extraction of its metal concentrates, and subsequent complete utilization of the slag in the national economy. Further expansion of the production of modifiers and foundry alloys is also required. In the coming years most capital investments will have to be directed toward construction and retooling of gas scrubbers and toward the introduction of engineering decisions directed toward creating a normal ecological balance. Planned improvements in the area of reducing damage to the environment include the design and construction of fabric filters at four of the subsector's enterprises and introduction of a set of engineering measures at the Chelyabinsk Electrometallurgy Combine designed to reduce sulfur compound emissions to a minimum and improve problems existing with electrode production. Efforts are also under way to mechanize the most laborious aspects of ferroalloy production and to create a standard automated technological process control system at the furnace, shop, and plant levels and, eventually, at the level of the subsector as a whole. Each of the subsector's individual enterprises and the subsector as a whole will have to work to accomplish the following: establish balances in meeting the country's need for ferroalloys and obtain information regarding user needs so as to be able to conclude mutually beneficial contracts; regulate cooperative ventures between plants; find the resources for scientific research work to solve plant, subsector, and interbranch problems; develop an infrastructure to assist plants in introducing advanced technologies and create a subsector base for developing and producing batches of mechanization and automation equipment; coordinate plants' activities; conduct foreign economic activity under the new economic conditions; and find ways of making more complete use of dust and slag wastes by recycling them into other products. Incorporating ferroalloy enterprises under the conditions of independent management will be impossible unless each has its own scientific subdepartment. One option is for individual plants to found their own scientific centers in the form of associations or small enterprises that would operate on a cost recovery and contract basis, perhaps even serving foreign clients.

Improvement of Steel Smelting Processes at Sector Enterprises. Western Siberian Metallurgy Combine

927D0020B Moscow STAL in Russian No 6, Jun 91
pp 22-32

[Article by R.S. Ayzatulov, N.A. Fomin, I.Kh. Romazan, V.F. Sarychev, N.F. Bakhcheyev, A.A. Krivosheyko, A.F. Sarychev, V.V. Ryabov, A.Ya. Buneyev, M.G. Korolev, G.N. Roldugin, A.I. Agaryshev, V.A. Sakhno, S.G. Melnik, O.V. Nosochenko and K.A. Bryzgunov]

[Abstract] This six-part article reviews improvements that have been made at the Western Siberia, the

Kuznetsk, the Magnitogorsk, the Novolipetsk, the Cherepovets, and the Azovstal metallurgy combines. The Western Siberia Metallurgy Combine is credited with developing a number of new resource-conserving and efficiency-boosting smelting processes, including a process in which carbon-containing materials are used during smelting, a technology of blasting steel on a three-tuyere stand, and a process (developed jointly with the Moscow Steel and Alloys Institute and the Leningrad Machine Building Institute) for blasting steel in large-capacity ladles by high-speed plane streams of neutral gas. Among the key improvements noted at the Kuznetsk Metallurgy Combine are the 1980 introduction of an electric steelmaking shop with 100-t arc furnaces, the introduction of a single-slag technology that increased furnace capacity and reduced the amounts of electric power and ferroalloys required for smelting, introduction of the country's first electric furnace equipped with water-cooled roof and wall elements, and developing of a way of improving martensite steel by killing it with a complex alloy containing Si, Ca, and V and by blasting the metal with Ar in ladles and then treating it with solid slag-forming mixtures. The Magnitogorsk Metallurgy Combine is said to have focused its efforts in recent years on improving the quality of its products, conserving raw materials, improving the environment, and developing new types of steel so as to meet user demands to the fullest degree possible. One of its most significant developments is said to be the introduction in its martensite shops of a process to blast metal with argon through a gate valve and to thereby achieve a severalfold reduction in the number of ingots not conforming to established standards. The combine has also developed processes for producing SV-08G2S steel in a two-stage process involving the production of an intermediate product conforming to 10sp steel. The Magnitogorsk Metallurgy Combine's developments in the area of improving labor conditions include the development of a new environmentally safe material for coating chill molds that does not contain above-norm amounts of phenol, benzopyrene, or other toxic substances and a technology for cleaning railroad cars transporting scrap metal that significantly reduces noise levels. The Novolipetsk Metallurgy Combine is credited with having made a number of improvements in the process of making converter steel and has made notable improvements in the processes for producing electrical, low-carbon, and kinescope steels. Since its beginnings in 1958, the Cherepovets Metallurgy Combine has also made a number of improvements in steel smelting processes. It was the sector's first combine to develop an integrated technology for smelting and extrafurnace treatment of 08-12Cr18Ni10Ti corrosion-resistant steel in large-capacity electric furnaces coupled with pouring on continuous blank-casting machines, and in an effort to reduce the detrimental effects of steel smelting on the environment, it has redesigned its double-vat units to operate in a straight-through mode. The Azovstal Metallurgy Combine is credited with paying ever-increasing attention to producing steel that meets user-specified requirements. The combine has developed and adopted

dozens of new production processes, including smelting converter steel by using top-grade burden materials, refining pig iron, using solid slag-forming mixtures to desulfurize and dephosphorize steel in a ladle, using synthetic slags and new foundry alloys to smelt steel, and developing new grades of steel (including hydrogen sulfide-resistant, high-strength, and pipe steels). Its new processes for producing plate steel are said to be especially noteworthy.

Past STAL Publications on Blast Furnace Processes Reviewed

927D0020A *Moscow STAL in Russian No 6, Jun 91*
pp 4-5

[Unattributed article]

[Abstract] Throughout its 60-year history the journal STAL has covered the key moments in the development of metallurgy and the metallurgy industry. The following are among the key blast furnace process and equipment developments that have been covered in past issues of STAL: manufacturing a self-fluxing agglomerate from Magnitogorsk ore and smelting it into cast iron (No 5-6, 1948); averaging Magnitogorsk ores (No 3, 1948); intensifying the sintering of Krivoy Rog ores (No 7, 1951); sintering finely pulverized concentrates (No 8, 1954); blasting reducing gases into blast furnace hearths (No 5, 1958); determining the composition of the gas in a blast furnace hearth fired by natural gas and conventional blasting (No 9, 1962); the operation of the natural gas-fired blast furnaces of the Cherepovets Metallurgy Plant (No 1, 1965); development of an experimental blast furnace melting using an oxygen-enriched blast (No 8, 1965); an experimental blast furnace melting using a combined blast with a low coke flow rate (No 3, 1978); and an experimental blast furnace using hot reducing gases and commercial-grade oxygen (No 4, 1970). Other topics that have been covered in past issues include the effectiveness of blast furnace melting using blast furnace gas with the CO₂ removed together with commercial-grade oxygen without blasting in gases from the atmosphere (No 4, 1971) and the comparative efficiency of different blast furnace melting regimens under conditions of a modern metallurgy plant (No 8, 1975). STAL has also reported on the introduction of important new pieces of blast furnace equipment, including the following: 2,000- and 2,700-m³ blast furnaces (No 2, 1956, and No 11, 1962); plans for new 3,200-m³ blast furnaces (No 6, 1972, and No 8, 1981); and 5,000- and 5,500-m³ blast furnaces (No 1, 1976).

The Properties of Highly Disperse Tungsten Carbide Powders Produced by the Method of High-Temperature Electrochemical Synthesis

927D0029A *Kiev POROSHKOVAYA METALLURGIYA in Russian No 8, Aug 91*
(manuscript received 8 Jan 89) pp 1-4

[Article by O.N. Grigoryev, Kh.B. Kushkhov, A.M. Shatokhin, G.Ye. Khomenko, and A.A. Tishchenko, Materials Science Problems Institute, Ukraine Academy of Sciences]

UDC 621.762.4.04

[Abstract] The authors of the study reported herein examined the properties of highly disperse tungsten carbide powders produced by the method of high-temperature electrochemical synthesis. Specifically, they examined the phase morphology and impurity state of tungsten carbide powders synthesized at a temperature of 700°C. Study and control tungsten carbide powder specimens were subjected to quantitative and qualitative phase analysis on DRON-2.0 and HZG-4 x-ray diffractometers and to electron microscopy studies on a JSM T-20 scanning electron microscope and a JEM-100CX transmission microscope. The impurity profile of the specimens was determined by chemical analysis, atomic adsorption and Auger electron spectroscopy, and emission spectroscopic analysis. Tungsten carbide powders synthesized under conditions of an excess of free carbon were found to lack W and W_2C lines in their roentgenograms but to contain between 2 and 10% (by mass) free carbon in the form of graphite and up to 6% (by mass) oxygen. The tungsten oxides and oxycarbides that were identified by electron microscopy in a handful of cases were removed by additional purification of the powder with hydrogen. This purification resulted in a residual oxygen content of 0.2-0.3% (by mass) and a residual carbon content not exceeding 0.1% (by mass). Slight amounts of tungsten were also found in some samples. The content of metal impurities was generally insignificant. Before purification the tungsten carbide powders had a specific surface of 10 to 15 m²/g; after cleaning, their specific surface generally ranged from 5 to 10 m²/g. The periods of the monocarbide lattice were found to virtually coincide with the literature values, and the periods of the W_2C lattice corresponded to an atomic carbon content of 32%. Depending on the exact synthesis conditions, the morphology of the particles varied widely as follows: monocrystalline platelike disk-shaped particles 0.1 to 0.5 μm in size and less than 0.1 μm thick, monocrystalline platelike uniaxial particles up to 10 μm long and less than 0.1 μm thick, incorrectly shaped monocrystalline platelike particles between 1 and 10 μm in size, polycrystalline particles up to 5 μm in size, and layered aggregates of monocrystalline thin plates. The platelike disk-shaped and elongated particles were virtually free of defects; the larger incorrectly shaped particles and their agglomerates contained growth dislocations and packing and twinning growth defects. The powders were found to undergo only insignificant recrystallization during sintering. The material produced had a hardness of 18 GPa under an indenter load of 100 to 500 N and 24 GPa under an indenter load of 2 to 5 N, which conforms to the hardness of fused tungsten carbide. The studies performed thus confirmed the promise of high-temperature disperse synthesis as a method of producing tungsten carbide powders for used in manufacturing ceramic and cermet materials. Figures 3; references 4: 3 Russian, 1 Western.

A System To Design Processes for the Hot Isostatic Compaction of Powder Materials. 2. Description of "Lower"-Level Models. A Method of Determining Rheological Coefficients. An Overall Schematic of the System's Operation

927D0029B Kiev POROSHKOVAYA
METALLURGIYA in Russian No 8, Aug 91
(manuscript received 14 Jun 90) pp 5-10

[Article by A.A. Frolov, O.B. Sadykhov, and G.Ya. Gun, Moscow Steel and Alloys Institute]

UDC 621.762

[Abstract] In a continuation of their ongoing research on a system to design processes for the hot isostatic compaction of powder materials, the authors of this article discuss the need to use what they term simplified lower-level models that will eventually be used to determine the various laws governing hot isostatic compaction processes. Specifically, they examine a zero-dimensional model describing the compaction of a compressible medium at some "point" under specified conditions and a one-dimensional model that makes it possible to give consideration to the contribution made by different compaction mechanisms. The two mathematical models explained are based on a discrete approach and are implemented in a set of programs written in Fortran-77 for Unified System (YeS) and IBM PC-compatible computers. The use of the new process design system is illustrated by way of the example of data from an experimental study of shrinkage of the alloy EP741 on a precision dilatometer in test regimens involving different temperatures, loads, and holding times. In essence, the process works as follows. In the first stage, the results of the experimental dilatometric studies are used along with calculations based on the zero-dimensional model to determine the rheological coefficients of the deformable medium. Next, computations based on the one-dimensional model are used to narrow the list of hot isostatic compaction modes in the given search field. This is accomplished by using selected criteria and by giving consideration to specified constraints. In the second stage, an expert takes the information obtained in the first stage and uses it to continue the process of designing the required hot isostatic compaction process. The expert accomplishes this in an interactive system based on a "higher"-level model. Figures 2; references 6: 3 Russian, 3 Western.

Radiation-Accelerated Sintering of Powder Materials

927D0029E Kiev POROSHKOVAYA
METALLURGIYA in Russian No 8, Aug 91
(manuscript received 21 Aug 89) pp 15-17

[Article by Yu.M. Annenkov, T.S. Frangulyan, and A.V. Voznyak, Tomsk Polytechnic Institute]

UDC 548.4

[Abstract] The authors of the study reported herein conducted a comparative analysis of the processes of thermal and thermal-radiation compaction of pressed specimens of potassium bromide. The powders were obtained by taking crystals grown by the Kyropoulos procedure, pulverizing them in an agate mill, and then passing them through a calibrated sieve with a cell diameter of 40 μm . The finished powders were then vacuum-dried at a temperature of 380 K for 2 days and then pressed into tablets. They were pressed into tablets under a pressure of 19 MPa and subjected to thermal and thermal-radiation annealing at temperatures ranging from 750 to 950 K. The radiation heating was implemented on an ELU-4 accelerator by an electron beam with an energy of 4 MeV, pulse current density of 4.5 to 5 mA/cm², pulse duration of 5 μs , and pulse following frequency of 220 Hz. High-power pulsed electron irradiation was found to result in an enormous increase in the coefficient of bulk self-diffusion in the potassium bromide pressed specimens studied. The effect of radiation activation of solid-phase sintering of alkaline halide crystal powders observed during the experiments was determined to be the result of acceleration of the process of anionic self-diffusion due to a significant reduction (by more than two orders of magnitude) in the process activation energy. Figure 1; references 7: 4 Russian, 3 Western.

The Effect of the Stability of the Phase Composition of Powders of Fe-Nd-B Alloys on the Structure and Hysteresis Properties of Sintered Permanent Magnets

927D0029G Kiev POROSHKOVAYA
METALLURGIYA in Russian No 8, Aug 91
(manuscript received 29 Aug 89) pp 70-75

[Article by A.A. Pavlyukov, O.S. Opanasenko, E.V. Krakovich, and N.G. Boroday, Materials Science Problems Institute, UkSSR Academy of Sciences]

UDC 669.781:857.12:538.248:621.762.242

[Abstract] The authors of the study reported herein conducted an experiment to determine whether the duration of mechanical grinding of Fe-Nd-B alloys in a ball mill affects the magnetic characteristics and crystalline structure of sintered alloys (permanent magnets). $\text{Nd}_{15}\text{Fe}_{77}\text{B}_8$ was smelted in an electric arc furnace with a nonconsumable tungsten electrode on a copper water-cooled hearth in an argon medium. The cast alloy was ground first in a metal mortar and then in a ball mill in isopropyl alcohol. The grinding bodies and ground material were in a 1:30 ratio. The powder was compacted in a magnetic field. After sintering at 1,330 and 1,410 K for half an hour, the specimens were held for 2 hours at 870 K and then cooled quickly. The phase composition of the cast and sintered alloys was subjected to x-ray and microscopy studies. The magnetic characteristics were measured on a U5056 unit. As the grinding time was

increased, the coercive force, residual induction, and density of the sintered powders all increased until reaching some maximum and then decreased. Differential dilatometric and thermographic analyses performed as the compacted powder specimens were heated and ground in a ball mill indicated that the said processes are accompanied by adsorption (as indicated by an endothermal peak at 930 K) and release of heat (as indicated by exothermal peaks at 1,430 and 1,470 K). The peak at 930 K was determined to correspond to a eutectic reaction, and the peak at 1,430 K was determined to correspond to a peritectic reaction. The residual induction of the study permanent magnets was found to depend on the perfection of the axial texture formed as a result of compaction of the powder in a magnetic field and on the amount of magnetic phase per unit volume of specimen, which is in turn determined by the specimen density. When all other conditions were equal, reducing product density resulted in a reduction in residual induction. The changes in the coercive force and residual induction of the sintered specimens as a function of powder-grinding time that was observed during the experiment was determined to be due primarily to the kinetics of the oxidation of the neodymium-enriched phase that is a structural component of the cast alloy. The grinding time required to achieve optimal values of the specified magnetic characteristics was found to be determined by the grinding conditions. When the ratio of the masses of the grinding bodies and the ground material in the ball mill was cut in half, this time increased. Figure 3; references 13: 5 Russian, 8 Western.

The Effect of Calcium Fluoride and Lead Content on the Structure Formation and Tribotechnical Characteristics of Copper-Based Powder Material

927D0029I Kiev POROSHKOVAYA METALLURGIYA
in Russian No 8, Aug 91 (manuscript received
14 Sep 89) pp 78-83

[Article by N.G. Baranov, V.S. Ageyeva, A.I. Il'nitskaya, V.S. Mokrovetskaya, Ye.A. Ganusets, V.S. Kuzmenko, and Ye.A. Leshchenko, Materials Science Problems Institute, UkSSR Academy of Sciences]

UDC 621.762

[Abstract] The authors of the study reported herein examined the structure and selected mechanical and tribotechnical characteristics of a copper-based composite containing calcium fluoride and lead in order to determine the effect of the two additives on structure formation and the aforesaid characteristics. Composites were produced from powders of PMS-1 copper, PS-1 lead, and calcium fluoride. The study composites were twice subjected to compaction and sintering to reduce their porosity. Both sinterings were performed at 800°C. Specimens 10 x 10 x 55 mm in size were measured to determine their bulk shrinkage, resistivity, and impact strength. They were also subjected to friction and wear

tests on a stand designed by the Materials Science Problems Institute. On the basis of the tests and measurements performed, the researchers concluded that calcium fluoride is a polyfunctional additive that participates in the formation of the copper-based composite's tribotechnical characteristic, increases bulk shrinkage, and impedes the sweating out of lead after sintering. Lead was found to help reduce the friction coefficient of the study composites; however, when its content was increased to 11% (by mass), the wear of the test materials fell sharply. This was attributed to the disordering effect of lead and to its distribution in the form of thin, elongated interlayerings between the copper grains. The studies further established that powder copper-based antifriction materials containing 6% (by mass) lead and 11% (by mass) calcium fluoride have a low wear coefficient (between 0.15 and 0.25) and a very low wear intensity (0.3 to 3.3 $\mu\text{m}/\text{km}$) when exposed to friction without lubrication and may therefore be recommended for use in high-speed friction nodes as effective replacements for copper-graphite materials. Figures 3, tables 2; references 17 (Russian).

The Production and Properties of a Cu-Ni Powder Alloy for Thermostatic Bimetals

927D00501 Moscow IZVESTIYA AKADEMII NAUK
SSSR: SERIYA METALLY in Russian No 5.
Sep-Oct 91 (manuscript received 30 Jan 90) pp 178-180

[Article by R.G. Samvelyan, S.G. Agbalyan, N.L. Akopov, and N.N. Manukyan, Yerevan]

UDC 621.762.4.016:539.389.2

[Abstract] The authors of this concise report developed a method of producing a Cu-Ni powder alloy with stable characteristics and a low resistivity with respect to thermostatic bimetals. As a starting compound they selected the powder alloy MN19-PS, which has a nickel content of approximately 19%. The study CuO-NiO oxides were synthesized in ceramic containers at a temperature of $920 \pm 20^\circ\text{C}$ for 4 to 6 hours. NH_4Cl in amounts ranging from 1.5 to 2.0% (mass) was used as an activating additive. Derivative thermogravimetric analysis was used to determine the mechanism and kinetics of the synthesis of the CuO-NiO oxides. The studies performed indicated that synthesis occurs autonomously. The synthesis of each of the two compounds $\text{NiO-NH}_4\text{Cl}$ and $\text{CuO-NH}_4\text{Cl}$ was essentially self-contained. The extrema on the curves of each at 195 and 197°C were united into an extremum at 180°C . The extrema at 270 and 280°C were shifted to 210 and 250°C , respectively, after which point the DTA and DTG curves were nearly identical. This finding was taken as an indication that the chlorination process occurs separately for all practical purposes and is completed at 315°C . Solid-phase synthesis reactions were found to follow this stage. Tests performed to determine the physicomechanical properties of the Cu-Ni alloy synthesized indicated that it may be recommended for use as an active layer for thermostatic bimetal materials with highly stable properties and an elevated per-unit-length bend. Its elasticity modulus is close to those of Invar and Superinvar, thus guaranteeing a thermostatic bimetal with maximum heat sensitivity. Figures 3, tables 2; references 5: 4 Russian, 1 Western.

The Structure and Properties of Welded Joints of Different Titanium Alloys

927D0026J Moscow METALLOVEDENIYE I
TERMICHEKAYA OBRABOTKA METALLOV
in Russian No 7, Jul 91 pp 23-25

[Article by A.A. Popov, A.G. Illarionov, M.A. Khorev, and N.A. Drozdova, Ural Polytechnic Institute imeni S.M. Kirov and All-Union Scientific Research Institute of Aviation Materials]

UDC 669.295:621.79

[Abstract] The authors of the study reported herein examined various changes in titanium alloys subjected to welding. Specifically, they examined the effect of welding on the following: structure, phase composition, microhardness, distribution of alloy-forming element in the main metal, and thermal effect zone. Welds of the following titanium alloy pairs were studied: VT6-OT4, VT6-VT20, VT23-OT4, VT23-VT6, VT23-VT19, and VT23-VT32. On the basis of studies performed by using the methods of metallographic analysis, x-ray crystallographic analysis, and x-ray spectral microanalysis, the authors concluded that the laws governing the formation of the structure and properties of the titanium alloys in a weld depend on the average conditional coefficient of β -stabilization ($K_{\beta w}$) of the weld. They then proceeded to develop a classification of titanium alloy welds and specific recommendations for heat-treating the alloys in each class. The first class developed includes VT6-OT4 and VT20-VT6 welds ($K_{\beta w} < 0.3$). The second class includes VT23-OT4 and VT23-VT6 welds ($K_{\beta w}$ 0.4 to 0.7). The third class includes VT23-VT19 and VT23-VT32 welds ($K_{\beta w} > 1.0$). For class 1 alloys the authors recommended a regimen of hardening heat treatment including hardening and aging procedures developed with consideration of the properties of both alloys in the melt. According to the recommendations, the final heat treatment for class 2 welds should include preliminary annealing to stabilize the structure and properties of the titanium alloys and hardening heat treatment based on decomposition of the metastable α'' -martensite and β -solid solutions. The hardening heat treatment recommended for class 3 welds includes aging sufficient to cause the decomposition of the β -phase formed during cooling of the weld zone following welding. Figures 2, table 1; references 4: 3 Russian, 1 Western.

The Quality of Ingots Forged From Low-Alloy Steel Subjected To Pulsation Treatment During Hardening

927D0026I Moscow METALLOVEDENIYE I
TERMICHEKAYA OBRABOTKA METALLOV
in Russian No 7, Jul 91 pp 21-22

[Article by A.N. Smirnov, Yu.B. Bychkov, T.V. Chernobayeva, and S.V. Pilguk, Donetsk Polytechnic Institute and VNIIPVtortsvetmet]

UDC 621.746.588:669.14.018.29

[Abstract] The authors of the study reported herein examined the effect of pulsation treatment on the formation of the macrostructure and physical and chemical inhomogeneity of forged ingots weighing 30 to 45 tons. The effect of pulsation treatment on the contamination of the said ingots with nonmetallic inclusions was also considered. Two ingots with a design weight of 36 tons were studied. In accordance with previously obtained results, the weights of the sinkheads of the said ingots were reduced by 2 tons each. 20CrNi steel was smelted in a 60-ton arc furnace. One of the ingots was subjected to pulsation treatment (by a submerged stream) for 60 minutes beginning 6 minutes after it had been poured. Lengthwise axial templates were cut from pulsation-treated and untreated ingots. The templates were subjected to deep etching with a 15% ammonium persulfate solution and a 10% nitric acid solution. The depth of penetration of shrinkage holes in the pulsation-treated ingot was reduced by 250 mm. Pulsation treatment was also found to reduce the length of zones of columnar crystals and to increase the slope of the dendrites' axes to the horizontal plane. The difference between the lengths of the columnar crystal zones in the test and control ingots was smaller in the bottom parts of the zone than in the middle and top parts, thus confirming that the pulsating stream's effect is diminished in the bottom part of the test ingot. The pulsation treatment was also found to affect the structure of the zone of equiaxial crystals, with this effect being most pronounced in the grain sizes and uniformity of the metal of the bottom part of the test ingot. In addition, pulsation treatment facilitated an increase in the number of solid particle nucleation centers in the melt. A comparison of eccentric liquation in the two ingots revealed that pulsation treatment causes the liquation filaments to shift from the zone hardened during the pulsation treatment process. The total length of the filaments in the test ingot was less than in the control ingot by a factor of about 1.2, and the slope of the filaments to the ingot axis in the test ingot was less than in the control ingot by a factor of 1.3 to 1.5 on average. The top part of the test ingot was found to contain fewer nonmetallic inclusions than the control ingot. This difference in the amount of nonmetallic inclusions was greatest in the zone hardened during the pulsation treatment process. Table 1; references 10: 7 Russian, 3 Western.

Quality Control of Heat Treatment of Components

927D0026H Moscow METALLOVEDENIYE I
TERMICHEKAYA OBRABOTKA METALLOV
in Russian No 7, Jul 91 pp 19-20

[Article by V.V. Pleshakov, S.A. Alimova, T.A. Pavlova, Moscow Instrument Making Institute]

UDC 658.56:621.78

[Abstract] The authors of this article have proposed a method for quality control of the heat treatment of

components. The new method is based on recording the parameters of the electromotive force due to the Barkhausen jumps arising when the magnetic polarity of the transducer being used for the inspection is reversed. The said transducer (sensor) consists of a magnetic flux-reversing winding and a measuring winding. A saw-toothed voltage providing a current of specified frequency and amplitude is fed to the flux-reversing winding. A signal is extracted from the measuring winding, and its parameters are correlated with the properties of the surface layer of the component being inspected. A statistical link between the signal's electromotive force parameters and the quality indicators of the surface layer was established experimentally on the basis of research of specimens (components) with known properties. Several modifications of the monitoring device have been developed, including a laboratory version that may be connected to a domestic or foreign IBM-type personal computer. The applications software that has been developed for use with the new inspection instrument and process permits quick and effective inspection of the properties of a surface during the processes of its manufacture, testing, operation, and repair. The American Strescan-500C is seen as an analogue of the new instrument. Unlike the Strescan-500C, which only measures the amplitude characteristics of a signal, the newly developed instrument also measures signals' spectral characteristics. The following are among the new instrument's technical characteristics: magnetic pole reversal current frequency, 0.1 to 50 Hz; magnetic pole reversal current amplitude, 0 to 3 A; and overall dimensions, 220 x 150 x 70 mm. The new instrument is ready for use in 3 seconds and may be powered by a municipal power system (200 V, 50 Hz) or else autonomously by 9 V. The range of parameters that can be measured by the new instrument may be changed by altering the strength of the polarity-reversing current. Tempering temperatures between 410 and 620°C may, for example, be measured by using a polarity-reversing current of 0.3 A, whereas a current of 0.5 A permits measurement of temperatures between 237 and 540°C. Figures 2; references 2 (Russian).

High-Temperature Thermoplastic Hardening of Steels St3sp and 09Mn2C

927D0026G Moscow METALLOVEDENIYE I
TERMICHESKAYA OBRABOTKA METALLOV
in Russian No 7, Jul 91 pp 18-19

[Article by A.G. Ksenofontov, M.Yu. Sinelnikova, I.V. Kozhevnikov, M.N. Krylov, and V.K. Fadeyev, and Moscow Higher Technical School imeni N.E. Bauman and All-Union Scientific Research and Design Institute of Metallurgical Machine Building]

UDC 621.977:669.14.018.29

[Abstract] The authors of the study reported herein worked to develop that high-temperature thermoplastic treatment process that would be best suited to the

specific requirements of hardening the steels St3sp and 09Mn2C. Hot-rolled bands of the study steels with a starting thickness of 30 mm were rolled in six passes at 950°C to a final thickness of 4 mm. Next, bands measuring 4 x 45 mm were subjected to high-temperature thermoplastic treatment on a commercial planetary deformation unit designed by the All-Union Scientific Research and Design Institute of Metallurgical Machine Building. The total heating and holding process, including both the preliminary and final stages, lasted about 6 minutes. Air and water were used as the cooling media. To suppress the development of recrystallization processes and obtain a fine-grained finely disperse structure, cooling of the bands was begun virtually immediately after the bands were removed from the deformation zone. The cooling was implemented at a rate of 100°/s to 500°C. On the basis of the studies performed, the authors concluded that the best regimen for high-temperature thermoplastic treatment of St3sp and 09Mn2C steels includes austenitization at 1,020°C, deformation (total deformation, 200%; one-time deformation, 5.7%) at 940°C, and cooling at a rate of more than 100°C/s. These process parameters were demonstrated to result in St3sp steel with an ultimate strength of up to 1,230 N/mm² and 09Mn2C steel with an ultimate strength of 960 N/mm². The tentative yield points of the said steels processed in the manner described were established at up to 1,100 and 840 N/mm², respectively. Tables 2; references 8 (Russian).

The Effect of Hardening Regimens Entailing Electrocontact Heating on the Structure and Properties of 36NiCrTiAl Spring Alloy

927D0026F Moscow METALLOVEDENIYE I
TERMICHESKAYA OBRABOTKA METALLOV
in Russian No 7, Jul 91 pp 15-18

[Article by G.M. Klykov, A.G. Rakhshadt, O.M. Khovova, and V.A. Uzakova, Moscow Higher Technical School imeni N.E. Bauman]

UDC 621.785.6:669.018.27

[Abstract] The authors of the study reported herein worked to assess the possibility of producing a fine-grained structure of the supersaturated solid solution in the alloy 36NiCrTiAl by using the method of rapid electrocontact heating during recrystallization after preliminary cold plastic deformation. For their studies they used commercial 36NiCrTiAl alloy containing 0.04% C, 35.85% Ni, 12.63% Cr, 2.96% Cr, and 1.06% Al. A soft strip of the alloy 0.8 mm thick was rolled to a thickness of 0.3 mm. The strip had a total reduction of about 60%, which conforms to the requirements established for the solid (workhardened) alloys generally produced by instrument making enterprises. Specimens measuring 0.3 x 5 x 150 mm cut out along the direction of rolling were used. The specimens were subjected to rapid heating on an experimental unit at the Arkhangelsk Forestry Engineering Institute. The unit permitted rapid

(up to 10^4 /s) heating of the specimens by passing a current through up to a specified temperature in the range from 600 to $1,200^\circ\text{C}$. This was followed by isothermal holding for a specified period and cooling by means of copper water-cooled plates (at a rate of about $500^\circ\text{C}/\text{s}$) or else by immediate cooling by the plates. The heating took place in an oxygen-free environment. Primary recrystallization of deformed 36NiCrTiAl alloy was not found to develop after electrocontact heating to 900°C at a rate of $3,000^\circ\text{C}/\text{s}$ and holding at that temperature for 12 seconds. When lesser heating speeds ($1,000$ and 300°C) were used, it was impossible to prevent the decomposition of the supersaturated solid solution of the deformed alloy as it was heated. Comparative analysis of the kinetics of the change in hardness under conditions of heating to temperatures of or above 950°C demonstrated that heating speed affects only the initial stage of primary crystallization. As expected, the aging of the deformed alloy during the process of heating at rates of 300 and $1,000^\circ\text{C}/\text{s}$ delays the onset of recrystallization and facilitates the formation of a finer-grained structure. The best combination of hardening, high plasticity, and good stampability was obtained by a regimen of recrystallization treatment with heating to $1,050^\circ\text{C}$ at a rate of $3,000^\circ\text{C}/\text{s}$ for 6 seconds. The best ratio of concentrated and even elongation was also achieved at this heating temperature and time. Comparative fatigue tests performed on the specimens under conditions of an asymmetric loading cycle (test base, 10^7 cycles) confirmed that electrocontact heating results in specimens with higher endurance limits than does conventional heat treatment. The method of recrystallization treatment (hardening) of deformed 36NiCrTiAl alloy by using electrocontact heating was thus demonstrated to be a promising and highly efficient method of producing alloy with a homogeneous structure. Figures 4, tables 2; references 10 (Russian).

The Effect of Nitrocarburization Regimens and Subsequent Oxidation on the Properties of Components

927D0026E Moscow METALLOVEDENIYE 1
TERMICHESKAYA OBRABOTKA METALLOV
in Russian No 7, Jul 91 pp 9-10

[Article by G. Wal, Germany]

UDC 621.785.533:669.15'24'26'28'-194

[Abstract] In view of the increasing importance of nitriding and nitrocarburization, the author of the study reported herein examined the effect that different nitrocarburization regimens followed by oxidation have on the properties of components made of various carbon and carbon-molybdenum steels. Specifically, he determined the hardness and thickness of the diffusion layer and the corrosion resistance of the following steels after nitrocarburization in salt baths at 580 and 630°C : C45, 42Cr4Mo4, 18CrNi8, X38CrMoV51, X20Cr13, X35CrMo17, and X10CrNi188. The said steels contain

medium and low amounts of carbon and between 0 and 18% chromium. The studies performed indicated that the structure and thickness of hardened steel have a significant effect on the corrosion and wear resistance of components made from it. When all other conditions are equal, the nitrocarburized layer formed after nitrocarburization at 630°C is nearly twice as thick as that formed after standard nitrocarburization at 580°C . After nitrocarburization at 580 and 630°C , the thicknesses of the layer formed on nonalloyed and low-alloy steels (the first three of the steels listed above) were about $15-18$ and $30-40\text{ }\mu\text{m}$, respectively. The layers formed on high-alloy steels were $6-8$ and $10-16\text{ }\mu\text{m}$, respectively. As expected, the thickness of the diffusion layer decreased as the chromium content in the different steels increased. After high-temperature nitrocarburization, the nonalloyed steel C45 and the alloy 42CrMo4 had a corrosion resistance that was either less than or nearly analogous to that after standard nitrocarburization (at 580°C) even though the hardened layer was thicker. All of the other materials studied had a higher corrosion resistance after nitrocarburization at 630°C . This improvement in corrosion resistance was attributed to the increased thickness of the diffusion layer and the presence of chromium nitride in the layer. X-ray and metallographic studies established that nitrocarburization (whether at 580 and 630°C) results in the formation of single-phase carbonitride layers. The studies performed confirmed that nitrocarburization of high-alloy steel in a salt bath at high temperatures results in a significant improvement in the corrosion resistance of components eventually made from the steel. This increase in corrosion resistance was found to increase as the thickness of the carburized layer increased. Subsequent oxidation was found to improve corrosion resistance even further. Steels containing nickel in addition to chromium were found to have a low corrosion resistance following the processing regimen studied. Figures 3, table 1; references 6 (Russian).

A Study of the Kinetics of the Dissolution and Formation of Complex Carbides and Their Effect on the Martensite Transformation in Corrosion-Resistant Steels

927D0026D Moscow METALLOVEDENIYE 1
TERMICHESKAYA OBRABOTKA METALLOV
in Russian No 7, Jul 91 pp 7-8

[Article by G. Garcia, L.F. Alvarez, M. Karsi, and M.R. Andres, Spain]

UDC 669.14.018.8:620.18.181.4

[Abstract] The authors of the study reported herein used the technique of high-resolution dilatometry to study the phase transformations that occur during the heating and cooling of high-carbon martensite steels of the type 45Cr13 and 60Cr13MoV. The studies were performed after the said steels were heated to $1,060$ and $1,050^\circ\text{C}$ (the temperatures generally used during hardening) and

1,120 and 1,100°C respectively. In all cases the heating was conducted at a speed of 0.5°/s, and the austenitization temperature was held for 60 seconds. Specimens 2 mm thick and 12 mm long were studied. Analysis of the measurement results demonstrated that heating speed has a significant effect on the degree to which ferrite is transformed into austenite in two study steels at all temperatures. The martensite transformation in the study steels was found to develop in an atypical manner with the demarcation of several different stages. The distinctions observed were explained on the basis of the theory of the nonisothermal transformation of austenites with different chemical compositions. In both steels studied, the subdivision of the martensite transformation process occurred differently for each heating temperature studied. These differences were explained in terms of the gradient of the concentration of carbon and carbide-forming elements (Cr, Mo, and V) in the austenite as a result of their release during the cooling process. Specifically, the main stage of the martensite transformation was characterized by the mass transition of austenite into martensite. The higher-temperature stage was linked to the presence of carbon- and carbon-forming element-depleted austenite zones. The stages occurring at lower temperatures than the basic stage were found to correspond to austenite zones enriched in the aforesaid elements. Figures 4, tables 2; references 2 (Western)

The Dissolution of Carbides and Nitrides During the Austenitization of Steels

927D0026C Moscow METALLOVEDENIYE I
TERMICHESKAYA OBRABOTKA METALLOV
in Russian No 7, Jul 91 pp 5-6

[Article by V.V. Popov and M.I. Goldshteyn, Ural Polytechnic Institute]

UDC 669.14.018.298:536.001.24

[Abstract] The degree of dissolution of carbides, nitrides, and carbonitrides in steels during austenitization determines the main structural factors dictating the key properties of steel (i.e., grain size, effectiveness of dispersion hardening, and subgrain structure). Austenitization regimens are usually designed so that total dissolution of carbonitrides (which are needed to restrain the growth of the austenite grain during heating) does not occur. On the other hand, the degree of carbonitride dissolution must be rather high in order to achieve noticeable dispersion hardening. In view of these facts, the authors of the study reported herein performed a series of thermodynamic calculations of the solubility of carbonitrides in steels with different compositions. The calculations were performed with consideration given to the fact that actual steels are multicomponent systems in which several phases form. Consideration was also given to the effect that alloy-forming elements have on components' activity in an iron-based solid solution. The calculation results were used to plot nomograms of the

most typical groups of machine building steels: vanadium-chromium, chromium-vanadium with nitrogen, chromium-molybdenum-vanadium and chromium-nickel-molybdenum-vanadium, and chromium-manganese-titanium. The nomograms were plotted for the most typical alloy-forming element contents in each group of steels. Carbonitride solubility was found to depend largely on the amount of carbon in the individual steels. Nitrogen content was also found to have a significant effect on carbonitride solubility. The nomograms presented are recommended for use in determining heat treatment regimens involving carbonitride hardening. Figures 3; references 7: 6 Russian, 1 Western.

The Reverse Martensite Transformation of Ferrite Into Austenite

927D0026B Moscow METALLOVEDENIYE I
TERMICHESKAYA OBRABOTKA METALLOV
in Russian No 7, Jul 91 p 4

[Article by Ya. Prokhazka and K.G. Maroti, Hungary]

UDC 620.181.5

[Abstract] The literature contains conflicting opinions regarding the possibility of a martensite transformation of ferrite into austenite in steels. One of the authors of the study reported herein has previously proposed a formula for determining the incubation period τ , of the $\alpha \rightarrow \gamma$ transformation that is reminiscent of Zener's dependence published in 1925. In a continuation of this line of research, the authors of the present study conducted a series of experiments on specimens cut from a steel wire. The test specimens were subjected to preliminary heat treatment and then polished to half their cross section and cut to a length of about 50 mm. To avoid oxidation of the polished surface, the specimens were placed (one at a time) in a gas flow containing 5% $H_2 + 95\% N_2$ and circulating in a silicon tube. The specimens were then heated by passing an electric current through at a frequency of 50 Hz. Hardness measurements taken of the specimens confirmed that no martensite transformation took place when the heated specimens were cooled. Because the test specimens had been heated for periods of less than 0.01 seconds, the authors concluded that this amount of time was insufficient for the formation of austenite from perlite in accordance with a diffusion mechanism. Figure 1; references 7: 4 Russian, 3 Western.

The Link Between Martensite and Bainite Transformation in Carbon and Alloy Steels

927D0026A Moscow METALLOVEDENIYE I
TERMICHESKAYA OBRABOTKA METALLOV
in Russian No 7, Jul 91 pp 2-3

[Article by V.M. Schastlivtsev, D.A. Mirzayev, A.I. Bayev, S.Ye. Karzunov, and I.L. Yakovleva, Metal Physics Institute, Ural Department, USSR Academy of Sciences]

UDC 620.181.4:669.14.018

[Abstract] Numerous researchers have studied the effect of cooling speed on the position of the critical points and morphology of transformation products in steels. In a continuation of this line of research, the authors of the study reported herein studied the martensite transformation in steels in a broad range of cooling speeds and worked to establish its link to the bainite transformation. For the studies, steel ingots were smelted in a vacuum induction furnace, homogenized, and subjected to hot rolling. To avoid decarburization, specimens 0.7 mm thick were first austenitized at 900°C for 10 minutes. The water-quenched specimens were polished to a thickness of 0.12 mm and then coated with copper. Next, they were heated by an electric current in a vacuum to 1,000°C, held at that temperature for about 100 hours, and then cooled. A continuous spectrum of cooling speeds was obtained by subjecting the specimens to bilateral cooling by streams of argon, alcohol, or distilled water at a pressure of 0.1 to 2.5 MPa. A dilatometer was used to examine the transformations occurring at the lowest speeds. Analysis of the experiments performed indicated that the martensite points of steels containing between 0.05% and 0.6% carbon remain constant in the cooling speed interval from 40 to 70 x 10³/s, drop abruptly, and remain unchanged thereafter. The analysis further indicated that the dependence of the martensite point on carbon content may be expressed in the form of two straight lines intersecting at a carbon content of 0.65%: M₁ = 540 to 420 (% C) and M₂ = 420 to 120 (% C). The structure of martensite of low-carbon steels was found to change upon the transition from the upper to the lower stage: the grid crystals of the martensite α_2 disperse while large plates containing twins typical for higher-carbon martensite form. The most significant difference between these two types of martensite was related to the residual austenite: No residual austenite was detected in the structure of steel with α_2 martensite. Studies of the bainite transformation occurring in the low-carbon steels studied indicated that as in the case of the martensite transformation, the bainite transformation occurs in several stages that are linked to the multistage kinetics of the $\gamma \rightarrow \alpha$ transformation in pure iron. The temperature of each stage was found to depend on the carbon content. It was further found that cooling speed does not affect the temperatures of the martensite stages. This finding confirmed results published in 1937 by S.S. Shteynberg. Figures 5; references 7: 5 Russian, 2 Western.

The Effect of Pressing on the Texture of Powder Magnets Made of Barium Ferrite

927D0050H Moscow IZVESTIYA AKADEMII NAUK SSSR. SERIYA METALLOV in Russian No 5, Sep-Oct 91 (manuscript received 18 Dec 89) pp 144-147

[Article by A.S. Kotenev]

UDC 621.762

[Abstract] The authors of this concise report worked to develop a method of determining those pressing

conditions that would result in barium ferrite powder magnets with the optimal texture. In essence, their efforts to optimize the pressing process revolved around refining the amplitude and frequency parameters of variable and constant magnetic fields. The unit developed to implement the new process contains components to shape the powder's texture, pack the powder, and measure its degree of texture (by means of a vibratory pressure gauge). The magnetic texture of the barium ferrite powder was shaped by using a technique published elsewhere. In essence, powder was poured freely into a nonmagnetic mold and then subjected to a variable magnetic field created by using an electric magnet. The movements and sizes of the particles and floccules in the powder stream are changed by manipulating the amplitude and frequency of variable and constant magnetic fields until the desired texture is obtained. Manipulations of the said magnetic fields are also used to orient the particles and floccules and mass them together so that they can be packed into the mold. The technique of combining variable and constant magnetic fields is used both to shape the texture of the powders and to arrive at a qualitative estimate of the magnetic texture of the specimens formed in the process. Both the shaping and measuring techniques are described in detail. Figures 4; references 5 (Russian).

The Mechanical Properties of the Alloy KhN35VTYu at Low Temperatures

927D00261 Moscow METALLOVEDENIYE I TERMICHESKAYA OBRABOTKA METALLOV in Russian No 5, May 91 pp 28-29

[Article by P.F. Koshelev, P.N. Nikitin, Ye.Yu. Bynin, and T.A. Pastukhova, State Scientific Research Institute of Machine Science and All-Union Scientific Research Institute of Electrical Mechanics]

UDC 620.17:669.14.018.44

[Abstract] The alloy KhN35VTYu is intended primarily for use at high temperatures. The literature also contains several communications regarding its use in cryogenic technology. In view of this fact, the authors of the study reported herein examined the effect of different heat treatment regimens and the effect of different patterns of stress concentration on the mechanical properties of KhN35VTYu at normal and cryogenic temperatures. The study specimens were cut lengthwise from a 50-mm-diameter bar of a commercial melt containing 0.07% C, 0.38% Si, 0.30% Mn, 15.17% Cr, 35.15% Ni, 3.01% Ti, 1.11% Al, 3.19% W, 0.008% S, 0.01% P, and 0.015% B. The blanks from which the specimens were cut were heat treated in electric chamber furnaces. The standard mechanical (i.e., strength and plasticity) properties and the effect of stress concentration on the study specimens' strength were determined at temperatures of

20, -196, and -153°C. Mechanical tests were performed on smooth specimens 4 mm in diameter and on specimens that had an annular notch and a diameter of 4 mm at their smallest cross section. The tests performed indicated that specimens of the alloy KhN35VTYu subjected to hardening at 1,050°C for 3 hours and cooled in air have high values of strength and plasticity indicators at both normal and cryogenic temperatures. Increasing the hardening temperature to 1,200°C was found to result in a significant reduction in the values found for the indicators $\sigma_{0.2}$ and $a_{0.25}$ (impact strength). Figures 2, table 1; references 4 (Russian).

The Structure and Properties of Cast Bimetal Composites for Tools

927D0026H Moscow METALLOVEDENIYE I
TERMICHESKAYA OBRABOTKA METALLOV
in Russian No 5, May 91 pp 17-22

[Article by V.V. Chekurov, Tashkent Machine Building Institute]

UDC 621.753.5:62-419.4

[Abstract] The most popular method of manufacturing a tool is to have the actual tool (which is made of the tool material) be an insert in a casing made of construction steel. The reliability and serviceability of such tools are determined mainly by the composition, structure, and properties of the composite's transition zone. In an effort to be able to forecast the possibility of producing a given composite during the tool design stage, the authors of the study reported herein have developed a thermophysical model of the formation of cast bimetal composites. In essence, the proposed model is based on two versions of the process of the formation of cast bimetal composites: 1) the melting of the skin on the insert surface until the beginning of bulk crystallization of the casting and the formation of a transition zone upon direct contact of the melt and insert due to the fusion of the surface layers and 2) retention of the skin on the insert surface until the beginning of bulk crystallization of the melt and formation of a transition zone due to a fusible intermediate layer or an insert made of a fusible material. The studies performed to substantiate this model revealed that the transition zone of tool steel-construction steel bimetallic composites produced by gasifiable-pattern casting is characterized by an elevated concentration of carbide-forming elements and by a sharply pronounced structural heterogeneity. It was further discovered that in the presence of stress concentrators, bimetal composites of the type examined are more crack resistant and durable than are one-piece specimens made to tool steels. This finding was attributed to the occurrence of internal residual compressive stresses in the tool steel insert and the high damping ability of the composites' transition zone. The formation of a transition zone in hard alloy-composition steel composites with retention of the skin between the steel melt and sintered hard ally was determined to result from the migration of the melt of the

intermediate layer and the surface layers that are dissolved in it and that bound this melt of solid surfaces. The formation of composites retaining the skin and a hard alloy insert of the system Fe-Cr-C was determined to involve the formation of a structure characterized by multiple layers with a sharp difference in composition and properties from one zone to the next. Cast bimetal composites of the type studied were found to be stronger, more reliable, and more durable than their soldered or melted counterparts. Figures 10, table 1; references 22 (Russian).

An Investigation of the Chemical Composition of the Surface of Specimens of High-Speed Steel With a Titanium Nitride-Based Coating After a Thermal Effect

927D0026G Moscow METALLOVEDENIYE I
TERMICHESKAYA OBRABOTKA METALLOV
in Russian No 5, May 91 pp 16-17

[Article by V.D. Kalner and A.K. Verner, ZIL Production Association]

UDC 669.14.018.252.3:621.785.53

[Abstract] Titanium nitride-based coatings have gained widespread popularity as a way of protecting cutting tool surfaces that are exposed to repeated heating and cooling during the course of their operation. In view of this fact, the authors of the study reported herein examined the effect that heating has on the chemical composition of the system coating-substrate as one of the characteristics determining both the properties of tool coating and the serviceability of the tool itself. As a test substrate, the authors used specimens of R18 high-speed steel that had been subjected to hardening and three cycles of tempering until a hardness (HRC) of 62-64 was achieved. The specimens were ground to a surface roughness (R_a) of 0.63 μm and then coated (by means of ion sputtering) with a titanium nitride-based coating up to 15 μm thick. The coating had a hardness of 1,800 to 2,000 HV. The coated substrates were subjected to short-term (duration, 10 seconds) heating to 600-800°C. Control specimens were subjected to vacuum annealing at the same temperatures for 1 hour. Electron spectrometry and Auger spectroscopy were used to determine the chemical composition of the test specimens' surfaces. The studies performed indicated that protracted heating of the coated test specimens in a vacuum results in processes of diffusion mass transfer in the system coating-substrate. Two regions were observed in coating specimens subjected to short-term high-speed heating: an outer oxygen-enriched, nitrogen- and carbon-depleted region and an inner region with an opposite element ratio. In these regions the oxygen was determined to enter from the surrounding atmosphere, whereas the carbon entered from the material of the substrate. The studies performed led the researchers to conclude that short-term heating makes it possible to control the processes of the

formation of $TiN_xO_yZ_z$ compounds with specified compositions. This in turn makes it possible to improve the service performance of the cutting tool being produced and optimize the material-working process. Figure 1.

The Effect of the Structure of the Hot-Rolled Band on Texture Formation in 80kp Steel

927D0026F Moscow METALLOVEDENIYE I
TERMICHEskAYA OBRABOTKA METALLOV
in Russian No 5, May 91 pp 14-16

[Article by V.Ya. Goldshteyn, A.V. Seryy, D.E. Berbovetskaya, G.A. Suvorova, and S.A. Burlakov, Metallurgy Scientific Research Institute, Chelyabinsk, and Karaganda Metallurgy Combine]

UDC 548.735:669.14

[Abstract] One promising way of increasing steel's capacity for deep drawing is to increase its $I_{(111)}/I_{(100)}$ textural component ratio and optimize its $I_{(332)}/I_{(112)}$ ratio within the limits from 1 to 2. The degree of deformation during cold rolling is very important in this respect. In view of these facts, the authors of the study reported herein worked to determine the link that exists between the structural state of a hot-rolled band and the degree of deformation during cold rolling on the one hand and the characteristic features of texture formation on the other hand. The studies were performed on specimens of a hot-rolled band of 80kp steel 3.5 m thick. The band structure was varied by varying the reeling temperature between 600-620 and 700-720°C after hot rolling on a 1700 KarMK mill. The temperature at the end of rolling ranged from 880 to 890°C. Commercial treatment of the hot-rolled bands included cold rolling on a 1700 five-cage mill to a thickness of 1.4 mm, recrystallization annealing in bell furnaces at 650°C for 10 hours, and subsequent tempering on a 1700 skin mill. Increasing the reeling temperature was found to result in the following: a rounding of the grain structure (especially in the surface layers of the hot-rolled band), the formation of a free-structure cementite along the grain boundaries, fuller formation of a disperse phase, and an increase in the textural inhomogeneity along the cross section. A link was found between the microstructures of the hot- and cold-rolled metal. This link appeared as the inheritance of a uniform fine-grained structure in the case of rolling with low-temperature reeling and in the form of the inheritance of coarse differences in grain size in the case of rolling with high-temperature reeling. Increasing reeling temperature was also found to result in structural nonuniformity along the length of the band. Reducing the reeling temperature to 600°C increased structural uniformity. Additional experiments established that the increase in degree of deformation during cold rolling and the reduction of reeling temperature help reduce the grain size of the recrystallized structure and increase its uniformity. Reducing the heating rate from 200 to 30°C/h increased the intensity of the octahedral component. This was especially true after reeling

at 600°C and subsequent deformation with degree of deformation (ϵ) > 60%. At a higher reeling temperature (700°C), an intensity of $\sigma_{(111)} > 3$ in the recrystallization texture was achieved when the degree of deformation during cold rolling was increased to greater than 70%. A high reeling temperature (700°C) and adequate formation of disperse phase during hot rolling were thus found to increase the lower bound of the degree of deformation during cold rolling and the rate of heating during annealing. Figure 1, table 3; references 4 (Western).

The Effect of the Duration of High-Temperature Tempering on the Elimination of Superheating Texture in Rotor Steels

927D0026E Moscow METALLOVEDENIYE I
TERMICHEskAYA OBRABOTKA METALLOV
in Russian No 5, May 91 pp 11-14

[Article by A. Borisov, TsNIITMash Scientific Production Association]

UDC 669-176:669.14.018.298

[Abstract] Commercial melts of 25CrNi3MoWN, 36CrNi3MoWN, and 25Cr2NiMoWN were studied in order to determine the effect of the duration of high-temperature tempering on the elimination of superheating texture in rotor steels. The steels were studied in two states: with superheating (i.e., after heating to 1,250°C, holding for 3 hours, and cooling in air) and without superheating (i.e., after standard normalizing or hardening from a temperature of 850 to 900°C). Tests were performed to determine the effect that duration of tempering at 640-650°C has on the mechanical properties, the semiembrittlement temperature (T_{50}), amount of austenite, coercive force, and density of the study steels. Hydrostatic weighing was used to determine the density of the metal specimens, x-ray crystallographic analysis was performed to identify structural changes induced by different tempering times, the technique of etching with a reactive compound was used to determine residual austenite in the specimens, and fracture and tensile strength tests were performed. Analysis of the study results revealed that when steel is tempered, processes of polygonization and subsequent recrystallization of the α -phase occur that result in a sharp decline in T_{50} , an increase in metal density, and significant attenuation of intragrain texture. The polygonization process slows down in the presence of a superheated structure (a more-alloyed α -phase) and is connected with a carbide transformation that disturbs orientation along the bainite plates. Increasing tempering time to 100 hours was found to result in recrystallization of the α -phase, which in turn caused a reduction in impact strength and an increase in T_{50} . The following guidelines were offered for use in designing regimens for heat-treating large forgings: the duration selected for the tempering of welded rotors should correspond to the time required for polygonization of the α -phase in the area around the weld; tempering sufficient for polygonization of the

α -phase is needed between two steel-hardening operations; and high-temperature tempering sufficient for polygonization of the α -phase is advisable after those operations that cause austenite grain growth (casting the blanks, hot plastic deformation, electroslag welding of the forgings, high-temperature treatment to straighten the grain). Figures 3, tables 2; references 8 (Russian).

Chemical and Heat Treatment of 5CrNiMo Die Steel

927D0026C Moscow METALLOVEDENIYE I
TERMICHEKAYA OBRABOTKA METALLOV
in Russian No 5, May 91 pp 7-8

[Article by N.Ya. Kudryavtseva, Yu.N. Gromov, and V.A. Kotofeyev, Kemerovo Food Industry Technology Institute]

UDC 621.785.5:66.14.018.258.2

[Abstract] A wide variety of chemical and heat treatment regimens are used to enhance the performance characteristics of dies used in hot deformation, including carburization, nitriding, boriding, surface alloying with chromium and vanadium, and chrome-calorizing. The literature does not contain any comparative data on the effect of each of these methods on such characteristics as resistance to scaling, heat resistance, and erosion resistance. For this reason, the authors of the study reported herein worked to find the optimal chemical and heat treatment regimen for 5CrNiMo die steel. Of all of the types of combined chemical and heat treatment regimens tested, single-phase boriding combined with surface alloying of chromium and vanadium resulted in the best combination of performance characteristics in the 5CrNiMo steels studied. The specimens subjected to surface alloying with chromium and vanadium demonstrated the best scaling resistance. In erosion resistance tests, specimens subjected to carburization developed cracks after 200 cycles, and nitrided specimens developed cracks after 500 cycles. The borided steels and those subjected to surface alloying with chromium and vanadium withstood 1,000 cycles without any visible crack formation. No significant differences in retention of hardness after heating to 700°C were found when specimens of steel subjected to boriding, nitriding, and surface alloying with chromium and vanadium were compared. Figures 2, tables 2; references 2 (Russian).

Carburization of Molybdenum- and Titanium-Containing Heat-Resistant Steels

927D0026B Moscow METALLOVEDENIYE I
TERMICHEKAYA OBRABOTKA METALLOV
in Russian No 5, May 91 pp 5-7

[Article by Ye.L. Gyulikhhandanov and A.D. Khaydorov, Leningrad State Technical University]

UDC 621.785.52:669.15-194

[Abstract] The authors of the study reported herein examined the carburization process and structure formation in diffusion layers of molybdenum- and titanium-containing low-carbon steels after different chemical and heat treatment regimens. Specimens of steels containing various percentages of C, Cr, Mo, V, and Ti were subjected to 2 hours of carburization in natural gas at a temperature of 1,000°C. The thickness of the carburized layer formed on each of the study specimens was calculated and also determined experimentally. Analysis of the measurement and calculation results demonstrated that the carburization kinetics of molybdenum-containing high-alloy steels may be satisfactorily described by both a model of internal carburization and a model of diffusion in the two-phase $\alpha + \gamma$ region. As expected, titanium-containing steels were found to be subordinate to a single-phase diffusion model. It was further discovered that monoalloy steels may be calculated based on a model of internal carburization by proceeding from the formation of TiC in the carbide layer. The structure of the diffusion layers of the study steels following carburization was determined after slow cooling and after direct hardening from the carburization temperature. Two zones containing carbides and austenite transformation products were discovered in the carburized layer of the molybdenum-containing steels. Carbide formations were found throughout the entire layer; they were rather finely dispersed. The structure of the carburized layer became more complex as the degree of alloying of the steel was increased: The carburized layer developed a multilayer structure, and the size and number of carbides increased. The surface layer of the molybdenum-containing study steels was found to contain martensite and residual austenite after hardening. The carbide formations were rather finely dispersed and evident only when there was a large increase in their number. In molybdenum-containing steels, heat resistance was maintained to 600°C. In titanium-containing steels, heat resistance was maintained to 500°C. The wear resistance of the titanium-containing steels was greater than that of the molybdenum-containing steels by a factor of 1.2. This finding was deemed grounds for replacing high-alloy steels by more economical titanium-containing steels. Figures 2, tables 3; references 5: 4 Russian, 1 Western.

Resource-Saving Technologies for Nitriding Steel in a Closed Space

927D0026A Moscow METALLOVEDENIYE I
TERMICHEKAYA OBRABOTKA METALLOV
in Russian No 5, May 91 pp 2-4

[Article by Ya.D. Kogan and Yu.A. Konovalov, Moscow Automobile Traffic and Highway Construction Institute]

UDC 621.785.532

[Abstract] Two versions of a new low-waste chemical treatment process for use in nitriding steel in a closed

space have been developed. The first is a cyclic (pulse) process, and the second is a combined two-stage process. The cyclic process entails periodically feeding a batching of saturating medium into the closed working space of a furnace and then holding it there until its saturation capacity has been completely used up. The combined two-staged nitriding process includes a stage of continuous nitriding followed by a stage of diffusion annealing in an atmosphere of nitrogen or dissociated ammonia in a closed space. The new processes make it possible to produce nitrided layers with a specified phase composition while reducing ammonia consumption by a factor of 2 to 8 depending on the individual process parameters. The new processes offer several advantages over the conventional process of nitriding in a flow of saturating gas. Specifically, they permit effective regulation of the phase composition of the diffusion layer and highly reproducible hardening results. Furthermore, the new processes are ecologically pure and involve a lesser amount of emissions of toxic gases into the atmosphere. Of the two new processes described, cyclic nitriding resulted in the greatest reduction in the amount of ammonia required. Figures 5, tables 2; references 5 (Russian).

Blast-Furnace Smelting With Injection of Hot Reducing Gases

927D0018A Moscow *STAL* in Russian No 8, 91 [signed to press 5 Jul 91] pp 7-13

[Abstract of article by A. P. Pukhov, G. M. Stepin, M. A. Tseytlin, V. S. Shvedov, L. S. Mkrtchan, and Yu. I. Gokhman; Tulachermet Scientific Production Association, Central Scientific Research Institute of Ferrous Metallurgy, and the National Institute of Metallurgical Plant Design (Gipromez)]

UDC 669.162.267.4:662.767

[Abstract] A fundamentally new modification of the blast-furnace process, injection of hot reducing gases, has been developed. In HRG injection, recirculated top gases from which the carbon dioxide has been removed are compressed, heated, and injected through the blast pipes into the furnace bosh. The top gases are compressed by two 900-31-2-type air blowers, each with a capacity of 50,000 to 60,000 cu m/hr and an output pressure of 360 kPa. The blowers are equipped with heat exchangers to bring the gas temperature down to 40°C. The carbon dioxide is removed from the gas by a scrubber consisting of two identical units with carbon dioxide absorbers utilizing an aqueous monoethanolamine solution. The carbon dioxide is removed from the MEA solution by steam heating the solution in a regenerator. The solution is then cooled and returned to the absorber, while the carbon dioxide is vented to the atmosphere. The cleaned top gases pass through a separator to remove the condensate and are then heated by a gas heater with three high-alumina refractory-lined regenerating chambers to a temperature of 1100 to 1150°C. The hot gases are then pumped into the furnace along with cold process oxygen supplied by compressors. The HRG injection installation has its own power and process substance supply system and instruments. HRG injection underwent extensive industrial testing from 1985 to 1990, when 250,000 tons of iron were smelted in the No. 2 blast furnace of the Tulachermet NPO. After some process adjustments and equipment modifications were made to eliminate problems associated with excessive scorching of the blast pipe assemblies, HRG injection proved to be reliable and efficient, reducing coke consumption to 280 to 300 kg/t of steel and increasing furnace productivity 25-30. Figures 1, tables 6; references 10: Russian.

The Resistance of Type 14CrNi3MoCuN Steel to Delayed Fracture During Double-Arc Welding

927D0037A Kiev AVTOMATICHESKAYA SVARKA
in Russian No 8, Aug 91 (manuscript received
25 Oct 89; after revision 21 Jan 91) pp 7-11

[Article by G.V. Burskiy, engineer, D.P. Novikova, candidate of technical sciences, and Yu.A. Sterenbogen, doctor of technical sciences, Electric Welding Institute imeni Ye.O. Paton, UkSSR Academy of Sciences]

UDC [621.791.75.052:669.14.018.295]:539.413

[Abstract] Using medium-alloy high-strength steels in welded structures provides significant engineering and economic gains over other types of steels. When such steels are welded, however, problems arise because the metal of the heat-affected zone is prone to the formation of cold cracks. In an effort to help alleviate this problem, the authors of the study reported herein examined the effect that the heating cycle used in double-arc welding has on the resistance of the heat-affected zone of joints of type 14CrNi3MoCuN steel to the formation of cold cracks during delayed fracture tests. The test joints were assembled so as to simulate a narrow gap. Sv-10MnNi2CMoCu wire 2.0 mm in diameter was used. A shielding atmosphere of 80% Ar and 20% CO₂ was used. The welding regimen for each of the arcs was varied within the following ranges: $I = 340$ to 450 A, $U = 30$ to 38 V, and $v = 14$ to 20 m/hr. The welding was performed in a special heat-releasing jig, and the heating cycle was recorded by using tungsten-rhenium thermocouples and an N-105 oscillograph. The hydrogen saturation of the metal of the weld was kept constant and controlled on the basis of the shielding mixture's dew point and the content of residual hydrogen in the welding wire and base metal. After welding, the specimens were subjected to a previously specified load while at a temperature of 100 to 120°C . If the specimens did not fracture after 24 hours had elapsed, the load was removed. The tests confirmed that double-arc welding may be used to regulate heating cycle parameters within a broad range. By varying the distance between the arcs and regulating the welding regimen for each arc, the researchers were able to cool the heat-affected zone at a rate guaranteeing a high resistance to delayed fracture. They further demonstrated that double-arc welding makes it possible to significantly increase the delayed fracture resistance of the heat-affected zone of welds of type 14CrNi3MoCuN steel without preliminary heating provided that low-alloy welding materials are used. Specifically, the greater the distance between the arcs, the slower the cooling that occurs in the range of temperatures of the lowest stability of austenite and in the range of temperatures of the martensite transformation. The studies performed showed that as a result of heating to $1,200^\circ\text{C}$, the austenite grain grows to 2-3 points. Cooling to 400°C does not, for all practical purposes, result in decomposition of the austenite. When subjected to repeated heating and austenitization at 940°C , the austenite grain becomes somewhat reduced (4-5 points). A rather

coarse-grained mixture of bainite and martensite forms during the subsequent cooling. If repeated heating and austenitization are performed at 820°C , recrystallization causes the austenite grain to reach a size of only 6-7 points, and a fine-needled bainite and martensite is formed. No phase recrystallization occurs upon repeated heating to 740°C , and the grain size achieved as a result of heating to $1,200^\circ\text{C}$ is maintained. The change in the resistance of the heat-affected zone of type 14CrNi3MoCuN steel to delayed fracture may thus be explained in terms of its increased tendency to grain growth under conditions of welding heating and its formation of large- or fine-grained structure as a result of the thermal effect of the second arc. Figures 3, tables 2; references 10 (Russian).

The Structural Transformations and Properties of Metal in the Heat-Affected Zone of Welded Joints of the Steel 10CrNiCu

927D0037B Kiev AVTOMATICHESKAYA SVARKA
in Russian No 8, Aug 91 (manuscript received
16 Feb 90; after revision 4 Mar 91) pp 12-16

[Article by P. Seyffarth, doctor of technical sciences and H.G. Gross, candidate of technical sciences, Rostock University, Germany; V.A. Dovzheko and V.G. Vasilyev, candidates of technical sciences, Electric Welding Institute imeni Ye.O. Paton, UkSSR Academy of Sciences; and A.P. Ammosov, candidate of technical sciences, M.A. Fedotova, engineer, and V.P. Larionov, doctor of technical sciences, Institute of Physics Engineering Problems of the North, Yakutsk Scientific Center, Siberian Department, USSR Academy of Sciences]

UDC [621.791.75.052:669.15-194.2]:620.18

[Abstract] The authors of the study reported herein compared data obtained in simulations of welding heating cycles. They also studied the quantitative relationships existing among the structural components and mechanical properties of different variations of type 10CrNiCu steel (which is a low-alloy steel that is widely used in machine building and shipbuilding). The dilatometric studies and quantitative phase analyses reported and analyzed were performed at Rostock University, the Ye.O. Paton Electric Welding Institute, and the Institute of Physics Engineering Problems of the North. The thermokinetic diagrams of the austenite transformation in type 10CrNiCu steel at each of these institutions were in very good agreement with one another: the temperatures of the beginning and end of the phase transformations and the cooling cycles on the individual diagrams virtually coincide with those on the others. Analysis of the dilatometric studies and the analysis of the set of mechanical properties of the heat-affected zone of welded joints of 10CrNiCu steel conducted at the three institutions revealed that the difference in the

content of the alloy-forming elements within the confines of the composition stipulated in its type specification does affect the formation of the end structure obtained when the steel is welded. The best joints of 10CrNiCu steel produced by mechanized CO_2 -shielded arc welding and submerged-arc are achieved when cooling rates of 3.5 to 55°C/s are used. The following conditions were found to result in welded joints of 10CrNiCu steel with the best cold resistance: steel thickness, up to 30 mm; shielding medium, CO_2 ; welding wire, Sv-08Mn2C; welding wire diameter, 1.6 and 2.0 mm; and per-unit-length energy, 10.0 to 21.0 kJ/cm (which corresponds to a cooling rate of 40 to 10°C/s). Figures 3, tables 2; references 7: Russian, Western.

The Effect of Preliminary Heating and Local High-Temperature Tempering on the Fracture Toughness of Welded Joints of 09Mn2C Steel

927D0037C Kiev AVTOMATICHESKAYA SVARKA in Russian No 8, Aug 91 (manuscript received 12 Oct 89; after revision 18 Mar 91) pp 17-21

[Article by V.S. Girenko and M.D. Rabkina, candidates of technical sciences, Yu.V. Pavlenko engineer, and V.N. Gorpenyuk and E.M. Dyskin, candidates of technical sciences, Electric Welding Institute imeni Ye.O. Paton, UkSSR Academy of Sciences]

UDC

[621.791.75.052:669.15-194.2:620.192.7]:621.78.013.7

[Abstract] The authors of the study reported herein conducted a series of experiments to assess the effect of preliminary heating and subsequent heat treatment on the fracture toughness of welded joints of 09Mn2C steel. A 1,600-mm-diameter shell (wall thickness, 60 mm) of 09Mn2C-12 steel was welded. A V-shaped bevel with a total angle of 50-55° was used along with a root face of 3 +/- 0.5 mm and a gap of 3.25-4.0 mm. The shells were assembled by using strong shackles secured from within. The standard technique for welding assembly joints was used to weld the annular joint. The root weld was made by using LB-52U electrodes with a diameter of 3.25 mm and a direct current of 100 to 110 A with straight polarity. The filler layers were made by using UONI-13/55 electrodes with a diameter of 4.0 mm, direct current, and reverse polarity ($I = 140-160$ A; $U = 22-24$ V). For half the length of the shell's circumference the weld was made without heating at an air temperature of 7°C; the other half of the weld was made with the joint heated to 120-150°C. After being welded, the joint was cut into two halves. One half was subjected to high-temperature tempering (heating to 650°C, holding for 2 hours, cooling in the furnace). The other half was not heat-treated. Four specimens were cut from the shell. These specimens reflected the following welding regimen modifications: 1. without preheating, without heat treatment; 2. without preheating but with heat treatment; 3. with preheating but without heat treatment; and 4. with

preheating and heat treatment. The chemical composition of the base metal and root zone of each of the specimens was determined. High-temperature tempering had very different effects in the root and filling layers of the metal of the weld: The fracture toughness of the root layers increased markedly after tempering, whereas that of the filler layers decreased somewhat from its initial fracture toughness. Preheating resulted in an even more noticeable reduction in the hardness of the root sections of the weld and, accordingly, in an increase in its fracture toughness values. This change was attributed to a reduction in the cooling rate of these sections during the welding process, to a small reduction in thermoplastic deformations, and to an intensification of the restructuring processes occurring when the filler layers were applied. When preheating and high-temperature tempering were combined, each had much the same effect as when used alone. Both preheating and high-temperature tempering were thus demonstrated to have a significant effect on the properties of the different segments of a weld. When both techniques were used together, the fracture toughness of the filler sections decreased somewhat. It is important to bear in mind, however, that this decrease occurs against the background of an increase in the fracture toughness of the root layers, where the likelihood of the appearance of defects is especially high. Thus, this decrease in fracture toughness is not decisive from the standpoint of the weld's reliability. Both preheating and high-temperature tempering increase the fracture toughness of root sections and thus increase their resistance to defect formation as well as the joint's overall reliability. Figures 2, tables 2; references 14: 5 Russian, 9 Western

The Effect of Carbide-Forming Elements on the Properties of Welds of Martensite Steels Containing 12% Chromium

927D0037D Kiev AVTOMATICHESKAYA SVARKA in Russian No 8, Aug 91 (manuscript received 2 Nov 88; after revision 18 Mar 91) pp 22-25

[Article by V.Ye. Lazkov, candidate of technical sciences, V.G. Kovalchuk, V.M. Yadrov, and M.I. Naumov, engineers, All-Union Scientific Research Institute of Aviation Materials [VIAM] Scientific Production Association]

UDC [621.791.754:293:669.15.194.3]:620.18

[Abstract] The authors of the study reported herein examined the effect that the complex molybdenum, tungsten, vanadium, and niobium additives in amounts totaling 0.9% have on the weldability of martensite steels containing 12% chromium. During the studies specimens of Cr12Ni2MoVNb steel 3 mm thick were argon arc-welded by using a filling material in the form of a "noodle" made of a sheet of 12Cr12Ni2Mo steel 3 mm thick. So that the metal of the weld would be close in composition to the filling material, the weld was made in a gap 3 mm wide. The mechanical properties of the metal

of the weld and filling materials were estimated after thermal hardening in accordance with the standard regimen (hardening and tempering at 680°C for 3 hours). The filling material was also tested to determine its resistance to the formation of hot and cold cracks, and the weld was subjected to metallographic studies to determine the crystallization parameters of the filling material. On the basis of the studies performed, the researchers concluded that replacing molybdenum with an equivalent amount of niobium, vanadium, or tungsten within the 0.9% limit results in a significant alteration in the structure and properties of the metal in a weld of the aforesaid steels. Resistance to hot crack formation was found to increase from 7 to 15×10^{-5} m/s and ultimate strength at 650°C was found to increase from 420 to 450 MPa. A complex additive consisting of 0.5% Nb and 0.4% Mo was found to produce a weld with the following set of optimal properties. Specifically, the additive resulted in welds with an ultimate strength of $\geq 1,000$ MPa at 20°C and ≥ 450 MPa at +650°C. At 20°C the weld had an impact strength of ≥ 0.75 MJ/m² and a resistance to hot crack formation of $\geq 10 \times 10^{-5}$ m/s. Figures 6, tables 2; references 14 (Russian).

The Effect of Design Parameters on Durability During the Thermal Cycling Life of Soldered Joints of Electronic Components Mounted on a Printed Circuit Board Surface

927D0037E Kiev AVTOMATICHESKAYA SVARKA in Russian No 8, Aug 91 (manuscript received 19 Dec 89; after revision 29 Oct 90) pp 30-34

[Article by V.I. Makhnenko, academician, UkSSR Academy of Sciences, and N.I. Pivtorak, engineer, Electric Welding Institute imeni Ye.O. Paton, UkSSR Academy of Sciences, and A.A. Grachev, candidate of technical sciences, and T.V. Sagaydachnaya, engineer, Scientific Research Institute for Industrial Technology and Organization, Kiev]

UDC [621.791.3.052:621.396.6]:539.43

[Abstract] The authors of the study reported herein examined the effect of design parameters on the durability of the soldered joints of electronic components mounted on printed circuit boards throughout their thermal cycling life. They considered the interactions occurring at temperatures ranging from -60 to +125°C in the system component lead-circuit board contact area when the following materials are used: ceramic, POS-61 solder, epoxy resin glass-base textolite, gold, copper, a ceramic chip element, air, and Kovar. Specifically, they estimated the elastoplastic deformations arising during thermal cycling in the said soldered joints as a function of the variation of the components' geometric parameters and the mechanical properties of the solder. Four tables of data summarizing these relationships are presented along with expressions for use in estimating the relationship between given parameters. The main conclusion resulting from the data presented is that

increasing the thickness of the solder in the soldered joints and reducing the overall dimensions of the connections will reduce the range of plastic deformations in the solder and thus result in more durable joints. Figures 4, tables 4; references 5 (Russian).

Preprocessing Welding Current and Voltage Signals for Input Into a Computer

927D0037F Kiev AVTOMATICHESKAYA SVARKA in Russian No 8, Aug 91 (manuscript received 23 Jan 89; after revision 7 Dec 90) pp 41-46

[Article by G.A. Butakov, V.V. Dolinenko, candidate of technical sciences, and A.G. Ter-Arutyunants and K.A. Shemetilo, engineers, Electric Welding Institute imeni Ye.O. Paton UkSSR Academy of Sciences, and B.P. Rzhannov, candidate of technical sciences, and A.A. Zinoviyev and A.Yu. Nikiforov, engineers, Southern Machine Building Plant Scientific Production Association, Dnepropetrovsk]

UDC 621.791.754*293.001.24:681.3

[Abstract] The authors of the study reported herein examined the problem of designing a feedback loop to monitor an argon-arc welding regimen based on a three-phase alternating-current arc. The feedback loop under consideration is intended to provide information about the running effective values of the currents and voltages in the arcs. The specific system analyzed contains an analog-to-digital converter, a radial parallel interface, a radial serial interface, and a signal filtration and normalization module. The system is designed to simultaneously read information along each of five feedback channels in a real-time mode. The main problem that had to be solved in order to develop the said feedback system was that of finding a suitable filtration system for the high-frequency components of the welding current and voltage signals. Detailed calculations of the signals that would have to be input into the monitoring computer and the requirements that a suitable filter would have to meet were performed and are presented. On the basis of their calculations, the authors concluded that a system for high-frequency real-time processing of welding current and voltage signals is indeed possible. They further concluded that using analog filters in input monitoring circuits makes the procedure of monitoring a welding regimen much easier. They developed five algorithms to monitor the welding currents and voltages in the arcs. The algorithms differed from one another from the standpoint of number of parameters estimated, complexity of execution, and precision of estimation. Least-squares method algorithms were used to calculate the effective values of the signals and determine their phase shifts. A correction was developed to compensate for the smoothing properties of least squares algorithms when used before the signal filtration and normalization module. The fourth algorithm was found to yield exact estimates both for the output and input signals of the

signal filtration and normalization module that coincided with estimates obtained when consideration was given to the signals' spectra. The fifth algorithm was designed for use solely in calculating the output signals of the signal filtration and normalization module. A correction had to be developed for use with this module in order to eliminate the loss of information associated with suppressing the high-frequency components of the monitored signals. A graph plotting the dependence of the bias of the estimate of the effective welding current as a function of its rated value has been included in the article for use in calculating this correction. Figures 5, tables 3; references 3 (Russian).

Magnetic Phenomena Occurring When ONi9 Steel Is Welded and Ways of Eliminating Their Effect on the Quality of Welded Joints

927D0037G Kiev AVTOMATICHESKAYA SVARKA in Russian No 8, Aug 91 (manuscript received 5 Jun 90; after revision 10 Jan 91) pp 47-51, 55

[Article by K.A. Yushchenko, corresponding member, UkSSR Academy of Sciences, V.A. Pestov, engineer, T.M. Starushchenko, candidate of technical sciences, and A.S. Yerashov, engineer, Electric Welding Institute imeni Ye.O. Paton, UkSSR Academy of Sciences]

UDC [621.791.75.052:669.15'24-194]:538.11

[Abstract] The increasing use of cold-resistant nickel steels containing 6 and 9% nickel in domestic cryogenic technology and in related structures has necessitated improvements in the processes used to weld such steels. One problem that arises when welding magnetically hard steels such as ONi9 is the phenomena of magnetic blow. The authors of the study reported herein report on their attempts to overcome the problem of magnetic blow while welding ONi9 steel during the process of manufacturing isothermal tanks to store ethylene. Specifically, they show that the changing direction and intensity of magnetic blow during the welding process results in the formation of various types of defects including pores, poor fusion, nonpenetration, and slag inclusions. They present an analysis of the distribution of the lengthwise, crosswise, and vertical components of the magnetic field that developed under the actual conditions of welding the walls of isothermal tanks and illustrate the interconnection between the aforesaid types of defects and the intensity of the three magnetic field components. They present a technique that enabled them to reduce the level of residual magnetic induction in the weld zone without preliminary demagnetization of the metal being welded. The essence of the new technique lies in creating the conditions for closing the magnetic circuit in the blanks being welded through a magnetically soft material. Placing a magnetic shunt right up against the edges of the product being welded makes it possible to reduce the intensity of the magnetic field in the beveling to values at which it will no longer have a significant effect on the welding process. The new technique served as the basis

of process guidelines that were used at the Sintezkauchuk Production Association in Sumgait to complete construction of 10,000-m³ isothermal tank made of ONi9 steel with the level of magnetic induction reaching 25 mT. Figures 5; references 7: 6 Russian; 1 Western.

Heating Devices in Units To Weld Dielectrics in an Electric Field

927D0037H Kiev AVTOMATICHESKAYA SVARKA in Russian No 8, Aug 91 (manuscript received 14 Dec 89; after revision 28 Sep 90) pp 63-66

[Article by N.N. Khomenko, candidate of technical sciences and O.A. Moseyev, engineer, Chernigov affiliate, Kiev Polytechnic Institute, and V.V. Yakovlev, V.V. Silantsev, and A.D. Kuzin, engineers, Institute of Electronic Machine Building, Ulyanovsk Microelectronics Center]

UDC 621.791.03-69:537.212

[Abstract] The manufacture of control and monitoring sensors containing welded subassemblies of semiconducting materials and glasses has necessitated the creation of special units for welding in an electric field. Because heating temperature is one of the most important key parameters of the welding process, the authors of the study reported herein examined various devices and techniques for heating the glass in units designed to weld dielectrics in an electric field. The following are among the main conclusions of their study. When welding subassemblies containing glass and metal components in an electric field, it is possible to heat the glass in one of two ways: by the direct action of infrared radiation with a wavelength of 3 to 5 μm or indirectly through a heat-transfer agent. The second method has proved to be best when welding components 1 to 3 mm high and with a large contact plane. A simulator specimen should be used to monitor the temperature when the indirect heating method is used. In order to obtain even heating in multiposition welding attachments, consideration must be given to that portion of the radiators' length that is effectively used. Special heat screens must be installed when the piece of glass being welded is large. Inert gases should be used to improve heat transfer during welding in a vacuum with indirect heating. Infrared radiators have been demonstrated to improve the productivity of the process of welding dielectrics, as well as reduce the overall dimensions of the heating devices required. Figures 7; references 3 (Russian).

Radiative Heat Transfer Coefficient Measurement in Heating Parameter Analysis of Infrared Radiation-Welded Polymer Tube Surfaces

927D0058F Moscow SVAROCHNOYE PROIZVODSTVO in Russian No 6(680), Jun 91 pp 36-37

[Article by V.V. Koshelev, V.V. Chigarev, Mariupol Shipyard and Mariupol Metallurgical Institute]

UDC 621.791.01:536.2-036.6/8

[Abstract] Several methods of calculating the radiative heat transfer coefficient which determines the magnitude of the incident radiation flux and significantly affects the length of heating to the welding temperature and the depth of the viscous flow state zone of the welded tube surface are discussed. The knowledge of this coefficient ϕ is important for selecting the heating parameter for welding polymer tubes by infrared radiation—an efficient way of producing quality welded joints. The radiative heat transfer coefficient is one of the main parameters determining the radiant flux utilization factor and radiator-heater efficiency. In order to increase it, it is necessary to ensure that the heating element size and shape match those of the welded surfaces. Analytical relations are derived for computing the coefficient ϕ for a given heating element and welded surface configuration and a given distance between them. Figures 4; references 3

Welding Electrodes for Low-Alloy Heat-Treated Steel Operating at Subzero Temperatures

927D0058E Moscow SVAROCHNOYE
PROIZVODSTVO in Russian No 6(680), Jun 91
pp 23-25

[Article by Yu.M. Nyagay, O.S. Kakovkin, D.V. Vitman, Yu.V. Svanidze, Scientific Production Association of the Central Scientific Research Institute of Machine Building]

UDC 621.791.75.042:669.15-194.2:536.485

[Abstract] The need to develop high-quality cold-resistant electrodes for manual arc welding capable of ensuring the serviceability and reliability of welded joints at subzero temperatures prompted by extensive construction of industrial complexes in Siberia and the Far North is identified and the effort to develop electrodes for welding low-alloy pearlitic steels widely used for erecting various large-scale structures is described. The specifications used in developing electrodes are summarized and test data on three new types of electrodes are presented. A comparative estimate of the welding properties and performance of existing and newly developed electrodes show that the latter are characterized by a better slag separability, a low sputtering, a good weld formation, and an arc-burning stability. Furthermore, welding by the new electrodes in the overhead and vertical position does not lead to problems even at high currents. The new electrode ensures a weld impact strength of $\geq 34 \text{ J/cm}^2$ at -50°C , a yield strength of 340-393 MPa, and an ultimate rupture strength of 440-490 MPa after heat treatment. Figures 3; tables 1; references 4.

Formation Features and Properties of N-2.5 Zirconium Alloy Joints With PT-3V Titanium Alloy During "Sharp Face" Projection Welding

927D0058D Moscow SVAROCHNOYE
PROIZVODSTVO in Russian No 6(680), Jun 91
pp 16-18

[Article by A.A. Chularis, M.M. Mikhaylova, A.I. Popov, Rostov-na-Donu Agricultural Machinery Industry Institute]

UDC 621.791.763.2.052:669.296+669.295

[Abstract] The problem of joining together zirconium, titanium, or their alloys even in a homogeneous combination and the shortcomings of nonconsumable electrode welding of these metals are discussed and the possibilities of using "sharp face" projection welding for joining the N-2.5 zirconium alloy (with 2.5% Nb) to the PT-3V titanium alloy (with 3.5-5% Al and 1.5-2.5% V) are investigated. Sheets of the PT-3V doped titanium pseudo- α -alloy and strips of the H-2.5 zirconium alloy with 2.5% Nb are used in the experiment; sample surfaces are degreased with acetone before welding. The mechanical properties of the resulting joints and their microstructure are examined. Three distinct zones are identified in the heat-affected area: a capillary zone in the middle and a fillet zone on either side of it. The microhardness distribution in welded joint zones and the chemical inhomogeneity of the element distribution in the welded joint zones are examined and plotted; the alloy HV hardness in various measurement positions is summarized. An analysis of the properties of joints produced by "sharp face" projection welding makes it possible to expect an adequate corrosion resistance of titanium alloy joints with zirconium alloy and recommend the method for commercial applications. Figures 3; tables 2; references 6.

Welding Characteristics of Porous Wire Mesh Materials

927D0058C Moscow SVAROCHNOYE
PROIZVODSTVO in Russian No 6(680), Jun 91 pp 8-9

[Article by A.F. Tretyakov, Moscow State Engineering University imeni N.E. Bauman]

UDC 621.791.4.01:539.378.3

[Abstract] It is shown that porous elements on the basis of metal meshes can be produced only by welding the wires to each other; consequently, it is necessary to investigate the process and determine the temperature, straining rate and magnitude, and medium necessary for producing porous mesh materials (PSM) with specified properties and the maximum layer peeling strength. In so doing, a physical model of wire crosshairs is developed to simulate welding of the porous mesh material elements. The welded joint quality is estimated by the relative peeling strength. The dependence of the peeling

strength of cruciform wire connections from steel 12Kh18N9T produced by percussive welding in a vacuum on the crosshair reduction at various temperatures, the dependence of the relative peeling strength of wire crosshairs from steel 12Kh18N9T and the mass transfer rate on the straining rate, and the dependence of relative elongation during the stretching of wire crosshairs from steel 12Kh18N9T produced by percussive welding in a vacuum on temperature are investigated and plotted. An analysis reveals a relative peeling strength maximum in crosshair elements produced by diffusion and roll welding; the low quality of welded joints formed at a 10^{-2} - 1 s $^{-1}$ reduction is attributed to the microirregularities' high resistance to straining and the low rate of diffusive mass transfer in the contact zone. It is recommended that porous mesh materials be produced by roll welding and that the loading rate be increased or the blanks be hammer-welded by hot straining. Figures 4; references 10.

Characteristics of Light-Beam Welding of Copper Hookup Wires

927D0058B Moscow SVAROCHNOYE
PROIZVODSTVO in Russian No 6(680), Jun 91 pp 3-5

[Article by M.I. Oparin, V.S. Mamayev, V.A. Frolov, N.S. Pronin, P.G. Volkov, Moscow Aviation Engineering Institute imeni K.E. Tsiolkovskiy]

UDC 621.701.72.78:621.315.5

[Abstract] The shortcomings of existing methods of hookup wire brazing, such as an increased consumption of scarce and expensive solder and ecologically unsafe working conditions, are addressed and a new light-beam welding process developed at the Aviation Engineering Institute imeni K.E. Tsiolkovskiy (MATI) as well as the new equipment designed for this purpose in order to eliminate them are described. An equation is derived for calculating the mean luminous flux density in the heating spot. The properties of light-beam welded joints, particularly the oxygen, hydrogen, and nitrogen concentration, are compared to those produced by arc welding with consumable carbon electrode and argon arc welding

with a nonconsumable electrode. The effect of the welding method and welding conditions on the weld metal's gas saturation is assessed by reduction melting in a "Leco" unit. The light-beam weld metal ductility is considerably higher than that obtained by other methods. Thus, light beam welding in the air of hookup copper wires results in a lower weld metal saturation with oxygen, hydrogen, and nitrogen, making it possible to recommend the method for commercial applications. Figures 3; tables 2; references 3.

Connection of High- T_c Superconductors With Normal Conductors

927D0058A Moscow SVAROCHNOYE
PROIZVODSTVO in Russian No 6(680), Jun 91 pp 2-3

[Article by S.K. Slizberg, A.I. Tokarev, V.N. Shaktarin, S.N. Pylinina, All-Union Scientific Research Institute of Electric Welding Equipment and All-Union Scientific Research Institute of Electric Motors and Generators]

UDC 621.791.052:621.315.5

[Abstract] Problems encountered in trying to connect high- T_c superconductors to normal conductors for electric testing or electrical design purposes are identified and the development of relatively inexpensive methods of making connections on $YBa_2Cu_3O_{7-x}$ massive ceramics which are not labor-consuming and use standard welding and soldering equipment is reported. Three contact-making methods are considered: plating the superconductor surface with indium and soldering the normal conductor; applying silver paste to the surface and burning out the organic binder, then soldering the conductor; and connecting the superconductor to a silver-plated multiconductor copper wire by the capacitor stored-energy spot welding method. The structure of joints obtained by various methods and their voltage-current (VAKh) characteristics are examined and the results of electric tests of samples are summarized. The results are at the level of world's best known methods and convincingly demonstrate the possibilities of the proposed designs for making connections with suitable contact resistivity. Figures 3; tables 1; references: 3 Western.

Effect of Cryogenic Treatment on Wear Resistance of Diamond Drill Bits

927D0060E Moscow RAZVEDKA I OKHRANA NEDR
in Russian No 5, May 91 pp 23-24

[Article by V.I. Vlasuk, Tula Branch of the Central Scientific Research Institute of Geological Prospecting]

UDC 622.24.051.71.001.76:536.483

[Abstract] The development of a cryogenic method of diamond drill bit and tool hardening by cooling them for 10-15 min in a liquid nitrogen medium at a -196°C temperature is reported. Although the practical results are good, the method's theoretical bases have not been developed. Consequently, a hypothesis is made that the treatment lowers the residual stress in diamond and increases the tool's wear resistance. The hypothesis is experimentally tested. To this end, samples of 17A4 drill bits are tested for abrasive wear at the Superhard Materials Institute; the results demonstrate that the wear resistance of treated samples rises by 25% while the necessary exposure to liquid nitrogen can be shortened to 3 min. An analysis shows that the mean increase in the diamond drill bit wear resistance as a result of cryogenic treatment is 27.7% at the Adrasman enterprise and 11% at the Altyn-Topkan enterprise. A comparison of test data indicates that an average increase in wear resistance is 10-30%. The methods's simplicity and its relative economic efficiency make it possible to improve diamond drilling indicators considerably. Tables 1; references 3.

Type Test Outcome of Drill Bits Reinforced With Metallized Diamond

927D0060D Moscow RAZVEDKA I OKHRANA NEDR
in Russian No 5, May 91 pp 22-23

[Article by N.I. Kornilov, A.I. Osetskiy, O.V. Shechepetova, All-Union Scientific Research Institute of Prospecting Technology]

UDC 622.24.051.71:621.793

[Abstract] The results of type tests of drill bits reinforced with metallized diamonds conducted in 1988-1989 in the framework of a program approved by the USSR Geology Ministry are discussed. Standard impregnated drill bits with granulated O2IZG-59 natural diamonds are used as the frame of reference. Test data are processed by the mathematical statistics methods (with a 0.9 confidence level). The results are summarized for each drill bit type, indicating the metallizing method, number of bits, diamond mass, drilling time, drilling volume, drill bit life, drilling speed, and diamond outlays. The commission conducting the tests recommended that diamonds impregnated by the KIB and KBU methods (cathode ion bombardment and Kabardino-Balkarskiy State University, respectively) be used; they ensure a normal service life of 36.8 and 24.9% higher than base

drill bits, respectively. Commercial production of such bits began in 1989 at the Kabardino-Balkarskiy Diamond Tool Plant. Tables 1.

'Garmonika-411' Laser Microscope in Engineering Mineralogy

927D0060C Moscow RAZVEDKA I OKHRANA NEDR
in Russian No 5, May 91 pp 20-22

[Article by L.B. Meysner, Ye.Yu. Yefimkina, A.I. Frez, R.M. Raguzin, All-Union Institute of Mineral Resources and Leningrad Optics and Mechanics Association]

UDC 621.385.833.2:549

[Abstract] The Garmonika-411 laser microscope intended for an automatic quantitative analysis of the luminescent (scheelite, cassiterite, zircon, etc.) and acen-tric (free quartz, nepheline, sphalerite, etc.) mineral phase concentration in disperse materials, laps, and polished microsections by the ray optics laser and quantum optic methods given a phase concentration of 0.001-100% is described; a microscope block diagram is presented. The microscope's main elements are a YAG:Nd³⁺ laser with a pulse repetition period of 25 Hz and an automation unit. The laser microscope's capabilities are illustrated. The Garmonika-411 makes it possible to study linear and nonlinear optical properties of minerals and monitor and control dressing and concentration processes. The ray optics laser method (LOG) made it possible for the first time quantitatively to measure low (<1%) and extremely low ($\leq 10^{-2}\%$) mineral phase concentrations in ores and concentrates, use ungraded materials, identify several luminescent phases, and analyze material on the conveyor belt. The microscope is expected to be widely used in science and industry. Figures 3; tables 3; references 6.

Coal Sampling by Petrographic Parameters of Unified Classification

927D0060B Moscow RAZVEDKA I OKHRANA NEDR
in Russian No 5, May 91 pp 14-17

[Article by A.S. Artser, I.V. Yerebin, Kuznetsk Scientific Research Institute of Coal Dressing and Fossil Fuel Institute]

UDC 550.85:552.574:522.2

[Abstract] The coal and anthracite classification on the basis of GOST 25543-88 used in the USSR, especially the principal petrographic parameters, is discussed and the problem of determining the number of samples sufficient for estimating the petrographic parameters with a given precision and grading coal in individual seams using a unified classification is formulated. A new geological-mathematical method of determining the sampling parameters relative to the geological conditions of the Kuznetsk Basin (Kuzbass) is developed and the results obtained with its help are presented. The vitrinite

reflectance R_0 and the concentration of mineral charcoal components ΣOK are used as the principal petrographic parameters. It is shown that the greater the parameter variability, the greater the necessary sample density; moreover, an attempt should be made to distribute the samples as uniformly as possible throughout the seam. Figures 2; tables 4; references 1.

Geological-Economic Assessment of Eastern Donbass Coal Deposits

927D0060A Moscow RAZVEDKA I OKHRANA NEDR
in Russian No 5, May 91 pp 11-14

[Article by V.K. Kabalov, G.I. Starokozheva, O.Ye. Faydov, All-Union Scientific Research Institute of Geological Coal Prospecting]

UDC 550.8:553.93/.96.003.1(470.61)

[Abstract] The role of geological-economic assessment of coal deposits in economic science of mineral feedstocks and raw materials is considered in light of the length of deposit detection, prospecting, and operation processes

and the lag between prospecting and mining as well as the uncertain nature of geological data. Coal resources in Eastern Don Basin (Donbass) are estimated at 20.8 billion tons, or 0.4% of the country's total. A geological-economic assessment of 21 out of 56 existing and prospective deposits is performed in four stages and economic-mathematical and analytical models are developed. The formal economic assessment procedure is described in detail. The results show that of the 21 sites evaluated, Gukovskaya Glubokaya, Belokalitvenskaya North, Yuzhno-Kamenskaya, Millerovskaya South, North, and East, Sulinskaya Glubokaya, and Belokalitvenskaya South are potentially the most profitable. Their rental profits vary from 1.09-10.4 ruble/t fuel equivalent in the worst case scenario to 13.3-22.79 ruble/t in the best case, with the average being 7.2-16.8 ruble/t. The total predicted resource value is estimated as 5.5 billion rubles or 47% of the total predicted resource. The resulting data are applicable to Eastern Donbass only yet the procedure itself may be used in other regions. Tables 1; references 1.

END OF

FICHE

DATE FILMED

5, May 1992